Novel Biosensors Using Intact Liposome Microarrays

by

Nikhil D. Kalyankar

A Dissertation Submitted to the Graduate Faculty in Engineering in Partial Fulfillment of the Requirements for the Degree of Doctor of Philosophy

The City University of New York

2007

UMI Number: 3283620

ProQuest Information and Learning Company
300 North Zeeb Road
P.O. Box 1346
Ann Arbor, MI 48106-1346

This manuscript has been read and accepted for the Graduate Faculty in Engineering in satisfaction of the dissertation requirement for the degree of Doctor of Philosophy.

_____	_____
Date	Prof. Alexander Couzis Chairman of Examining Committee
_____	_____
Date	Prof. Mumtaz Kassir Executive Officer
	Prof. Alexander Couzis (Mentor) _____
	Prof. Charles Maldarelli (Co-Mentor) _____
	Prof. M. Lane Gilchrist (Co-Mentor) _____
	Prof. David H. Calhoun _____
	Prof. Stavroula Sofou _____
	Supervisory Committee

THE CITY UNIVERSITY OF NEW YORK

Abstract

Novel Biosensors Using Intact Liposome Microarrays

By,

Nikhil D Kalyankar

Advisor: Prof. Alexander Couzis

We have developed protocols to array individual, intact small unilamellar vesicles (liposomes) onto chemically modified microwell substrates. The substrates have microarrays of 1.2 μm diameter wells in a square pattern fabricated by photolithography and reactive ion etching on a silicon wafer coated with silicon dioxide layer. The background of the wells is modified using polyethylene glycol terminated silane self assembled monolayer using contact printing with a PDMS stamp and the wells are modified to have Neutravidin™ in subsequent steps. Liposomes of about 1μm diameter, with 5% Biotin lipid in the lipid bilayer, are exposed to these substrates, which results in the selective attachment of intact individual liposomes into wells by a 'Biotin-Neutravidin' interaction. We envision the use of these arrays as biosensors using membrane proteins or receptors incorporated in the lipid bilayer of the arrayed liposomes.

This thesis also describes the use of this platform to display a cell membrane ganglioside and its use in detecting the presence of a corresponding toxin. The lipid bilayer of the liposomes is modified to have 5 % monosialoganglioside GM1, which is used as an antigen and a highly selective receptor for cholera toxin. After arraying these liposomes individually into the chemically modified microwell substrates, these arrays are exposed to fluorescently tagged Cholera Toxin Subunit B to verify selective

attachment of cholera toxin to GM1 liposomes. Various control experiments involving exposure of Cholera Toxin Subunit B to chemically modified microwell substrates with no liposomes and with liposomes without GM1 receptors, are performed to show high selectivity of cholera toxin towards GM1 receptor modified liposomes arrayed on microwell substrates. Various steps involved in the protocol are confirmed using Atomic Force Microscopy, Fluorescence Microscopy, Particle Size Analysis, Zeta Potential measurements and Confocal Laser Scanning Microscopy.

Preface

Microarrays are tools for screening the binding interactions of biomolecules. In the usual design, different biomolecules are printed by fluidic dispensing from a robotic spotter into designated positions (spots), hundreds of microns in diameter, to form a spatially indexed array of probe or capture molecules. The array is exposed to an analyte solution containing a target biomolecule, which can potentially bind to one or more of the capture molecules in the array. After allowing the binding to proceed, the surface is washed and analyzed to identify the conjugation of targets; usually by labeling the targets with a fluorophore whose signature fluorescence is detected at the positions where the printed molecules have bound targets. As the size of the array spots is of the order of hundreds of microns in diameter, a chip with an active area of 1 cm x 1 cm and thousands of elements can screen a very large number of interactions with a very small volume of target analyte (approximately 1 ml to cover the active area). The high throughput, high capacity nature of the microarray tool has brought it to pre-eminence in clinical diagnostics, and drug discovery efforts. The above approach to microarraying, however, is not suitable for the display of cell membrane receptors and membrane proteins because these biomolecules require their native membrane lipid environment in order to retain their binding capacity. This problem is very important to drug discovery efforts, which usually target membrane receptors to achieve their therapeutic effect, and in which the screening of lead compounds with membrane receptors is essential in designing molecules, which bind strongly and with great specificity to the receptor. At present drug discovery research cannot take advantage of the high throughput nature of microarrays, since active membrane receptor molecules cannot simply be spotted onto the surface. Our

approach for implementing a membrane receptor microarray is to use liposomes to host the membrane receptor probes in order to retain their binding activity, and then array the liposomes onto a surface to display the receptors. This thesis outlines a strategy for arraying intact, micrometer sized unilamellar phospholipid bilayer liposomes on a surface by situating and immobilizing the liposomes individually in microwells that have been etched onto the surface in a regular pattern. Reconstituting membrane proteins in a lipid environment of intact liposomes and arraying these liposomes on a surface can prove to be a flexible platform for the development of high-density membrane protein arrays. A further advantage is that the intact liposome format can be geared toward probing membrane protein mediated transport or pore formation in vitro.

In the ongoing research, the surfaces used are microwell arrays of 1.2 μm diameter fabricated by Photolithography[1] on a silicon wafer coated with silicon oxide layer. Chapter 2 describes the microfabrication of these substrates. A flat block of Polydimethylsiloxane (PDMS) impregnated with polyethylene glycol (PEG) terminated silane is used to put down a PEG-terminal background phase using Contact Printing [2]. PEG terminated monolayers are resistant to protein/liposome adsorption. The 'bare' wells are then backfilled using amine terminal 3-Aminopropyltrimethoxysilane (APS). These amine microwells are biotinylated using NHS-PEO_4-Biotin (NPB). Next Neutravidin is attached to the Biotin islands to form patterned Neutravidin arrays capable of binding more Biotin. Chapter 2 also describes various other methods used to prepare these bifunctional substrates. Low T_g lipid formulations containing 5% biotinylated lipids are used to prepare liposomes of about 1 μm diameter using an extrusion technique. The patterned Neutravidin microwell array is then exposed to the liposome solution, which

results in attachment of intact liposomes into wells by 'Biotin-Neutravidin' interaction. The specific binding of the liposomes to the surface using the biotin-avidin linkage [3, 4], together with the resistant nature of the PEG background [5] and the physical confinement of the wells, allows the liposomes to remain intact and to not unravel, rupture, and fuse onto the surface. The size of liposomes is matched with size of the wells so that there is only one liposome attached per well. The intactness of liposomes after attachment is verified by co-localization of fluorescence signal from 'cargo' incorporated inside the liposomes, fluorescence signal from the fluorescent tag incorporated in the lipid bilayer of liposomes, and the fluorescence signal from Neutravidin grid on the surface using Confocal Laser Scanning Microscopy. Other steps involved in the protocol are confirmed using Atomic Force Microscopy, Fluorescence Microscopy, Particle Size Analysis, and Confocal Laser Scanning Microscopy. Chapter 3 covers all the experiments involved in intact arraying of liposomes.

This theses also describes various methodologies to array liposomes with different fluorescent identities on the same substrate. These methods are essential for arraying more than one membrane proteins on the same substrate and using this multi-receptor array to detect more than one ligand-receptor type of interactions in applications such as molecular screening for drug discovery. Chapter 4 describes two different methods to prepare liposome arrays with multiple fluorescent tags: mixed adsorption and sequential adsorption. Also, to show that the microarray format can indeed be used to display membrane proteins or receptors, which are biologically functional, this thesis describes the use of this platform to display a cell membrane ganglioside and its use to detect presence of corresponding toxins. The lipid bilayer of liposomes is modified to have 5 %

monosialoganglioside GM1, which is used as an antigen and a highly selective receptor for cholera toxin. After arraying these liposomes individually into the chemically modified microwell substrates, these arrays are exposed to fluorescently tagged Cholera Toxin Subunit B to verify selective attachment of cholera toxin to GM1 liposomes. These experiments show high selectivity of cholera toxin towards GM1 receptor modified liposomes arrayed on microwell substrates. In another set of experiments, liposomes with and without G_{M1} receptors were arrayed on the same substrate and exposed to fluorescently tagged toxins to show the selectivity of cholera toxin biding and hence proving the claim that this microarray format can indeed be used for molecular screening type of applications. Various steps involved in the protocol are confirmed using Atomic Force Microscopy, Fluorescence Microscopy, Particle Size Analysis, Zeta Potential measurements and Confocal Laser Scanning Microscopy. Chapter 5 describes the details in this set of experiments.

Acknowledgements

I truly thank my advisors Prof. Alexander Couzis and Prof. Charles Maldarelli for being the best mentors. They have given me the freedom and independence that nurtures original thinking and creativity, which is needed in a PhD student. They have been great friends to me both in my academic and professional life during the five years of my PhD research and I feel very proud to be a part of this wonderful research group. I thank my co-advisor, Prof. M. Lane Gilchrist for his continued hands on support during various stages of my PhD work. I also thank Prof. David Calhoun and Prof. Stavroula Sofou for providing valuable feedback and comments.

I thank my colleagues who worked with me at the City College: Anil, Ashish, Rajesh, Shyam, Manoj, Makonnen, FenFen, Jon, John, and Rohit. Also, thanks to Michael Skvarla and Rob Illic from The Cornell Nanofabrication Facility (CNF) for their valuable help in the photolithography work. Thanks to Andy, Xu and Lisa for non-academic and administrative help. I also thank all the graduate faculty members of Chemical Engineering Department at City College for their help in various academic matters. During my stay in New York as a graduate student, I made many wonderful friends and I would like to thank them all for being so helpful and fun to be around.

I dedicate this thesis to my parents, Mr. Deepak U. Kalyankar and Mrs. Sunita D. Kalyankar. It is the result of their enduring and continuous efforts, love and support that I have been able to undertake this task and do justice to it. They gave me the freedom to choose my career path and always encouraged me to achieve higher and higher goals in life. I also thank my sister Ms. Ashwini D. Kalyankar for her affection and support.

Contents

List of Tables

Chapter 3

List of Figures

Chapter 1

Chapter 2

Chapter 3

Chapter 6

Chapter 1:

Introduction and Literature Survey

1.1 Motivation for membrane protein or receptor arrays:

Membrane protein is a protein molecule that is attached to, or associated with the membrane of a cell or an organelle. Membrane proteins can be classified into two groups: 'integral membrane proteins' which are firmly attached to the membrane and 'peripheral membrane proteins' which are attached to integral membrane proteins by non-covalent interaction, usually by electrostatic bonds. Figure 1.1 shows schematic diagrams for both types of membrane proteins.

Many of the interactions studied in the biological and biomedical sciences occur with receptors at membrane surfaces. Prominent examples are neurotransmitters, cytokine receptors, tyrosine kinase receptors, ligand-and voltage-gated ion channels, G protein-coupled receptors, and antibody receptors. Interactions with these receptors are of special importance not only to academics, but also to the pharmaceutical industry as almost half of the 100 best-selling drugs on the market are targeted to a membrane receptor. [6, 7]. More than 50% of current drug targets are membrane-bound [8]. Naturally, there is a great interest in development of sensors using membrane proteins for drug discovery and high-throughput screening for detection of pathogens/toxins.

1.2 Various approaches for development of membrane protein based sensors:

The main problem associated with the use of membrane proteins for bio-detection is their strict requirement for the cellular membrane environment to stay biologically active and to protect their structural integrity. Whole-cell-based approaches are popular for studying the function and dynamic targeting of molecules/ligands to membrane-bound targets; but because of the complexity of cellular networks and interactions [8], it is difficult to unambiguously ascertain the target compound binding. Most techniques for

detailed kinetic analysis of molecular recognition events are applied in solution phase using a truncated, soluble form of the receptor. Membrane receptors, however, possess significant hydrophobic domains and are likely to have different tertiary structures and binding affinities in solution relative to those occurring in a membrane environment. Hence this type of approach is limited to receptors containing a single trans-membrane domain, does not allow the study of signaling cascades triggered by ligand binding to a receptor, nor the investigation of complex membrane proteins which often homo-or hetero-dimerize or oligomerize [6]. Hence artificial lipid membranes tailored for specific applications for various membrane proteins/receptors is an attractive option to develop these sensors. These membranes are available in the form of liposomes, which are spherical particles in an aqueous (water) medium (eg, inside a cell) formed by a lipid bilayer enclosing an aqueous compartment (Figure 1.2). Liposomes can be tailored to have various surface properties and functionalities such as charge, receptors etc. Various studies report techniques to reconstitute membrane proteins and receptors in the lipid bilayer of liposomes [9-11].

There are two main approaches discussed in literature for development of membrane protein based sensors using artificial membranes.

1.2.1 Use of solid supported artificial membranes:

This approach involves use of membranes on solid supports called supported planar phospholipids bilayer (SPB) [12-24]. SPBs are formed when liposomes are adsorbed onto hydrophilic surfaces such as glass or silicon oxide after their fusion (see figure 1.3). A hypothetical course of interaction in between the solid substrate and the liposome may result in: (1) vesicle approach and adhesion to the surface; (2) vesicle

fusion or rupture; and (3) lateral spreading to form supported bilayers [25-27]. Biosensors and screening assays based on solid supported membranes have been described in many studies [28-31]**.** The transient formation and regulation of protein complexes both at intracellular and extracellular sides of the cell membrane are difficult to reproduce using solid supported membranes because of the presence of solid phase on one side of the membrane. This drawback limits the use of SPBs for bio-detection using membrane proteins. There are several other limitations of this approach. The proximity of membrane proteins to a solid surface may lead to structural changes and hence, a loss in biological function. It is proven in literature that the mobility of lipid bilayers reduces substantially in contact with a solid support [32]. This may lead to reduction/loss in biological function in case of membrane proteins/receptors incorporated in the supported bilayer, because in certain applications, more than one receptors/proteins have to form aggregates for the binding to occur [33]. Also signaling in cells consists of a series of exquisitely coordinated binding events and enzymatic transformations beginning at the cell surface and ending in the nucleus, with built-in feedback to appropriately terminate the signaling cascade. The SPBs cannot be implemented to mimic this process.

1.2.2 Use of intact liposomes adsorbed on a substrate:

This approach involves use of intact liposomes arrayed on various substrates to display membrane proteins/receptors. Since liposomes mimic cells in their membrane structure, their intactness provides an ability to reproduce both intracellular and extracellular sides of the cell membrane. Intact liposomes have been successfully attached to a surface using a strategy in which the surface is chemically functionalized to

present two chemistries, one to prevent adsorption and unraveling of liposomes (as shown in figure 1.3) and one to anchor the liposomes to the surface. In this strategy, the surface is modified uniformly with a passivating chemistry that is designed to block the nonspecific adsorption of lipids, liposomes, and proteins (e.g., passivation with SPBs and HBMs, [34, 35] bovine serum albumin (BSA), [36] poly(ethylene glycol) (PEG) coatings including grafted PEG polymers [37, 38] or poly(L-lysine)-poly(ethylene glycol) copolymers (PLL-*g*-PEG) [39-41] and PEG oligomers attached to a surface using SAMs. [42-45] The matrix of the passivating layer is functionalized with chemical groups designed to couple to binding partners localized on the liposome exterior. Liposomes are brought to the surface and attach only at the anchoring points of the second functionality and are prevented from rupturing and fusing by the surrounding passivating layer. To bind the liposome to the surface, early studies used antibody coupling [46] or disulfide linkages, [47] but recent techniques have used one of two methods. In the first, [48-51] ssDNA is attached to the surface of the liposomes (usually by covalent binding to the lipid headgroups of the bilayer) with the strands extending out from the liposome surface. A surface is prepared that consists of an SPB, and DNA strands complimentary to those extending from the liposome are attached to the bilayer by covalent linkages to the headgroups or to molecules (e.g., cholesterol) that embed themselves inside the bilayer. The liposomes are then attached to the surface by hybridization to form a double-stranded tether; because the surface bilayer is mobile, the tethered liposomes can laterally translate over the surface. In the second method, [52, 53] the receptor-ligand pair biotin-streptavidin is used to link the liposome to the surface. Streptavidin-biotin coupling proceeds by conjugating biotin to the headgroup of a phospholipid and incorporating this

lipid in a few percent mole fraction into the liposome. A passivated surface is prepared and biotinylated, linked with streptavidin, and then conjugated to the liposomes with biotin on its surface. (See refs [47] and [48] using HBMs and SPBs, respectively, as passivating layers, refs [54] and [55] using a poly-(ethylenimine) background, and refs [56] and [57] using avidin or BSA as the background.) By examining the surface using principally a quartz crystal microbalance, scanning force microscopy, and fluorescence techniques, these studies found the attached liposomes to be intact.

Platforms for the large-scale micro arraying of different liposomes were fabricated using photolithography to etch square 50 μm X 50 μm wells in glass, with the wells arranged in a checkerboard pattern. [58] Direct pipetting of picoliter solutions of liposomes into the wells formed SPBs on the well floors; this platform can then be used to pipet and tether proteoliposomes in the wells to form SPBs with embedded membrane protein or tether liposomes to previously assembled SPBs using DNA tethering. (46) Similarly, Boxer et al. ([44], [45],[59-64]) used microcontact-printing to assemble a square grid of fibronectin (100μm X 100μm) on a glass coverslip. In a microfluidic cell, adjoining stream of two liposome solutions, with each solution containing liposomes with the same ssDNA tether (although the two liposome solutions had different tethers), were passed in a parallel flow over the coverslip to fill in the bare square grid with SPBs. The two-stream microfluidic flow patterned the squares of the grid with SPBs, with squares in a row completely underneath one or the other stream forming an SPB with only that stream's tether while some squares underneath the interface where the stream join forming SPBs with a mixture of tethers. The fibronectin grids resist adsorption and function as barriers between the square domains. The patterned surface was then exposed

to a solution of liposomes. Each liposome had on its surface strands of DNA complementary to one of the two types of strands extending from the SPB surface squares. The liposomes hybridize to the complementary strands extending from the surface, forming two rows of squares with a single type of liposome and DNA strand and separated by a row of squares with a mixture of the two kinds of liposomes. Similarly, another study, [65] using photolithography, fabricated a matrix of square regions (200μm X 200 μm) consisting of a biotinylated PLL-*g*-PEG polymer grafted to the surface. DNA tethers were attached to these regions by streptavidin-biotin binding, and the squares were surrounded by a passivating layer of PLL-*g*-PEG. Liposomes with complementary strands of DNA were linked to the tethers in the square regions to create a liposome array displaying one kind of liposome.

Individual liposomes have been arrayed using two methods. In the first approach, a square array of micrometer-sized dots of BSA conjugated to biotin was microcontact printed onto a glass surface, and the remainder of the surface was then backfilled with BSA. [66] Surface biotinylated liposomes on the order of 100 nm in diameter were coupled from liposome solutions to the dots by streptavidin with approximately one liposome to an island under very dilute conditions. In a different approach, [67] photolithography was used to pattern a silicon oxide surface with a square array of TiO2 nanopillars approximately 100 nm in diameter. The surface of the pillars was biotinylated while the surroundings were passivated with PLL-*g*-PEG; biotinylated liposomes were then bound onto the pillars with streptavidin to array the liposomes individually.

1.3 Introduction to our approach for arraying of intact liposomes:

In this study, we provide a novel format (Figure 1.4) for arraying individual

liposomes with membrane proteins/receptors by situating micrometer-sized liposomes individually in wells (with diameters of the same order as the diameter of the liposomes). The wells are inscribed on a silicon oxide surface in a square pattern by using photolithography techniques. The area surrounding the wells is passivated using a self-assembled monolayer (SAM) of a PEG oligomer. The interior of the wells is functionalized with an amine SAM that allows conjugation to biotin. Biotinylated liposomes are then linked to the well interiors using avidin as a linker molecule. The size of liposomes matches the size of wells, so that there is only one liposome attached per well. We use confocal laser scanning microscopy to verify a one-to-one placement of the liposomes in the wells and to establish that they remain intact. Recessing the liposomes in wells rather than openly displaying them on tethers has the advantage that it further isolates the liposomes from each other, preventing fusion. Liposomes also tend to conform to the shape and size of the wells to maximize binding interactions of biotin-avidin linkage preventing further attachments.

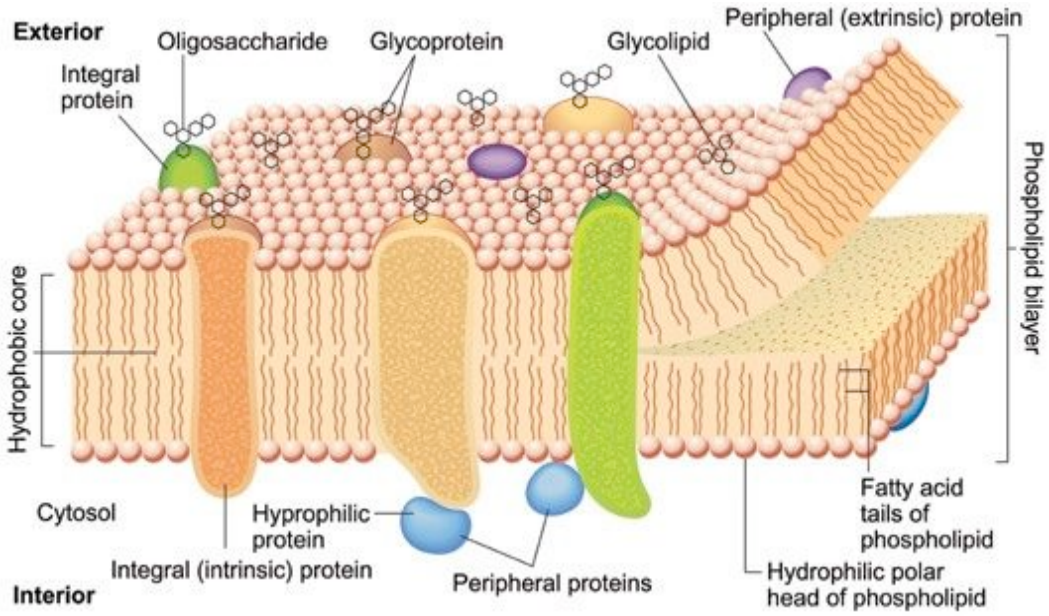

Figure 1.1: Types of membrane proteins.

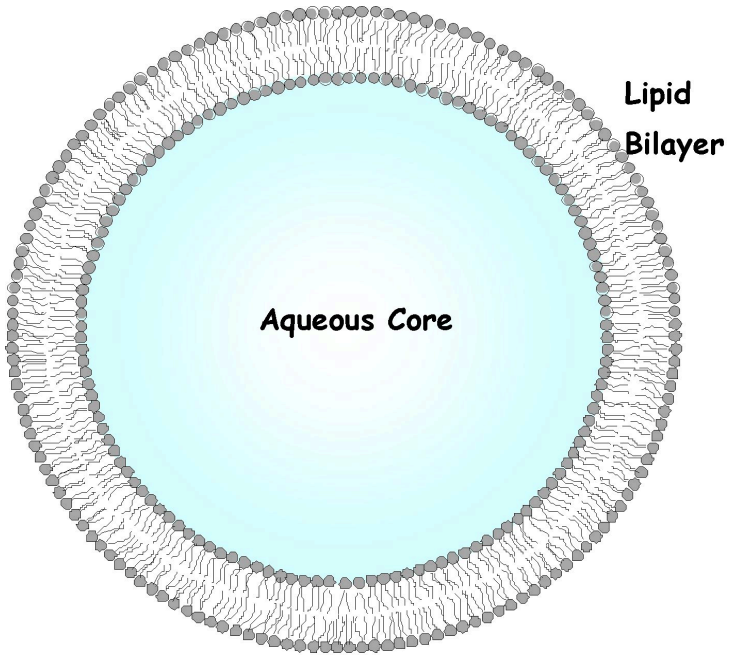

Figure 1.2: Schematic of a liposome.

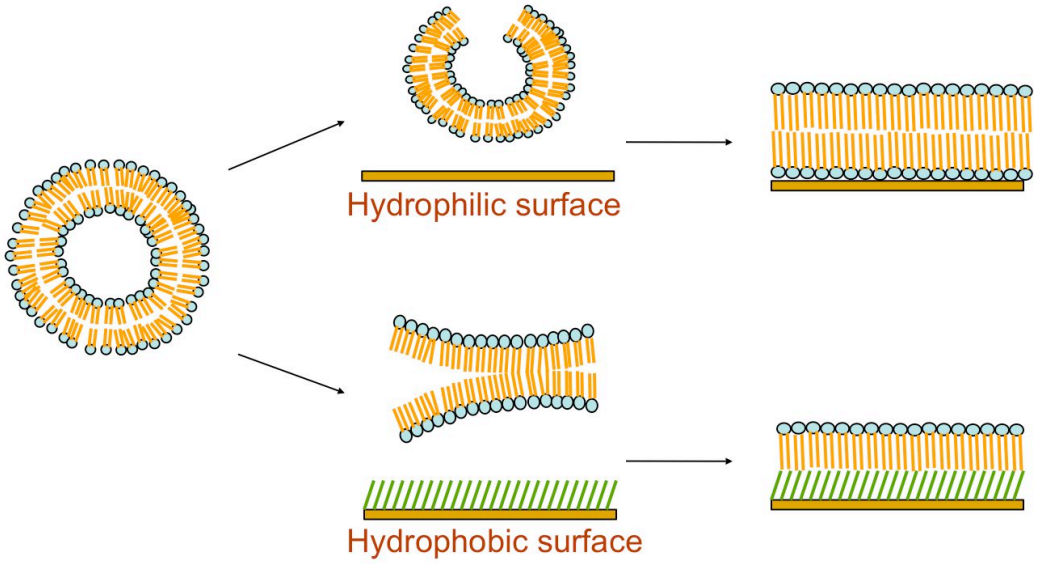

(a)

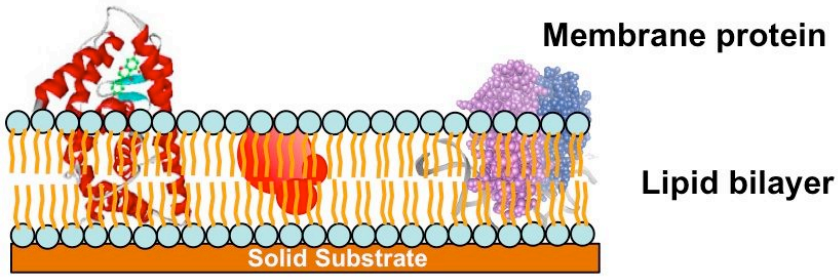

(b)

Figure 1.3: (a) Unraveling of liposomes to form supported lipid bilayers on hydrophilic surfaces and supported lipid monolayers on hydrophobic surfaces.
(b) use of SPBs for displaying membrane proteins

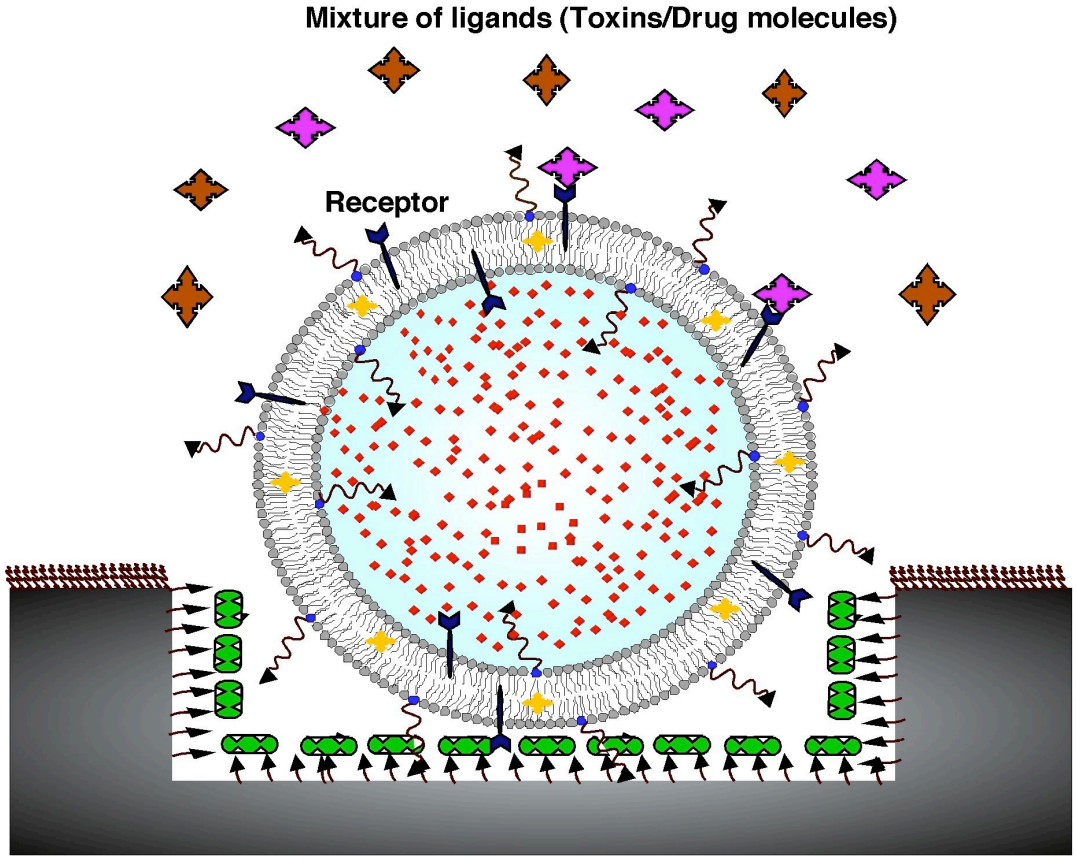

Figure 1.4: Project concept drawing.

Chapter 2

Preparation of bi-functional substrates for the liposome arrays

2.1 Need for a bi-functional substrate:

Liposomes with membrane proteins need to be arrayed on a substrate in intact form for them to be used for sensing applications. Ideally a substrate with attractive regions to attach intact liposomes surrounded by a region resistant to liposome attachment and unraveling is desirable. This need lead us to search Self Assembled Monolayers (SAMs) literature [68-73]. SAMs are formed by surfactant molecules, which adsorb on the surface, and dangle terminal functional groups off of the surface to provide desired functionality. A bi-functional SAM with active micron sized regions useful to attract liposomes in the background of a repulsive phase, which doesn't let them unravel/attach is needed. One of the objectives of this research work is to have only one liposome attached per active site so that the array is easily quantifiable. Hence the size of an active site should match the size of liposomes (around 1 micrometer).

There are several ways to form micron scale bi-functional SAMs; dip-pen nanolithography [74], nanoshaving [75], photochemical lithography[76, 77], phase separation [78] etc. to name a few. Most of these techniques are serial techniques in which each active region is generated one by one. These techniques cannot be scaled up for commercial production. Phase separation based methods [78] [79] such as co-adsorption/sequential adsorption of SAMs don't have a good handle to control the size and density of active regions. Hence we chose microcontact printing [2, 80] to fabricate substrates with bi-functional SAMs.

2.2 Introduction to Microcontact Printing:

Micro-contact printing (μCP) is a parallel pattern transfer technique in which a polymeric stamp with the positive of the pattern is used to transfer surfactants/molecules only in selected region of the substrate by conformal contact in between the stamp features and the substrate (See figure 2.1). Typically, polydimethylsiloxane (PDMS) stamps inscribed with a positive of the desired surface pattern are formed by pouring the uncured liquid polymer over silica or PMMA substrate with a negative of the desired pattern (master), and cured until the polymer gets stiff and achieves desired material properties. The PDMS stamp is then carefully peeled from the master to form a positive relief, and then the relief is inked using a SAM amphiphile to be printed on the substrate. The 'ink' is a solution of amphiphile (few mM in concentration) in a suitable solvent. Typical amphiphiles are alkyl silanes, which are printed on silica substrates and alkyl thiols, which are printed on gold/silver/copper substrates[80]. The inked stamp is then carefully placed onto the substrate, and pattern transfer occurs by physical contact between the stamp features and the substrate. The process is one of 'conformal contact' as the stamp is not pressed against the surface of the substrate as in a conventional printing processes; rather it contacts the surface in such a way that the only pressure experienced by the stamp is due to interfacial forces [2] and by its own weight. The PDMS deformability allows the stamp to conform to the irregularities in surface smoothness of the substrate surface. PDMS is chosen as the stamp material because of its easy commercial availability, its dense sponge-like nature which allows it to take up liquid (ink) only at the surface, its non adherence to fluorinated silica or PMMA masters enabling easy peeling, its excellent structural replication and its stiffness (the Young's

modulus Y is equal to 5 Mpa) which provides ease of handling during printing [2]. Once the first SAM is printed in a definite pattern onto the substrate, the rest of the 'bare' substrate can be backfilled using another amphiphile to form a bi-functional patterned SAM.

Advantages of μCP over other methods mentioned earlier in section 2.1 are:

(i) It is a 'parallel technique' of pattern transfer i.e. all the features of the pattern transfer simultaneously. Consequently, it can be easily be integrated to an industry level process.

(ii) It doesn't need clean room environments and demanding protocols.

(iii) It doesn't need sophisticated equipment; hence it is cost effective.

(iv) The stamp, once fabricated, can be reused many times [81].

(v) Any desired micro-pattern can be printed. The pattern transfer is not subject to diffraction limitation. The minimum feature size obtained using μCP is of the order of a few 10nm.[82, 83]

(vi) The process can be optimized to have precise control over island size and their surface distribution.

(vii) μCP can be used to print submicron features on curved substrates as well. [84]

The aspect ratio (the ratio of width to the height of features) of features on the stamp should be around 0.5 to 2 for better printing results [85]. This is important so that there would not be significant distortion of the features during stamping, which leads to blurred boundaries and feature broadening in the stamped monolayer because of non-contact ways of ink transfer[86]. Higher aspect ratio features (>1) on masters lead to distorted features (sagging) on the stamp because of their inability to withstand stresses associated

with inking and interfacial contact between the stamp and substrate during printing. Below an aspect ratio 0.5, significant transport occurs from areas in-between raised regions in the stamp, causing blurring of the desired pattern **.** Also features of aspect ratio less than 0.5 fall under its own weight [85].

2.3 Fabrication of microwell patterned substrates (masters) using photolithography:

The masters used in the stamp-making step of μCP are generally Si/SiO_2 substrates patterned using photolithography and different etching techniques [87]. The diffraction limitation of the photolithography step places a limit on the minimum feature size on masters that can be obtained as around 200 nm (using deep UV photolithography). We need features of around 1 micron size; hence photolithography is a technique of choice. A typical stamp to transfer islands of 1 micron diameter on a substrate would have pillars with about 1 micron X-section diameter and aspect ratio of 0.5–2 (as discussed in section 2.1). Hence the masters should have wells of similar dimensions. These masters were fabricated using photolithography at *The Cornell Nanoscale Science and Technology Facility (CNF)*, Ithaca, New York.

Following are various steps involved in fabrication of the masters:

2.3.1 Mask Fabrication:

The first step in the mask fabrication is to have a CAD (Computer Adapted Design) of the mask features with all the dimensions (pitch and diameter of wells) specified. The dimensions on the mask are decided based on the type of exposure used in the UV exposure step. We planned to use a stepper for UV exposure with a 5X size reduction. The desired master was supposed to have 1 micron diameter wells spaced 3

microns apart (center to center) on a total effective area of 25 sq mm (5mm X 5mm). So on the mask, the well diameter was specified as 5 microns with a pitch of 15 microns with an effective area of 25 mm X 25mm. The CAD file is then converted into a pixel data file readable on the He-Cd laser-writer Heidelberg DWL 66, which operates at 442 nm. Readily available non-patterned photomasks (a rectangular thin glass plate coated with few micron thick chrome layer with a few 100nm thick positive photoresist layer at the top) were exposed under the laser writer to write a pattern onto the positive photoresist layer. The positive resist depolymerizes upon exposure to the focused laser beam forming acid in the exposed regions on the mask. Alkaline developer solution was used to remove the exposed depolymerized regions on the photoresist layer to get a patterned resist. The mask was then exposed to CR-14 chrome etch solution to transfer the pattern into the chrome layer underneath the developed resist. The remaining photoresist was then striped in a series of resist strip baths containing acetone and isopropanol. The final mask obtained in this step is as shown in Fig 2.3.

2.3.2 Spin coating of photoresist onto an atomically smooth SiO_2/Si surface:

Atomically smooth silicon wafers with a thermally grown oxide layer of about 1 micron were used for fabrication of masters. The oxide layer facilitates further surface modifications using silane chemistry. A positive photoresist (Shipley 1813, Diazonapthoquinone based) was chosen for the application based on charts available for usage of different substrates in photolithography. The thickness of the resist was chosen based on relative etch rates of the resist and the substrate in the final etching step. This is important to make sure that complete resist thickness will not get reacted before the etching reaches the desired depth in the substrate. The speed of rotation of the spin

processor was chosen using thickness-rpm curves for the resist. Application of 'Primer' onto the wafer before resist coating helps in better binding of the photoresist onto the wafer. One method uses liquid P-20 primer (20% HMDS) and an alternative for even better binding properties is vapor prime in which the wafer is kept in an oven for half an hour and exposed to HMDS (Hexa Methyl Di Silazane) vapors. After application of the primer, the wafer was centered on the vacuum chuck of the spin processor precisely. Failure to center the wafer on the chuck leads to non-homogeneous coated resist thickness. The photoresist was dispensed at the center of the wafer and the spin processor was rotated for about 30 seconds. The change in reflectivity of the wafer with time can be noticed while spinning the wafer and finally it shows a uniform color, which is an indication of uniform thickness of the photoresist on the wafer. The wafer was post baked to remove excess solvent on a hot plate at 115C for one min and was checked for thickness at different locations using ellipsometer. After cooling, the wafers were placed with great care in secured enclosures away from light.

2.3.3 Alignment and exposure to UV light through photo-mask using 5X steppers:

There are two 5X steppers for exposure to UV light through the mask at CNF, GCA Autostep i-line (365nm) 5X stepper and GCA g-line (436nm) 5X stepper. The i-line stepper can be used down to feature sizes of 0.5 microns and g-line stepper gives good features down to 0.9 microns. The mask was loaded into the previously decided stepper. A resist coated test wafer was also loaded into the stepper. The number of active regions was decided by area and spacing calculations. Eg. a 4-inch diameter wafer with a 1 cm gap in between active regions can produce 48 squares of 25 sqmm. The number of active regions was also decided based on ease of cutting the wafer later on. The test wafer was

exposed to UV light through the mask by varying the exposure time and focus (angle) along rows and columns. The UV exposure causes the photoresist to depolymerize forming indene carboxylic acid at regions of exposure. The wafer was developed in the developer (alkaline solution, Shipley 300MIF). The wells formed on the photoresist layer on different active regions after development were checked using a microscope and the best exposure settings were decided by visual observation. The exposure settings were narrowed close to optimum so as to get the best features on at least a few of the active regions on each wafer. After developing the wafer using the alkaline developer Shipley 300MIF, it was baked using the hotplate for 1 min at 115C. This step is optional and it helps in better resist adhesion to the wafer for the next RIE step. But this step also makes it difficult to remove the resist after the RIE step.

2.3.4 Etching into the substrate using Reactive Ion Etcher (RIE):

RIE gas was chosen on the basis of type of etch needed (SF_6 : Isotropic etch, CF_4, CHF_3 : Non-isotropic etch for silicon oxide surface). CHF_3 was chosen based on the need to have as vertical walls of wells as possible. There are three RIE systems mostly used for etching into SiO_2/Si substrate: Plasma Therm (PT-72) RIE system, Applied Materials Research RIE system and Oxford 100 RIE system. Each RIE has different pre-studied recipes for various substrates and itching chemistry combinations. The most suitable recipe was chosen based on the substrate type and the desired type of etching. Recipes differ in operating pressures, gas, purge cycles, etch rate etc. The time of exposure was decided based on the pre-determined etch rate for the particular recipe. It was found that it differs considerably in real from the pre-determined etch rate. A 33% lowering of actual etch rate was observed as compared to the pre-determined etch rate using AFM

analysis of test wafers after RIE step and resist strip. This can be attributed to fluctuations in vacuum levels during the RIE operation. The wafer was put in the RIE system. It was centered and supported using glass chips from all the sides to prevent it from sliding. The standard operating procedure was used to carry out the etching operation. RIE step yielded wafers with active regions having patterns transferred into the substrate as desired. The next step was to remove undesired photoresist material on the wafer.

2.3.5 Resist strip:

The photoresist remaining on the wafer after RIE step can be removed by using two methods:

1. Dissolution into organic solvent baths of acetone and isopropanol.
2. Oxidation of the organic photoresist in aura 1000 plasma stripper.

In all cases, the later technique was used because of its ease of handling multiple wafers and resist removal rates at 2.8 microns per minute.

2.3.6 Cutting of the wafers for separating the active regions:

There are two ways to cut the wafers for separation of active regions: Using diamond cutter or using the K&S 7100 dicing saw. The later method gives better cuts with uniform size of each active region. The wafer was coated with photoresist in order to avoid the deposition of particulate matter on the active regions during cutting. It was then laminated using a thin polymer film and cut along rows and columns using the dicing saw. The active regions can be then taken out of the polymer film one by one and the resist layer can be removed by sonication in acetone and isopropanol sequentially for a few minutes. Figure 2.4 shows an image of a laminated wafer cut using dicing saw.

Figure 2.5 shows AFM images of the SiO_2/Si masters obtained using the techniques described above. These masters yield stamps with pillars of similar dimensions as wells. The stamps thus fabricated, can be used to print island phase of silane SAMs on silicon wafers using μCP technique.

2.4 Passivation (fluorination) of Si/SiO_2 masters:

One of the most important aspects of fabrication of Polydimethylsiloxane (PDMS) stamps with well-defined features is the separation of the stamp from the patterned Si/SiO_2 master. This separation process should take place with least peel off stresses. The ease of separation between any two surfaces is governed by the work of adhesion, which is defined as the work required to separate reversibly the interface between two bulk phases from their equilibrium separation to infinity. (See fig 2.6)

$$W_{adh} = \gamma_\alpha + \gamma_\beta - \gamma_{\alpha\beta} \qquad (1.1)$$

where,

W_{adh} = Work of adhesion γ_α = Surface tension of phase α,

γ_β = Surface tension of phase β $\gamma_{\alpha\beta}$ = Interfacial tension between phases α and β

This is the famous ***Dupre Equation*** formulated in 1869. An alternate way to define work of adhesion is to term it as the Gibbs free energy reduction per unit area when an interface is formed in between two individual surfaces.

For effective separation of PDMS stamp from the master, the work of adhesion between them should be as small as possible. Surface tension values of PDMS and silica at 20^0C are 19.8 dyne/cm *(*Wu [88], table 3.7, pg 88) and 78dyne/cm (Hiemenez [89], Table 6.4, pg.291*)* respectively. The interfacial tension can be calculated using Good and Girifalco equation as follows [88]:

$$\gamma_{\alpha\beta} = 2\Phi\sqrt{(\gamma_\alpha \gamma_\beta)} \qquad (1.2)$$

Assuming the parameter Φ to be 1 (the Fowkes approximation to Good-Girifalco equation [89]), for the PDMS-silica system, the work of adhesion value is 19.21 dyne/cm. To reduce this work of adhesion value further, the micropatterned silica surface was fluorinated using a monolayer of a fluorosilane (heptadecafluoro 1,1,2,2 tetrahydrodecyl) trichlorosilane)[86] .The interfacial tension value for the fluorinated surface is 12 dyne/cm. The work of adhesion for silica-fluorine system is 0.97 dyne/cm. Thus fluorination of silica surface reduces the work of adhesion value between the PDMS stamp and the silica master 20 fold. This helps in easy peel off of the PDMS stamp from the master.

Figure 2.7 shows the water contact angle data for different fluorination experiments carried out on cleaned silicon substrates at 4.5^{o}C using chloroform as solvent. It shows that the hydrophobicity of silicon substrates increases with increase in deposition time at all the concentrations. Figure 2.8 is the AFM image of the sample with 0.5mM concentration taken after 1 hr of deposition time. It shows complete coverage without multilayer formation. Thus the optimum protocol for fluorination of master involves using 0.5 mM fluorosilane for 60 min in chloroform as a solvent. This helps in making surface highly hydrophobic, with complete coverage by fluorine terminal SAM and gives the least possible work of adhesion with PDMS.

2.5 Fabrication of the PDMS stamps:

Sylgard 184 silicone elastomer kit by Dow Corning company is used as the raw material for fabrication of polydimethylsiloxane (PDMS) stamps. Sylgard 184 comes in two parts: base solution, which is a PDMS oligomer, and a curing agent, which is the catalyst to crosslink the oligomer to form a PDMS network. The structural formula of PDMS is given in the figure.

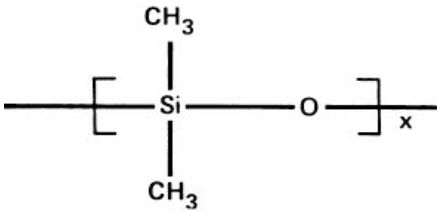

PDMS structural formula

The base solution is highly viscous (viscosity = 3900 mPa-sec). Hence, it is mixed with the curing agent in 10:1 volumetric proportion using a mechanical stirrer for about 3 minutes. After homogenous mixing of curing agent with the base solution, it is poured over passivated masters kept in a passivated glass petridish to form a 1 cm thick layer of uncured PDMS over the masters. The biker used for mixing sylgard 184 is also pre-passivated so that the remaining PDMS can be easily removed before use the next time. During mixing and pouring of the elastomer solution, air bubbles get entrapped in the uncured polymer. The Petri dish containing the masters and the uncured PDMS is then placed in a Branson 5200 Sonicator and sonicated for about 30 min to remove majority of the bubbles from the polymer solution. A degassing step is needed since any bubbles tend to migrate towards highly hydrophobic master surfaces or the surface of the passivated Petri dish, causing defects in the fabricated stamps. Typical curing time as given in the sylgard 184 data sheet is about 48 hr at room temperature. Hence no substantial curing

occurs during the degassing process. After degassing the solution, the petri dish is kept in a Precision Economy oven set at 60^{o} C for 18 hr for curing. During this step, the oligomer undergoes crosslinking and forms a network of PDMS giving it stiffness (Y= 5Mpa [2]). The petri dish is then taken out of the oven and allowed to cool. A steel knife is used to remove a PDMS disk from the glass petri dish since the entire glass dish is also fluorinated. During stamp making, the uncured polymer solution also goes below the fluorinated masters. Hence, the masters also come out while removing the PDMS disc. The same knife is used to carefully remove the PDMS thin film behind masters and masters are then easily removed by holding its edges using a sample holder. These masters can then be reused for the next batch of PDMS stamps. Figure 2.9 shows a PDMS disk of about 1 cm thick with 6 active regions; each approximately 8mmX8mm. These active regions are carefully cut and their opposite sides are marked to avoid confusion about the active region. These are then used as stamps for μCP.

Figure 2.10 show AFM images of a stamp fabricated from the microfabricated CNF masters. The pillars in the stamp correspond to holes in the original master. The stamps are rounded at the top of the features, which can be related to stresses during cross-linking process. The depth of features is around 450 nm and the width of stamps at the top is around 1.3 microns, which indicates there is a slight feature broadening after the stamp is peeled off from the master. This feature broadening can be attributed to release of the stresses in bulk of the PDMS after its peeling from the substrate surface. These stamp images clearly indicate the great deal of accuracy with which features can be replicated in PDMS at micro-scale.

2.6 Fabrication of bi-functional substrate for liposome arraying:

Two approaches are used to prepare bi-functional substrates for arraying intact liposomes individually on substrates:

1. Use of microcontact printing and surface chemistry modifications to prepare a planar bi-functional substrate.
2. Modification of microwell surface (master) to incorporate liposome-attractive functionality in the wells surrounded by an inert and liposome-resistive functionality in the plane of the substrate.

The later approach was developed because of some shortcomings in the first approach as discussed in chapter 3**.** The interaction with which liposomes are attached to active sites is well-known 'avidin-biotin' interaction. The active sites have avidin functionality and the surrounding region is polyethyleneglycol (PEG) terminated self-assembled monolayer (SAM). Liposomes are modified to have biotin functionality on their surfaces and hence, they can be selectively attached to the avidin active sites on the substrate.

The avidin functionality is introduced in the active sites using a three-step process:

1. Introduction of amine terminal functionality at the active sites.
2. Modification of amine functionality using NHS-PEO_4-Biotin to have biotin terminal active sites.
3. Modification using Neutravidin (a tetrameric protein with 4 active sites for biotin) to have avidin-terminal active sites.

2.6.1 Use of microcontact printing to prepare planar bi-functional substrates:

a. Preparation of substrate:

Polished silicon wafers were cut in approximately 7mm X 7mm size and cleaned by sonicating (Branson 5200 at 40 KHz**)** in a mixture of Nochromix and 98% sulfuric acid for about 30 min, followed by sonication in DI water for 30 min. They were then dried in a stream of nitrogen.

b. Microcontact printing:

The protocol used for microcontact printing is 'contact inking'[82, 87] as shown in Figure 2.11. In this method, flat PDMS sheets are fabricated by following the standard stamp fabrication protocol using fluorinated flat silicon chips as masters. These flat PDMS sheets are dipped in the ink solution (3-aminopropyltrimethoxysilane, APS, 5mM in Chloroform) for about 2 hrs, dried under nitrogen and used as a stamp pad to ink the previously cleaned stamp prepared using protocol as described in section 2.4. The stamp is kept onto the flat PDMS block impregnated with ink for 30 seconds, separated and dried for 15 seconds and kept onto the cleaned substrate for printing for 30 seconds. APS gets transferred only in the contact regions between stamp and the substrate. Use of contact inking minimizes feature broadening, and reduces non-contact modes of ink transfer**.** Figure 2.12 shows AFM images of a silicon substrate modified using microcontact printing. The average height of the features is 6Å, which corresponds to height of APS SAM deposited from solution.

c. Surface chemistry modifications of the substrate:

Next step after amine island micro-contact printing is their modification into biotin islands. The micro-patterned surfaces with amine islands are dipped in 15ml of 1mM

sodium hydroxide solution to deprotonate the amine terminal functional groups. They are then exposed to 2 ml of a 1mg/ml solution of NHS-PEO_4-Biotin in a filtered (0.2 μm pore size membrane) phosphate buffer solution of pH 10 for 1 hr. In this step, NPB reacts with primary amine group giving it a PEO_4-Biotin tether and NHS gets released. Figure 2.13 shows AFM height image in which the height of the islands has substantially increased (40 Å) because of the added PEO_4 – Biotin tether. They were then thoroughly washed with DI water, dried and dipped in 15 ml of PEG-silane (2-[methoxy(polyethyleneoxy) propyl]trimethoxysilane, 0.5 mM in chloroform) solution for 1 hr. Background of the biotin islands on the substrate now have a polyethylene glycol (PEG) terminal SAM which is resistant to protein/lipid/liposome adsorption**.** The substrates are then washed with DI water, dried using a stream of nitrogen and then dipped in 2 ml of a Neutravidin®-FITC solution (filtered using 0.2 μm pore size membrane) of 40 μg/ml concentration in a phosphate buffer of pH 10 for 1 hr. The substrates are then cleaned using buffer to remove unattached Neutravidin® and stored in a phosphate buffer solution of pH 10. Figure 2.14 shows confocal laser scanning microscopy images of a planar silicon substrate with Neutravidin-FITC islands. This image clearly indicates that Neutravidin-FITC is only present in the printed regions. Neutravidin, being a protein, doesn't attach to PEG-silane SAM in the background of biotin islands. Thus using this protocol, bi-functional substrates with Neutravidin islands in the background of PEG-silane SAM can be prepared. Figure 2.15 shows a schematic representation of the entire protocol. Confocal laser scanning microscopy (CLSM) is used to image the fluorescently labeled substrates and liposomes using the Leica TCS SP2 AOBS confocal microscope. This CLSM is equipped with an acousto-optical beam splitter and a prism

spectrophotometer detector, which negates the need for dichroic mirrors and bandpass, filters, furthermore, this microscope is based on a single pinhole design that ensures accurate co-localization over the entire visible range. All images were acquired using an 8-bit pixel depth setting.

2.6.2 Use of microwell patterned substrate (master) to prepare a bi-functional surface:

Because of problems associated with arraying liposomes on bi-functional surfaces fabricated using protocol 2.6.1, we developed a new protocol using the microwell-patterned substrates.

a. Preparation of substrate:

The microwell patterned substrates are cleaned using Nochromix® and sulfuric acid in a Branson 5200 sonicator for 30 min followed by sonication (40 KHz) with DI water for 30 min and drying under a stream of nitrogen. The surfaces are then imaged under a Nanoscope III (Veeco Instruments, Inc) atomic force microscope (AFM) in contact mode in air using silicon nitride tips with a force constant of 0.58 N/m (see fig 2.5).

b. Contact printing:

Polished silicon wafers are cut in approximately 7mm X 7mm size and cleaned by sonicating (Branson 5200 at 40 KHz) in a mixture of Nochromix and 98% sulfuric acid for about 30 min, followed by sonication in DI water for 30 min. They are then dried in a stream of nitrogen and exposed to 15ml of 0.5 mM fluorosilane solution in chloroform for 1 hr, rinsed with pure chloroform and dried. Highly viscous polydimethylsiloxane (PDMS, Sylgard® 184, DuPont) is mixed with the curing agent, poured onto these flat

surfaces and cured overnight at 60 ^{0}C. Flat blocks of PDMS are then peeled off of the surfaces after being cooled to room temperature. These blocks are cleaned using chloroform, dried in a stream of nitrogen and impregnated with a 15ml PEG-silane solution of 1mM concentration in chloroform for 2 hr to make stamp pads. These stamp pads are dried under a stream of nitrogen and used for printing via conformal contact on the micropatterned surfaces for 3 minutes. Thus, PEG-silane gets transferred onto the plane of the micropatterned surfaces leaving the wells uncoated.

c. Surface chemistry modifications of the substrate:

The micropatterned surfaces are then immediately dipped into 15ml of 5mM APS solution in chloroform for 30 minutes, rinsed with chloroform and dried. This step coats wells with APS SAM giving them primary-amine functionality. The micropatterned surfaces with amine wells are then dipped in 15ml of 1mM sodium hydroxide solution to deprotonate the amine terminal functional groups. They are then exposed to 2 ml of a 1mg/ml solution of NHS-PEO_4-Biotin in a filtered (0.2 μm pore size membrane) phosphate buffer solution of pH 10 for 1 hr. They are then thoroughly washed with DI water, dried and dipped in 2 ml of a Neutravidin®-FITC solution (filtered using 0.2 μm membrane) of 40 μg/ml concentration in a phosphate buffer of pH 10 for 1 hr. The micropatterned surfaces are then cleaned using buffer to remove unattached Neutravidin® and stored in a phosphate buffer solution of pH 10. This protocol yields microwell patterned substrates with Neutravidin coated wells in the background of PEG-silane SAM. Figure 2.16 shows a schematic of the entire protocol.

Figure 2.17 shows confocal laser scanning microscopy images of Neutravidin®-FITC fluorescence collected from the chemically modified microwell patterned surfaces

for two different detection regions (z sections). This analysis was performed using a 488nm laser for exciting the FITC fluorophore. The detection window for fluorescence was 510-535nm. Figure 2.17a is the fluorescence image collected at a detection region close to the top of the micropatterned surface. Figure 2.17b is a zoomed in image of figure 2.17a, which indicates the presence of negligible background fluorescence. Hence there is no indication of Neutravidin® present in the background of the wells, in agreement with the fact that PEG-terminated monolayers are resistant to non-specific protein adsorption[45]. Furthermore the amino-terminated silane during the backfilling step only reacted with the bare silica in the wells of the microwell-patterned surface.

Figure 2.17c, which is the fluorescence image of the micropatterned surface focused on the bottom of the wells, shows that Neutravidin®-FITC was present both along the walls of the wells and also at the bottom of the wells. Different z-sections were taken along the depth of wells starting from the top of the surface while imaging using confocal laser scanning microscopy and our results show that the intensity distribution in the wells becomes more uniform as the bottom of the well is approached (data not shown).

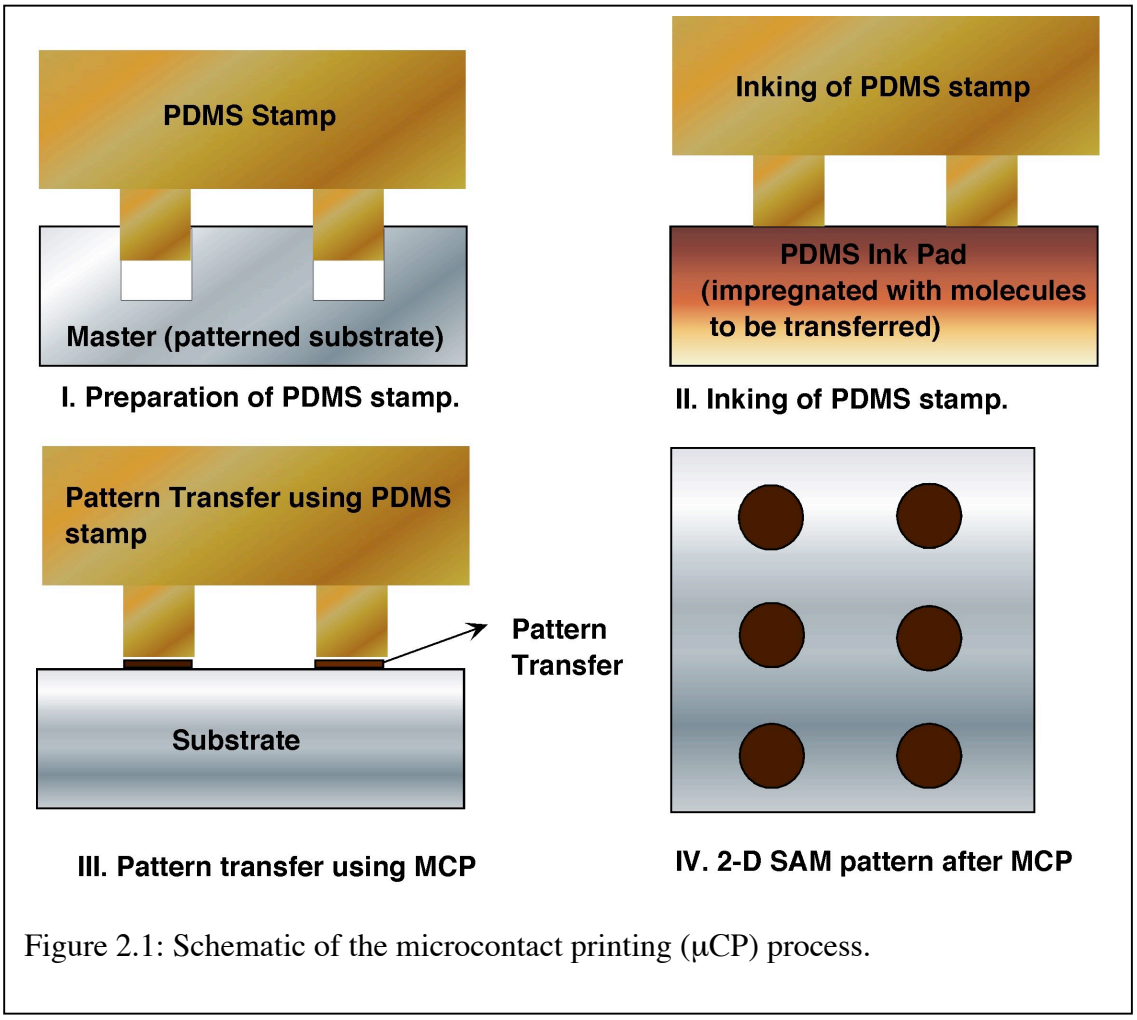

Figure 2.1: Schematic of the microcontact printing (μCP) process.

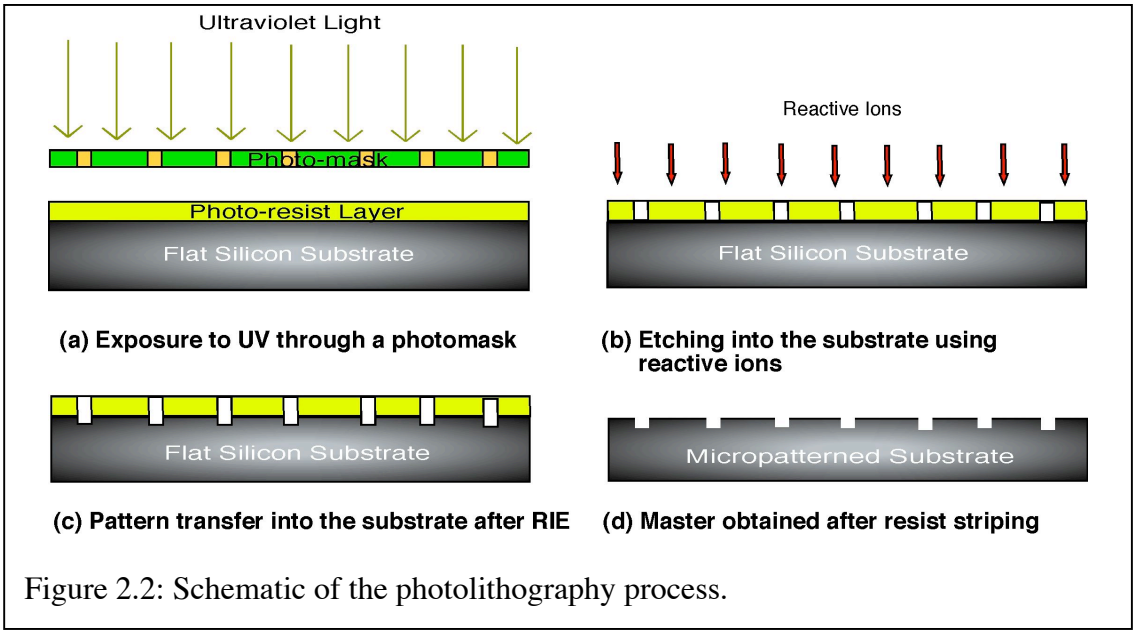

Figure 2.2: Schematic of the photolithography process.

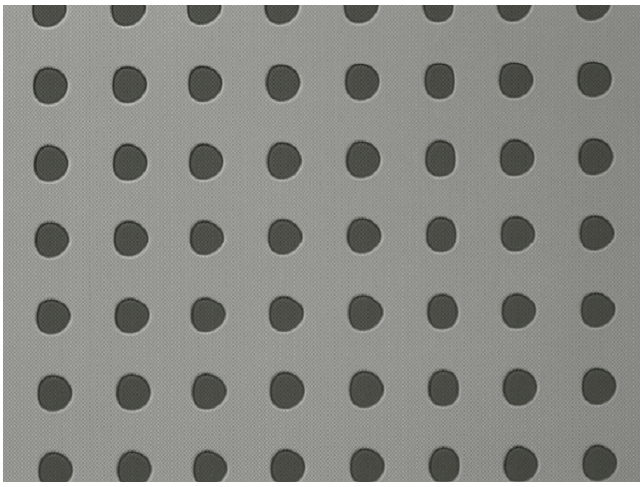

Fig 2.3: Photo-mask fabricated at CNF. The dark holes are exposed glass and the light background is chrome which is non transparent to UV light. Diameter of holes = 5μm, Pitch = 15μm.

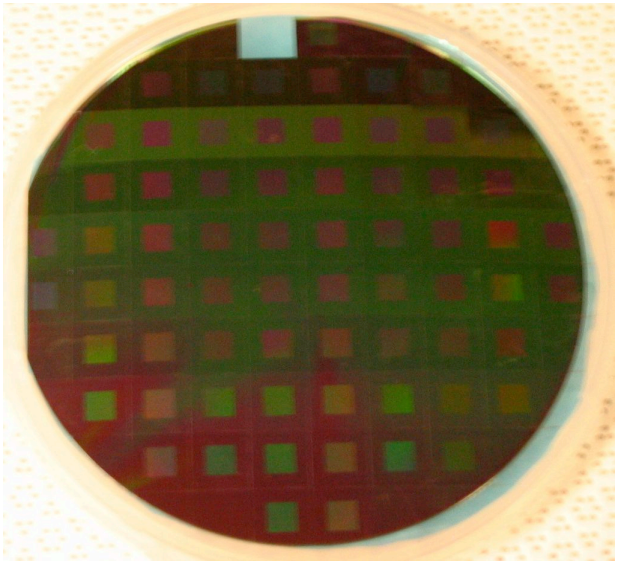

Fig. 2.4: CNF wafers cut using dicing saw: the wafers are still inside the lamination sheets

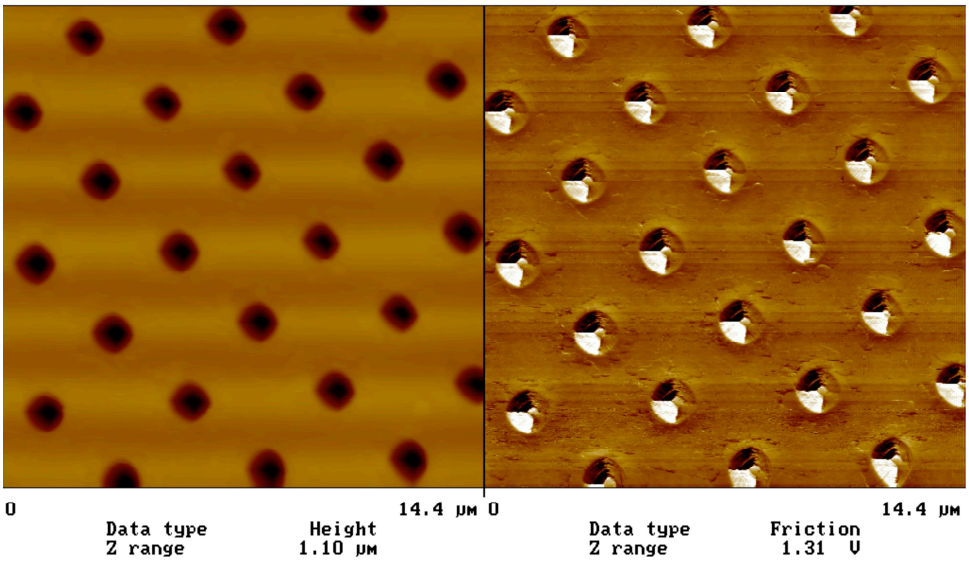

(a) Height and friction images

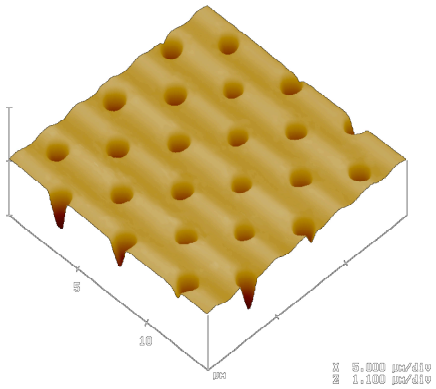

(b) Surface plot

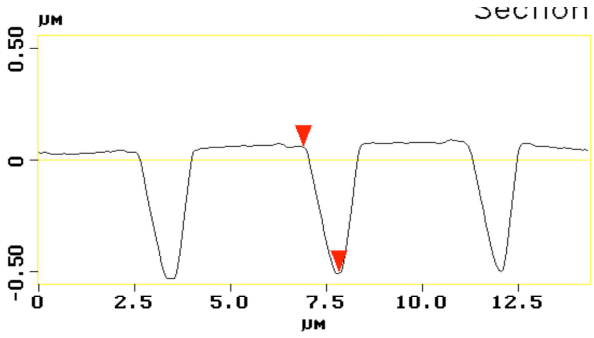

(c) Section image

Fig 2.5: Contact mode AFM images of SiO_2/Si masters with wells fabricated at CNF. Diameter of wells = 1.3 microns, Pitch = 3 microns, Depth =560nm

$$W_{adh} = \gamma\alpha + \gamma\beta - \gamma\alpha\beta$$

where W_{adh} is the work of adhesion,
$\gamma\alpha$ is the surface tension of phase α,
$\gamma\beta$ is the surface tension of phase β and
$\gamma\alpha\beta$ is the interfacial tension between phases α and β.

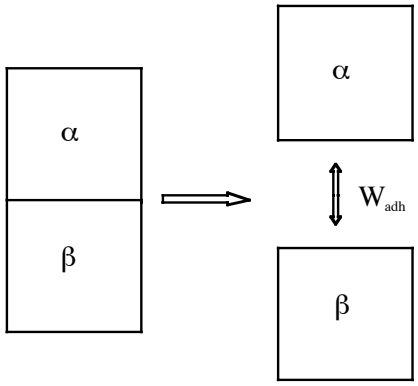

Fig 2.6: The concept of work of adhesion.

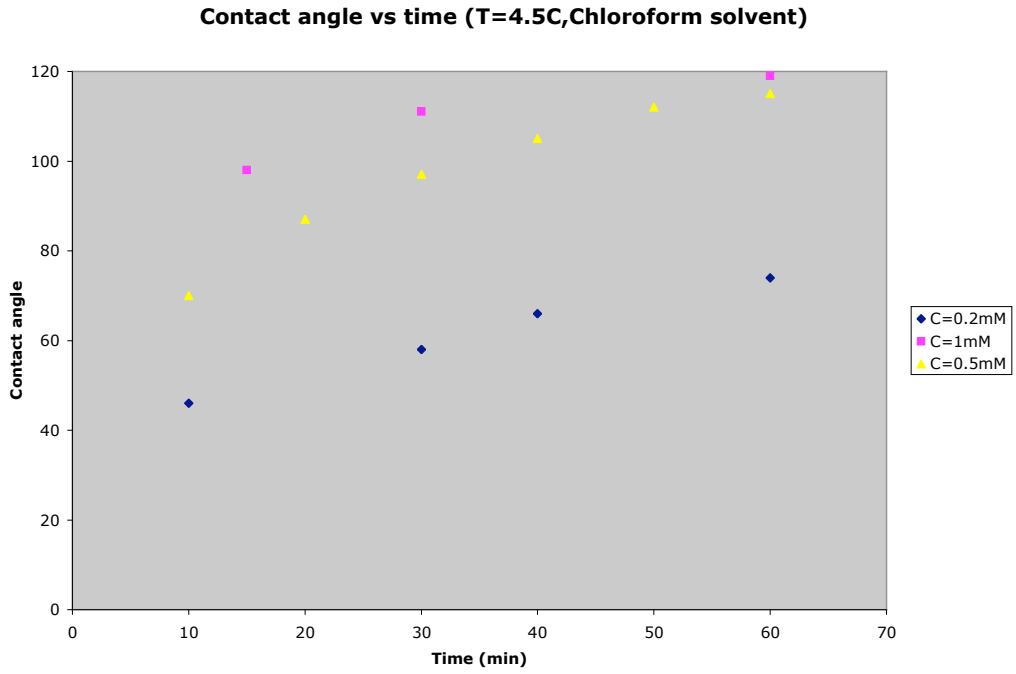

Fig 2.7: Contact angle data for fluorination experiments on silica substrate at 4.5^0C

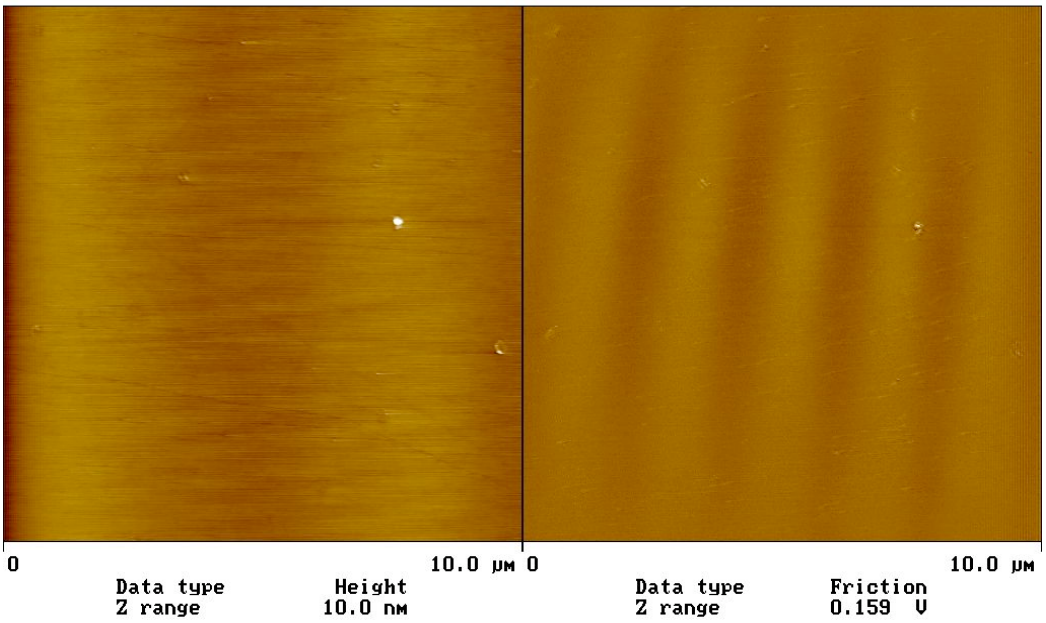

(a)

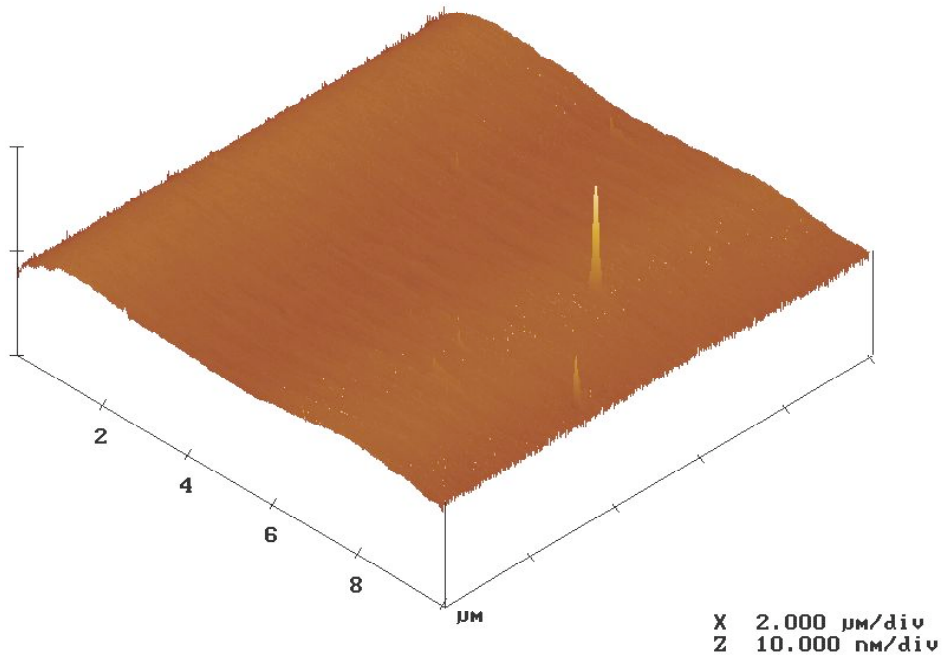

(b)

Fig 2.8: (a) Contact mode AFM height and friction images of fluorination experiment using 0.5mM fluorosilane in chloroform at 4.5^0C (b) The 3-D image of the height image in fig a.

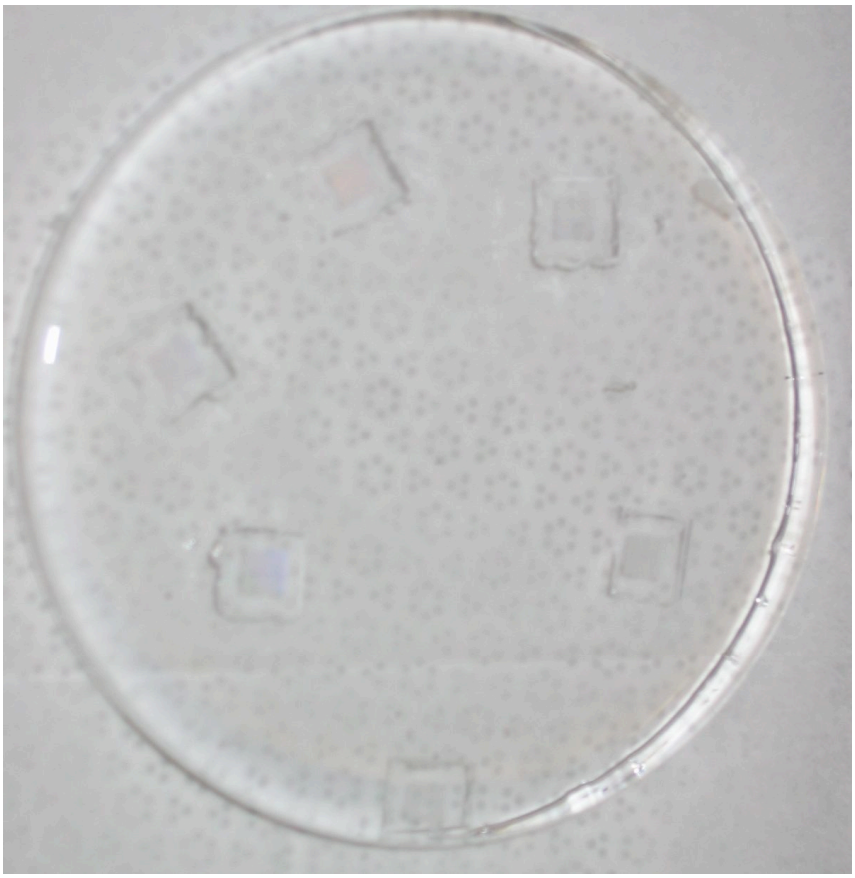

Fig. 2.9: PDMS stamp disc peeled off from 6 CNF masters. The active areas on masters are the squares clearly visible at the center. The size of the active regions is 5mmX5mm.

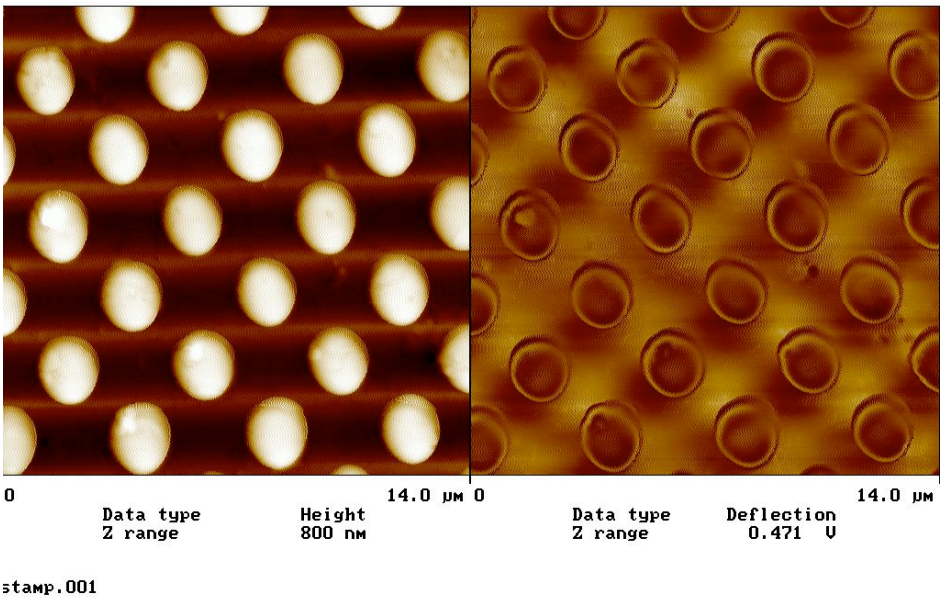

(a) Height and friction images of the PDMS stamp

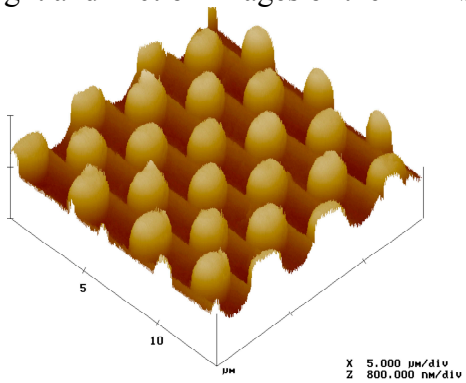

(b) 3 D image of the PDMS stamp

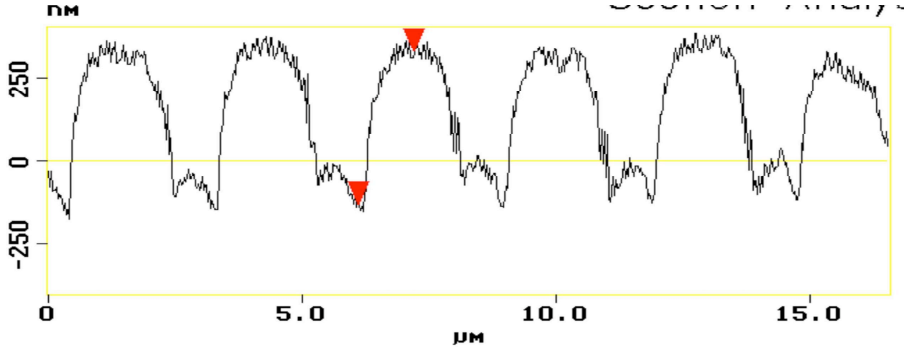

(c) Section image of the pillars on the PDMS stamp

Fig.2.10: Tapping mode AFM images of the PDMS stamp replicated from CNF master of the previous figure 2.5.

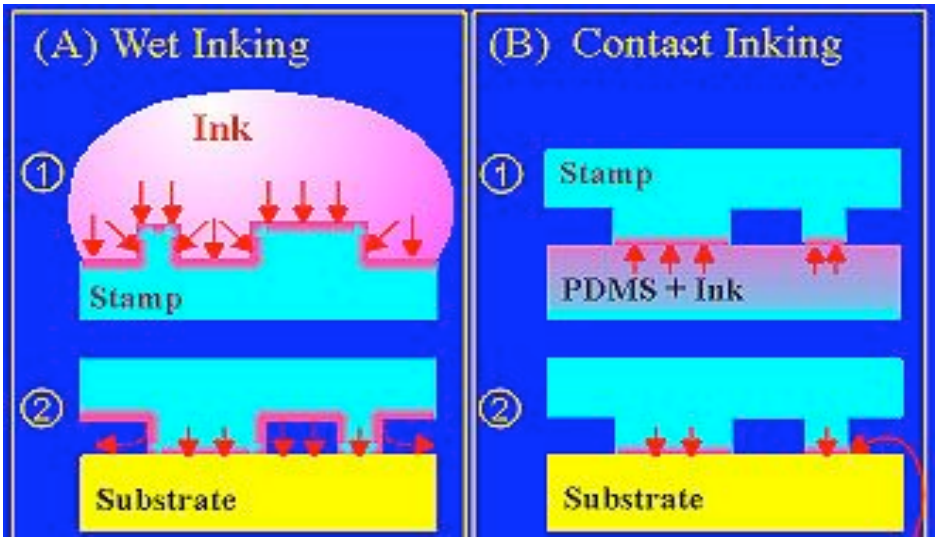

Fig 2.11: Methods of inking in the microcontact printing process.

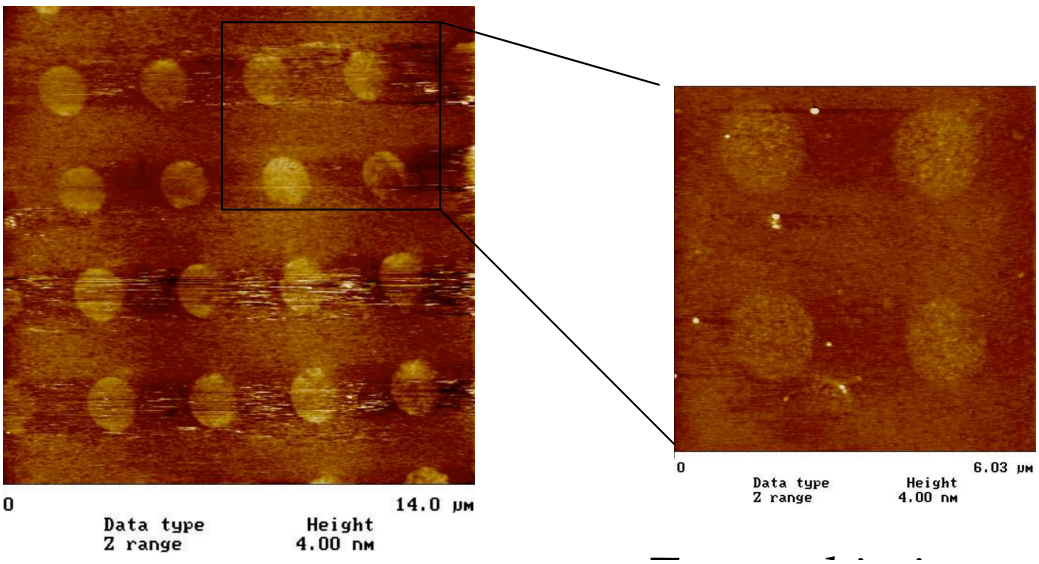

a. AFM Height image (z-range: 1nm) b. Zoomed in image

Fig. 2.12: Microcontact printing of APS islands on flat silicon substrate.

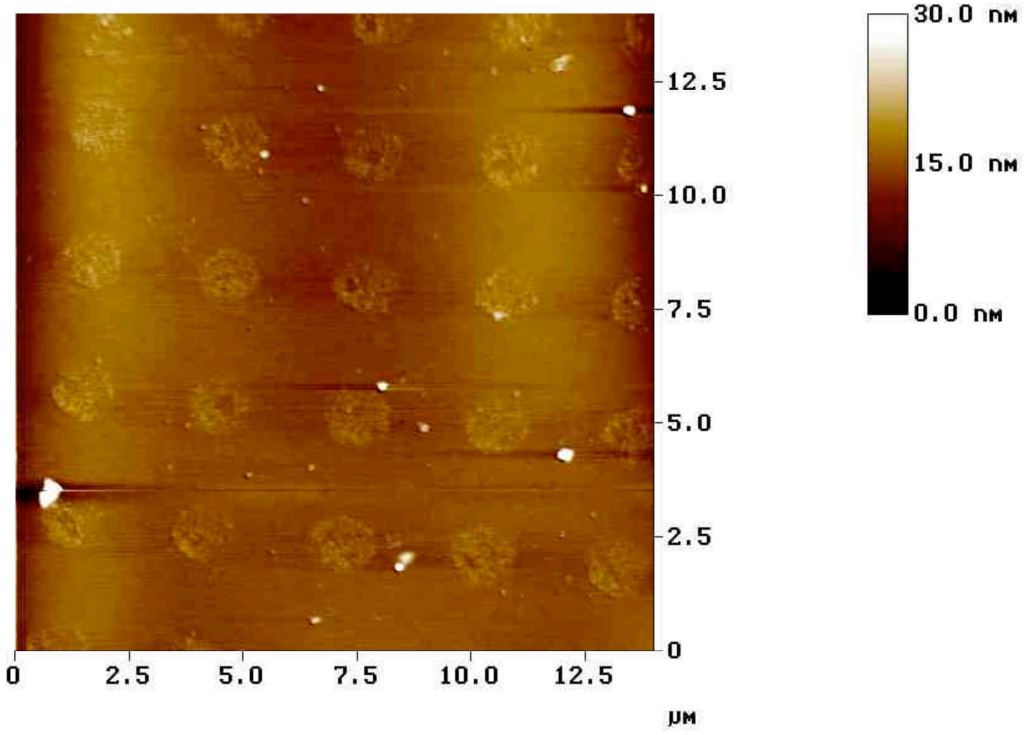

Fig 2.13: NHS-PEO_4-Biotin modified amine islands on flat silicon substrate.

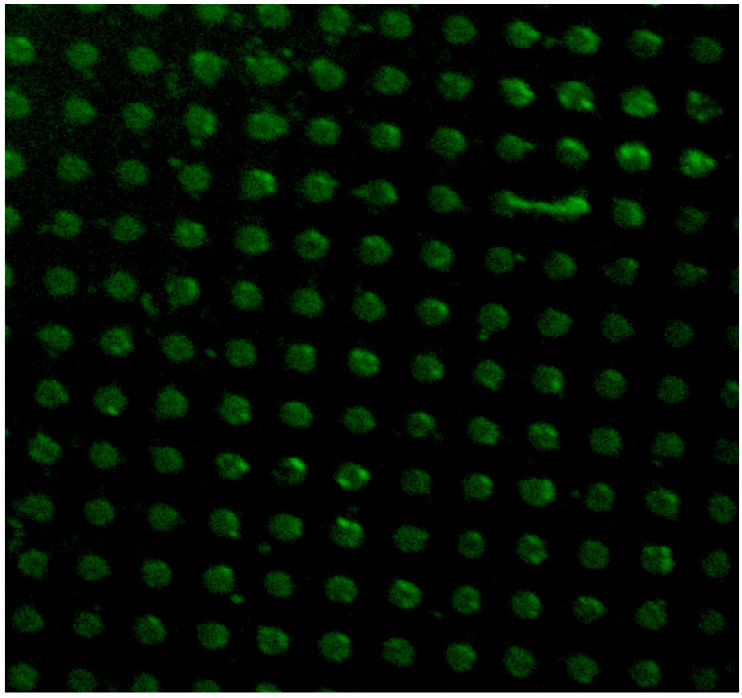

(a)

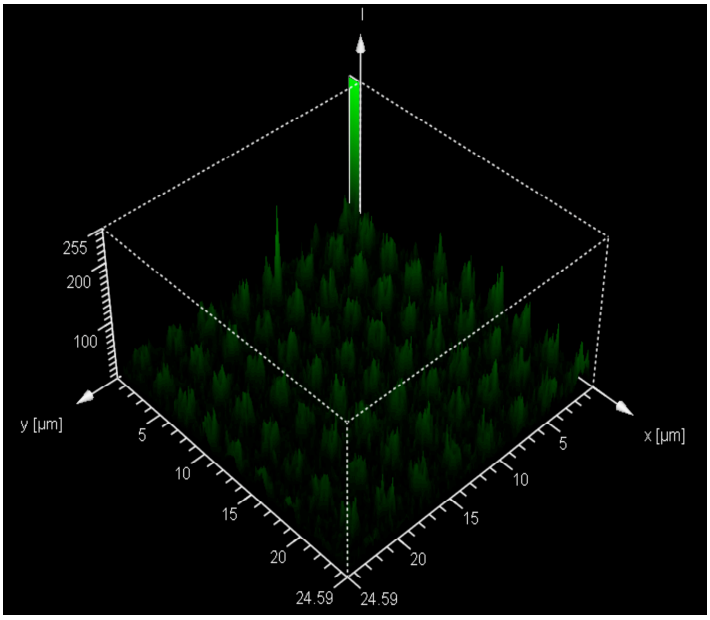

(b)

Fig 2.14 Neutravidin-FITC islands on flat silicon wafer. (a) Fluorescence data collected using CLSM. (b) 3-D intensity profile.

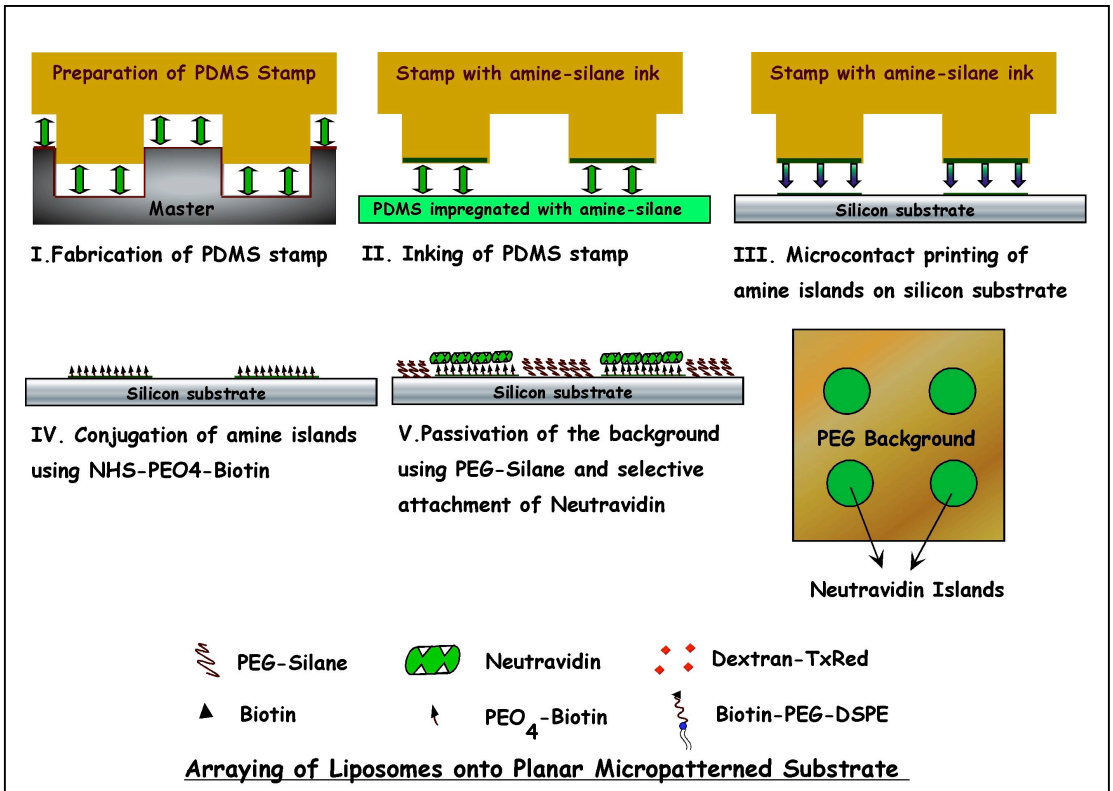

Fig. 2.15: Schematic representation of the fabrication process of planar bi-functional substrates.

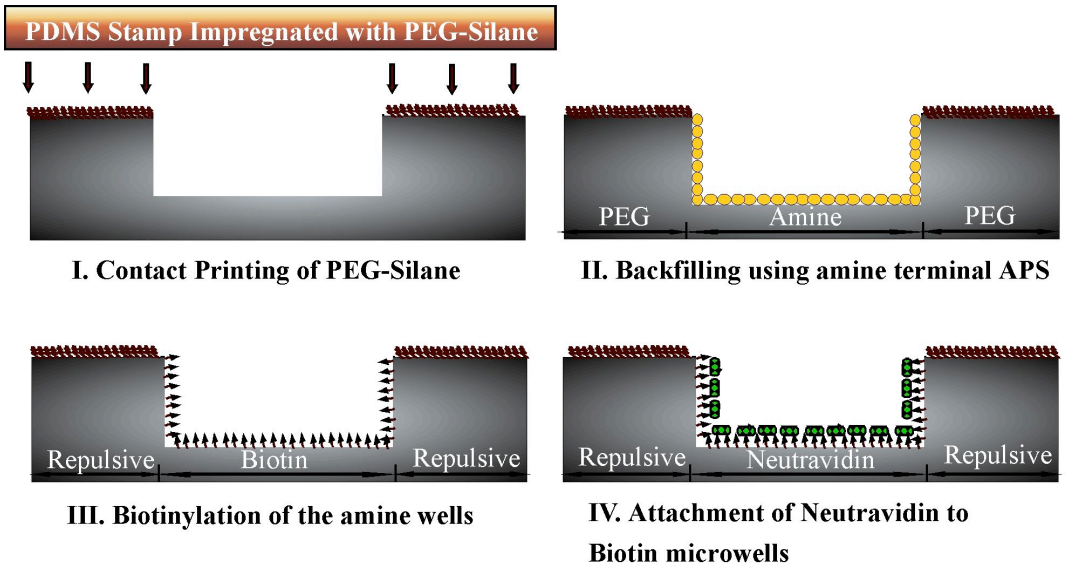

Fig2.16: Schematic representation of the fabrication process of the microwell bi-functional substrates.

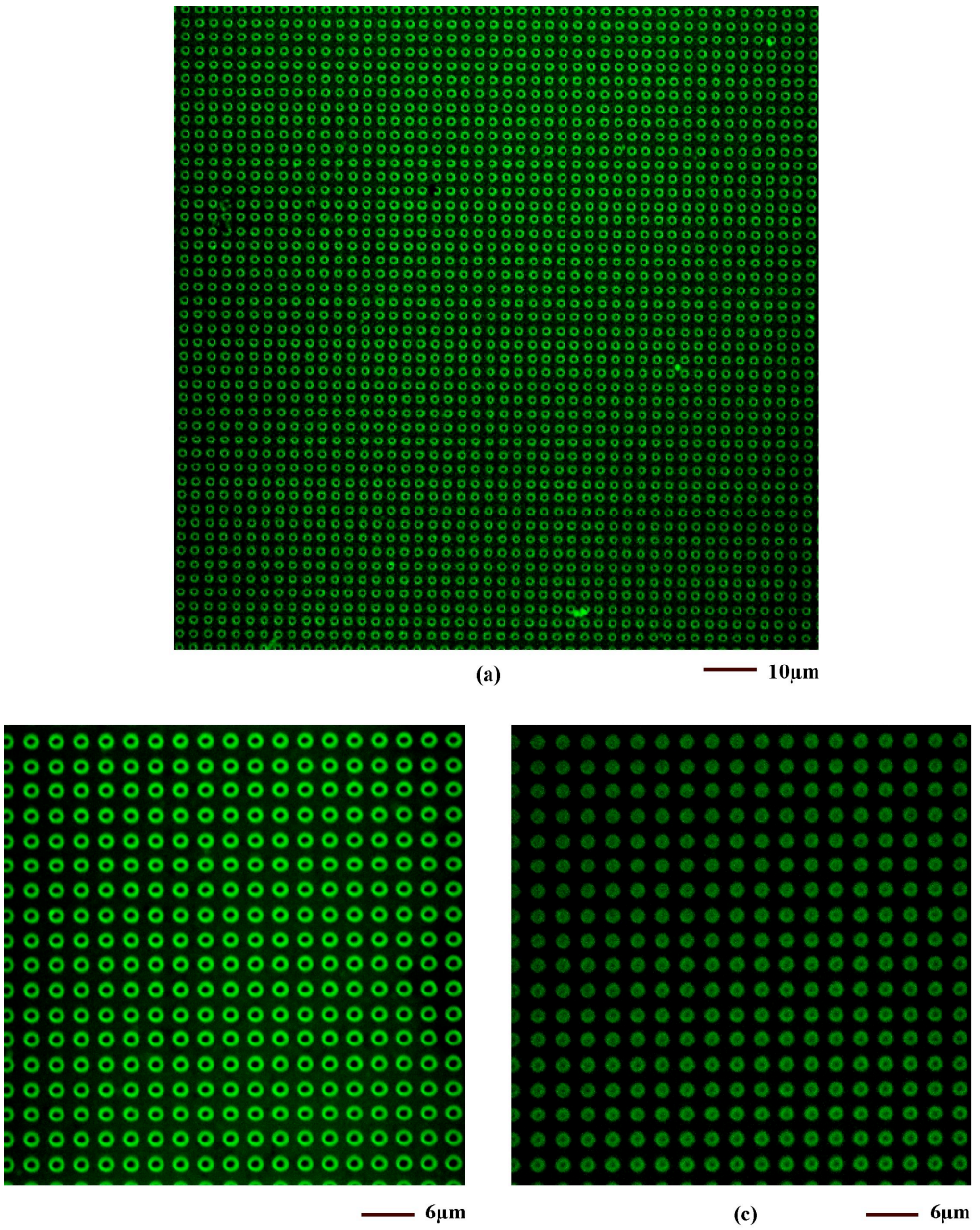

Fig 2.17: Bi-functional substrate with Neutravidin-FITC coated microwells in the background of PEG-silane SAM. (a) CLSM image of the fluorescence collected from the FITC tag close to the top of the microwells. (b) zoomed in image close to the top of the microwells implicating that Neutravidin is present along the walls of the wells. (c) zoomed in image close to the bottom of the microwells showing a relatively uniform fluorescence profile along the cross-section of the wells. (Note: negligible background fluorescence from the background of the wells)

Chapter 3

Liposome preparation and their exposure to bi-functional substrates

3.1 Procedure to prepare liposomes:

The procedure to prepare liposomes of desired size and surface properties is as follows:

3.1.1 Preparation of lipid films:

Phospholipids and cholesterol are dissolved in pre-decided amount of chloroform in airtight vials with enough care to avoid excess contact of the chloroform to humid air. These solutions are mixed to have a lipid mixture containing the three constituents with calculated molar proportions. This solution is divided in aliquot amounts in different vials such that each vial contains about 2 mg of lipid mixture dissolved in chloroform. The aliquots are then kept under vacuum until all the solvent has evaporated and a thin lipid film is formed on the walls of the vials. The vials are sealed using parafilm under nitrogen and stored in the refrigerator at -20^0C. Typical shelf life of these vials is about 3 months.

3.1.2 Preparation of buffer for hydration:

A slightly alkaline buffer (pH=7.5) is prepared by using following constituents in de-ionized water:

1. HEPES (H-3784, Sigma Aldrich): 20mM $\Rightarrow$15.62 g in 3litre water
2. NaCl: 100mM $\Rightarrow$ 17.53 g in 3litre water
3. EDTA: 1mM $\Rightarrow$ 1.12 g in 3litre water

The solution is mixed using a magnetic stirrer and the pH is monitored using the digital pH meter. The pH is adjusted using standard NaOH (5M) or HCl (6N) solutions. Millipore Sterivex- GV 0.22micron size membrane is used to remove large size particles from the buffer solution. The buffer is then degassed by bubbling pure argon gas through

it for approximately 15 minutes and stored in airtight containers. It is filtered again before each use.

3.1.3 Hydration of film to form MLVs (large multi-lamellar vesicles):

The temperature of the hydrating medium (buffer) should be above the gel-liquid crystal transition temperature (Tc) [90] of the lipid with the highest Tc before adding to the dry lipid. Thus the lipid bilayers formed are in the liquid crystal phase at the temperature of the system. After addition of the hydrating medium, the lipid suspension should be maintained above the Tc during the hydration period. The lipids used in our experimental protocols are low Tc lipids. Hence thawing of the lipid films to room temperature and use of hydrating medium at room temperature is sufficient enough to ensure compliancy to this requirement.

1 ml of HEPES buffer of pH 7.5 is added to a vial containing approximately 2 mg of the lipid mixture at room temperature. A vortexer is used to mix lipid in the buffer solution. The solution becomes turbid indicating that multilamellar vesicles have formed in the solution. It is kept in freezer at -20^0C for 15 min, taken out, shaken till it comes to room temperature, and vortexed till it is mixed nicely. This freeze-thaw step is repeated thrice. This procedure yields a solution containing large multi-lamellar vesicles (MLVs) with a narrower size distribution (Figure 3.1, taken from avanti lipids). It is reported that putting the hydrated lipid vial in freezer (-20^oC) overnight improves size distribution even more and makes sizing easier (data not shown).

3.1.4 Extrusion of the hydrated MLV solution to form SUVs (Small uni-lamellar vesicles):

Mini extruder by Avanti lipids is used for extrusion process to form liposomes in desired size range. The detailed procedure for handling of extrusion unit is given in a manual available online on Avanti Lipids website*. Figure 3.2 shows a schematic of the extrusion unit. The extrusion unit mainly consists of two micro-syringes; an assembly consisting of hexagonal-nut based steel casing and Teflon cylinders to hold the membrane and filter supports, and a stand to support the complete extrusion assembly. The syringes and Teflon assembly parts are thoroughly rinsed using deionized water and buffer before each extrusion step. There are membranes available of various sizes: 50nm, 100nm, 200nm and 1 micron. A membrane of right size is chosen and supported by using a pair of filter supports on both sides. It is then put in the previously cleaned extrusion assembly. Initially buffer is passed through the extrusion system in order to make the entire system wet. The MLV solution, at room temperature, is taken in one of the micro-syringes and passed through the extrusion assembly in such a way that it gets collected into the micro-syringe on the other side. The other micro-syringe is used to push the MLV solution through the extrusion assembly so that the solution is collected at the other end in the original micro-syringe. This procedure is repeated at least 11 times. The number of passes must be more than 11 and an odd number so that the SUV solution is taken out from a different micro-syringe than the original micro-syringe filled with the MLV solution initially. This helps in eliminating any errors due to mixing of extruded solution from the remaining non-extruded solution if any in the original syringe. Figure 3.3 shows a schematic involving the overall protocol in extrusion.

*** http://www.avantilipids.com/**

3.2 Selection of lipids for the preparation of liposomes:

Lipids selected for liposome arrays are always low T_c lipids ($T_c < 20^0$C or room temperature). As mentioned earlier in section 3.1, the temperature during hydration of lipid films and extrusion should be above the T_c of the lipid constituent in the mixture, which has highest T_c. This ensures that all the lipids are in gel phase and can easily form MLVs during hydration or SUVs during extrusion/sonication at room temperature. Cholesterol is used in all lipid formulations because it helps in improved stability of lipid bilayers of liposomes and also makes them less permeable. All the lipid formulations contain:

a. One major lipid constituent, which forms the bulk of the lipid bilayer.

b. Cholesterol in equivalent molar amount to the major lipid constituent

c. 5% molar lipid containing biotin, which gives biotin functionality to the liposome surfaces so that they can be selectively directed towards active regions on patterned substrate containing avidin functionality.

d. 1% molar fluorescently tagged lipids for visualization of liposomes using fluorescence/ confocal laser scanning microscopy.

Table 3.1 represents a list of lipids including their gel-crystal phase transition temperatures, which are used for the preparation of liposomes for arraying onto functionalized substrates. Figure 3.4 shows molecular structures of corresponding lipids. Table 3.2 represents a list of fluorescently tagged lipids including their excitation/emission maxima for corresponding dyes and figure 3.5 shows their molecular structures. Figure 3.6 shows sample emission curves of fluorescent tags of various lipids used in this study. To check the intactness of liposomes, sometimes fluorescently tagged

water soluble polymeric Dextran (MW 10,000) is incorporated in the aqueous core of the liposomes. If liposomes are broken open, the Dextran fluorescence signal does not colocalize with the fluorescence signal of the lipid bilayer. This is an important way to check if the liposomes are intact after arraying them on a substrate. Table 3.2 also has information about these dextrans, which are referred to as fluorescent cargos. Table 3.3 shows mean particle sizes of liposomes extruded using various membrane pore sizes.

3.3 Preparation of lipid formulations and liposomes:

Lipid films are prepared with two different formulations while standardizing the intact arraying protocol;

I) POPC: Cholesterol: Biotin-PEG-DSPE in 0.63:0.31:0.06 molar proportions.

II) POPC: Cholesterol: Biotin-PEG-DSPE: lipid tag in 0.62:0.30:0.06:0.02 molar proportions.

These constituents are mixed using chloroform and dried overnight under vacuum resulting into approximately 2 mg of lipid films in glass vials. These vials are sealed under nitrogen using Parafilm (Fisher Scientific) and used as needed. 1 ml HEPES buffer (HEPES 20mM, sodium chloride 100mM, EDTA 1mM) of pH 7.5 containing 1mg of Dextran-Texas Red dye is used to hydrate these films to form multilamellar vesicles. After three freeze-thaw cycles each lasting 15 min, this solution is extruded using 1μm pore size membrane in a mini extruder by Avanti Polar Lipids to form unilamellar vesicles (liposomes) of the same size range as the pore size of the membrane. Particle size analysis of the extruded liposomes using a Nano-series Zetasizer (Malvern Instruments) confirmed the presence of liposomes of approximately 0.85μm average diameter. To exclude the dye (Dextran-Texas Red) outside the liposomes, the solution is

passed through a column packed with Sephadex G75 gel using a BioLogic HR workstation and a BioFrac Fraction collector setup (BIO-RAD). After separation, the purified fraction is checked for correct particle size using the Zetasizer and the absence of any background Dextran-Texas Red fluorophore using epi-fluorescense microscopy (Nikon ECLIPSE TE 200 inverted microscope). The liposomes are also characterized for their zeta potential. A typical zeta potential for these formulations is –1.7 mV. Slight negative charge on liposome surfaces maybe due to the fact, that Biotin-PEG-DSPE is a charged lipid. This charge also helps in stabilizing the liposomes and prevents them from fusion. These liposomes are found stable using particle size analysis over a period of one week.

3.4 Exposure of liposomes to the bi-functional substrates:

3.4.1 Exposure of liposomes to the planar bi-functional substrates:

Liposomes in this set of experiments were prepared using formulation II as described in section 3.3 with T1395 (Excitation: 592nm, Emission: 612nm) as the fluorescent lipid tag. Substrates used were planar bi-functional substrates as described in section 2.6.1 with Neutravidin-FITC islands in the background of PEG silane SAM. Typical exposure time of liposome solution to the substrates was around 3 hrs. After exposure to liposomes, the substrates were thoroughly rinsed with HEPES buffer of pH 7.5 to minimize non-specific attachment of liposomes. Confocal laser scanning microscopy was used to detect the presence of liposomes arrayed on the substrate. Figure 3.7a shows one of these images. Red fluorescence in the image is from the lipid bilayer of liposomes. This data indicates that liposomes are present along the periphery of islands apart from sitting on the top of the islands and defeats the purpose of having one

liposome per island. This problem could be attributed to availability of more active sites for liposome attachment once a liposome attaches to an island. Figure 3.7b shows the conceptual visualization of the data. Various experiments using different liposome concentrations and exposure times were performed to achieve one to one attachment of liposomes without any desired results (data not shown). These results directed us in using bi-functional microwell substrates instead to achieve one to one attachment of liposomes onto islands.

3.4.2 Exposure of liposomes to the microwell patterned bi-functional substrates:

The microwell surfaces with Neutravidin®-FITC grid as described in section 2.6.2 are glued to previously cleaned glass microscope slides (obtained from Fischer scientific) using Permabond® industrial grade elastomer bonding adhesive. Press-to-seal™ silicone isolators are used to prepare the sample cell around these surfaces and 500 μl of liposome solution is exposed to them for 3 hr. Multiple rinsing steps using pre-filtered HEPES buffer of pH 7.5 are used to wash off liposomes which are not attached to the surface and excess dye. Cover slips (clean and with a monolayer of PEG-silane) are used to cover the surfaces under HEPES buffer of pH 7.5 for confocal laser scanning microscopy.

The microwell grid labeled with FITC-Neutravidin® in the well interiors is imaged using confocal laser scanning microscopy (Excitation: 488nm, Detection: 510-535nm). To image the immobilized liposomes prepared using formulation I as described in section 3.3, the laser lines at 488nm and 594nm are used to excite the FITC tag on the Neutravidin® functionalized microwell grid and the Dextran-Texas Red cargo inside the liposomes, respectively. Imaging is done at several locations on the surface and the

detection windows are 500-560nm and 610-670nm for FITC and Texas Red, respectively. To image the immobilized liposomes prepared using formulation II with D3815 lipid tag (Table 3.2), the laser lines at 488nm, 514nm and 594nm are used to excite the FITC tags on the Neutravidin® functionalized microwell grid, the BODIPY tag incorporated in the lipid bilayer of the liposomes (D3815), and the Dextran-Texas Red cargo inside the liposomes. Imaging is done at several locations on the surface and data is collected for the three probes using sequential scanning mode. In this mode, emitted photons comprising the fluorescence intensity in the images are collected in a sequential fashion in which only one excitation laser and detection channel are turned on at any one time. In this way we minimize bleed-through, often termed detection channel-to-channel crossover or crosstalk, due to the overlap of emission spectra. The fluorescence detection windows for FITC, BODIPY and Texas Red are 510–535nm, 550-580nm and 610-690nm, respectively.

Figure 3.8 shows fluorescence data taken after exposing loaded liposomes (with Dextran-Texas Red cargo) prepared using formulation I to Neutravidin®-FITC inside the wells on the microwell patterned surfaces. The two fluorophores were chosen on the basis of their well-separated emission spectra (refer to Fig. 3.9) in order to minimize crosstalk between detection channels. Appropriate spectral detection regions were chosen while imaging FITC and Texas Red fluorescence simultaneously using confocal laser scanning microscopy. Figure 3.8 a shows the fluorescence (Excitation 488nm: Emission 500-560 nm) from the green FITC tag on Neutravidin® molecules present inside the microwells on the micropatterned surfaces. Figure 3.8b shows the fluorescence (Excitation. 594nm: Emission 610-710 nm) from Dextran-Texas Red cargo encapsulated inside liposomes.

Figure 4c, which is an overlay image of a and b, clearly shows the co-localization of the fluorescence from the two dyes. This suggests that liposomes are residing inside the chemically functionalized microwells as conceptualized in Figure 1 and are intact. The occupancy level of the microwells is remarkable and was obtained in essentially quantitative yield, with fewer than 5 out of over 1500 sites remaining unoccupied. Based on the 0.85μm average diameter of the liposomes, measured using a Malvern Zetasizer, which is of the order of the microwell dimensions (1.2 μm), and based on the uniform intensity of the Dextran-Texas Red fluorescence at each site over a moderate sample size, suggests that there is only one liposome in each microwell.

The circled wells in figure 3.8b show absence of red fluorescence at places where corresponding FITC fluorescence is present. This is an indication of an empty well. To check this hypothesis, we have plotted the intensity line profiles of the green and red fluorescence incorporating one of the empty wells in the analysis as shown in figure 3.8d. It shows the marked decrease of Dextran-Texas Red fluorescence intensity corresponding to an individual microwell. This result appears to be attributed to the case of a well occupied by a liposome that subsequently released its contents, or a well never occupied by a liposome.

The above evidence does not directly fluorescently visualize the bilayer of the liposome, but only the cargo inside the liposome. As such the cargo could be localized onto the grid by adsorption without the need for the lipid bilayer. To directly confirm the presence of the liposome coexisting with the cargo we utilized formulation II, which places a dye in the lipid bilayer. Figures 3.10 and 3.11 show fluorescence data taken after exposing loaded liposomes (with Dextran-Texas Red) prepared using formulation II

which has BODIPY fluorophore tagged lipids (Molecular Probes D-3815). This dye was selected on the basis of an emission profile and maxima that lies in between that of FITC and Texas Red. (refer Figure 3.12). Appropriate spectral detection regions were chosen while imaging FITC, BODIPY and Texas Red fluorescence in sequential scan mode in which each dye is sequentially excited to suppress signal cross talk or bleed-through (fig 3.12). Figure 3.10 shows the fluorescence data obtained from a detection region close to the bottom of the microwells as depicted in the schematic model in figure 3.10e. Figure 3.10a is the fluorescence from the FITC (Excitation: 488nm, Detection: 510nm-535nm) tag on Neutravidin® molecules present inside the microwells on the micropatterned surfaces. Figure 3.10b shows the fluorescence from BODIPY (Excitation: 514nm, Detection: 550-580nm) tag of D-3815 present in the lipid bilayer of the liposomes. Figure 3.10c shows the fluorescence from Dextran Texas Red (Excitation: 594 nm, Detection: 610-690 nm) cargo encapsulated inside liposomes. Figure 3.10d, which is an overlay image of a, b and c shows the microwell co-localization of fluorescence from the three dyes with negligible background fluorescence. The co-localization of the lipid and cargo dyes provides strong evidence that intact liposomes and not just the cargo are situated inside the chemically functionalized microwells. Figure 3.10f shows line intensity profile taken along a section shown in figure 3.10d. The green (FITC) and yellow (BODIPY) curves are relatively flat across the cross section of the wells, since fluorescence data is collected from the bottom and the walls of the wells are excluded. The red (Dextran-Texas Red) line intensity profile curve shows a centrally symmetric distribution of the cargo present inside the liposomes, a co-localization finding consistent with the presence of intact liposomes within the microwells.

Another set of data was collected in a detection region close to the top of the microwells offset by 800nm in the Z direction, images from this optical section are shown in figure 3.11. Identical detection windows as the data in figure 5 were used to collect the fluorescence from the three dyes (refer fig 3.12). Figure 3.11a is the fluorescence from the FITC tag on Neutravidin® molecules present inside the microwells on the micropatterned surfaces. Figure 3.11b shows the fluorescence from the BODIPY tag present in the lipid bilayer of the liposomes. Figure 3.11c shows the fluorescence from Dextran Texas Red cargo encapsulated inside liposomes. Figure 3.11d, which is an overlay image of a, b and c further supports the claim that the liposome attachment was selective to the inside of the microwells on the chemically functionalized micropatterned surfaces. Figure 3.11f shows line intensity profile taken along a section shown in figure 3.11d. The green (FITC) and yellow (BODIPY) curves have a minima close to the center of the microwells since majority of the fluorescence collected in this region is from the walls of the microwells and the lipid bilayers of liposomes present inside them respectively. The red (Texas Red) curve shows a centrally-symmetric distribution of the cargo present inside the liposomes, as expected, with two shoulders present from an optical artifact caused by multiple reflections of the emitted fluorescence within the microwell (see Figure 3.13 and explanation below). This centrally-symmetric distribution for this highly-water soluble cargo could not have been realized if the liposome had ruptured, as is shown in Figure 3.14.

In addition to the two sections shown in figure 3.10 and 3.11, a series of four additional z-sections were taken in order to reconstruct a 3-dimensional image, shown in figure 3.15. The optical sections start near the top of the microwell (tentative midsection

of the liposome) and extend down into the silicon substrate over 0.87 mm with a step size of 0.28 mm. Figure 3.15 was obtained from the view directly above the array. This data was processed to intersect the center of a set of microwells along the rightmost and bottommost edges to display the co-localization of dyes within the wells in 3D. This figure clearly shows the encapsulation of the cargo by the BODIPY tagged lipid and is the clearest demonstration of the intactness of the immobilized liposomes.

Surfaces with intact liposomes were exposed to a 1M NaCl solution for 1 hr in order to lyse the liposomes. The surfaces were then washed with pre-filtered HEPES buffer of pH 7.5 and imaged using confocal laser scanning microscopy to check for the presence of the dyes. It was found that Neutravidin ® FITC fluorescent grid could still be observed, but there was no fluorescence signal obtained from the BODIPY fluorescent tag. Texas Red fluorescence was also systematically absent from the microwells, but in some areas appeared randomly smeared over the surface. This picture contrasts sharply with the organized co-localization of the three dyes for the case of the intact liposome arraying.

To demonstrate the importance of the microwells in confining and preventing the unraveling of the liposomes, liposome solutions were brought into contact with uniformly functionalized surfaces. For pure silicon surfaces the liposomes ruptured upon exposure to these untreated surfaces, as concluded from the fact that the Dextran-Texas Red fluorescence signal was smeared over the entire surface and was not localized in a regular pattern. Liposomes prepared using formulation II, and loaded with Dextran-Texas Red cargo, were also exposed to uniform Neutravidin^{TM}-FITC coated flat silicon wafers. Confocal laser scanning microscopy results (figure 3.14) showed a remaining uniform

FITC fluorescence (figure 3.14a) and that liposomes ruptured and released their fluorescent cargo. Dextran-Texas Red was smeared over the Neutravidin^{TM}-FITC layer on the flat silicon surface (figure 3.14c) and lipid dye was present in small amounts, in the form of islands, over the surface (figure 3.14b). This result further supports the use of patterned and chemically modified microwell surfaces to array intact liposomes.

Figure 3.11c, which is the fluorescence data of Dextran Texas Red present inside the liposomes arrayed on the microwell patterned surfaces taken close to the top of the microwells, shows the presence of two shoulders in the line intensity profile. We attribute this result to the complex optical reflections of the signal from the fluorescent cargo inside the microwells. To support this explanation, negatively charged 1μm diameter carboxyl functionalized fluorescent particles (Excitation maxima: 529nm, Emission maxima: 546nm) were arrayed instead of the liposomes into the microwells of our patterned surfaces. The same microwell patterned surfaces, functionalized with an amine SAM at the well bottom and a PEG SAM in the space between the wells, were exposed to a 0.0025 weight % solution of particles (1 micron diameter) for 24 hrs, then rinsed with DI water and imaged using the confocal laser scanning microscope. The negatively charged particles were electrostatically coordinated with the positive amine termination of the wells [91, 92]. The passivating PEG functionality surrounding the wells allowed for the easy removal of the non-coordinated particles. Figure 3.13a shows confocal laser scanning microscopy data collected in a detection region close to the top of the microwells using the 514 nm laser for excitation and a 535-615nm detection window. Figure 3.13b is a vertical slice (z-slice), which confirms the presence of the particles inside the microwells. Examination of figure 3.13a shows that the fluorescent pattern is

identical to the pattern observed for the Dextran cargo from the liposome immobilization experiments on these patterned surfaces (see figure 3.11c). In particular both figures exhibit a fluorescent concentric pattern consisting of a bright ring, a dark region, and a bright center. This pattern can be easily explained by assuming that the fluorescence of the centrally located particle (or liposome) is reflected off of the cylindrical inside surfaces of the wells. This reflection pattern is clearly shown in the z-slice image shown in figure 3.13b.

Table 3.1: Lipids used for the preparation of liposomes

SR NO	NAME	TYPE	ABBREVIATION	STRUCTURE
1	L-∝- Phosphatidylcholine (Egg, Chicken)	Major	POPC	Fig 3.4 a
2	1,2-Distearoyl-sn-Glycero-3-Phosphocholine	Major	DSPC	Fig 3.4 b
3	Cholesterol	Major	CHOL	Fig 3.4 c
4	1,2-Distearoyl-sn-Glycero-3-Phosphoethanolamine-N-(Biotinyl(polyethyleneglycol)2000)(ammonium salt) Powder	Biotin lipid	Biotin-PEG-DSPE	Fig 3.4 d
5	1,2-Dipalmitoyl-sn-Glycero-3 Phospho-ethanolamine-N-(Cap Biotinyl) (Sodium Salt)	Biotin Lipid	Biotin-PE	Fig 3.4e

Table 3.2: Fluorescently tagged lipids and cargo incorporated inside liposomes.

SR NO	NAME	ABBREVIATION	EXCITATION MAX	EMISSION MAX	STRUCTURE
1	2-(4,4-difluoro-5-methyl-4-bora-3a,4a-diaza-s-indacene-3-dodecanoyl)-1-hexadecanoyl-sn-glycero-3-phosphocholine (BODIPY® 500/510 C_{12}-HPC)	D3793	500	510	Fig 3.5 a
2	2-(4,4-difluoro-5,7-diphenyl-4-bora-3a,4a-diaza-s-indacene-3-pentanoyl)-1-hexadecanoyl-sn-glycero-3-phosphocholine (-	D3815	530	550	Fig 3.5 b

	BODIPY® 530/550 C_5-HPC)				
3	2-(4,4-difluoro-5-(4-phenyl-1,3-butadienyl)-4-bora-3a,4a-diaza-s-indacene-3-pentanoyl)-1-hexadecanoyl-sn-glycero-3-phosphocholine (-BODIPY® 581/591 C_5-HPC)	D3806	581	591	Fig 3.5c
4	Texas Red® 1,2-dihexadecanoyl-sn-glycero-3-phosphoethanolamine, triethylammonium salt (Texas Red® DHPE)	T1395	592	612	Fig 3.5 d
5	N-(6-tetramethylrhodaminethiocarbamoyl)-1,2-dihexadecanoyl-sn-glycero-3-phosphoethanolamine, triethylammonium salt (TRITC DHPE)	T1391	555	585	Fig 3.5 e
6	Dextran, Texas Red 10,000 MW, lysine fixable	Dextran TxRed	592	612	-
7	Dextran, Alexa Fluor 647; 10,000 MW, anionic, fixable	Dextran Alexa647	647	667	-
8	cholera toxin subunit B (recombinant), Alexa Fluor® 647 conjugate	CT647	647	667	-

Table 3.3: Mean size of liposomes after extrusion

SR. NO.	SOLUTION	PEAK POSITION(S)
1	100 nm membrane extruded liposomes	180.9 nm
2	200 nm membrane extruded liposomes	197.6nm
3	1000nm membrane extruded liposomes	743 nm
4	Non extruded LMV solution	1799nm
5	Buffer solution (filtered through 200nm filter)	1.935nm, 147nm

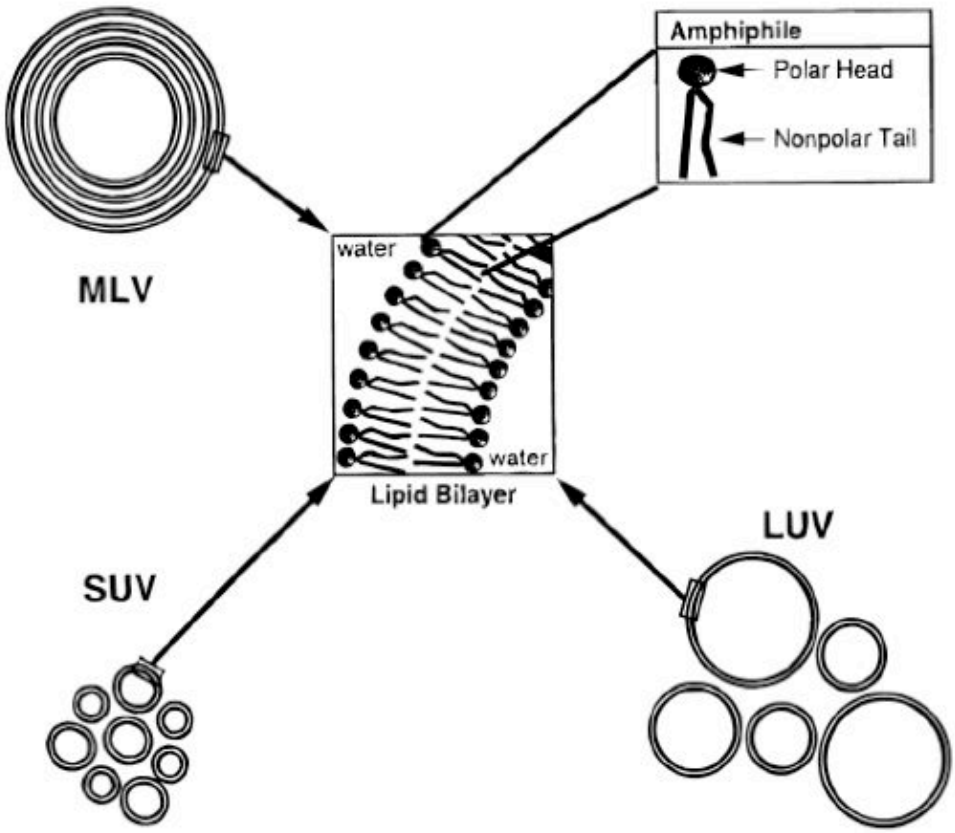

Fig 3.1 Schematics of Multilamellar Vesicles (MLV), Small Unilamellar Vesicles (SUV) and Large Unilamellar Vesicles (LUV). Coutersy: Avanti Polar Lipids

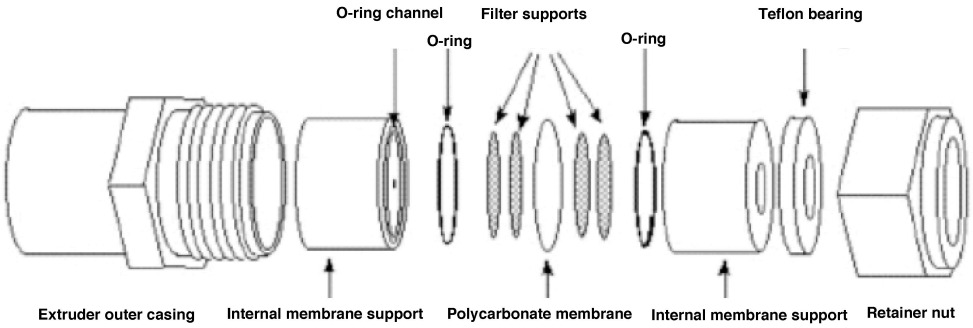

Fig 3.2: Extruder assembly for liposome preparation. (courtesy: Avanti Polar Lipids, Inc.)

Fig 3.3: Extrusion under progress. (courtesy: Avanti Polar Lipids, Inc.)

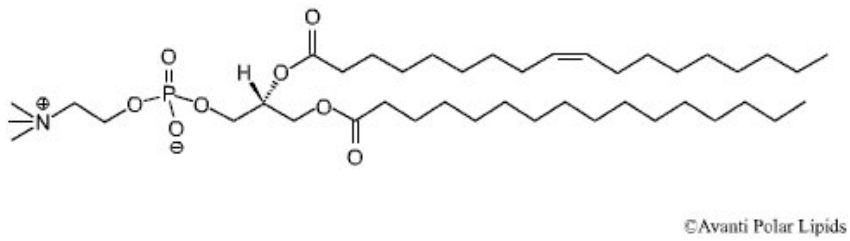

(a) L-∝- Phosphatidylcholine (Egg, Chicken) **(POPC)**

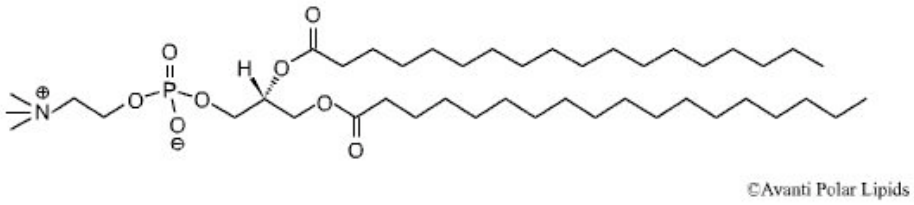

(b) 1,2-Distearoyl-sn-Glycero-3-Phosphocholine **(DSPC)**

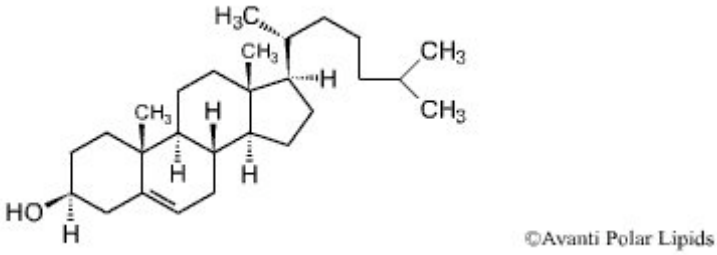

(c) Cholesterol

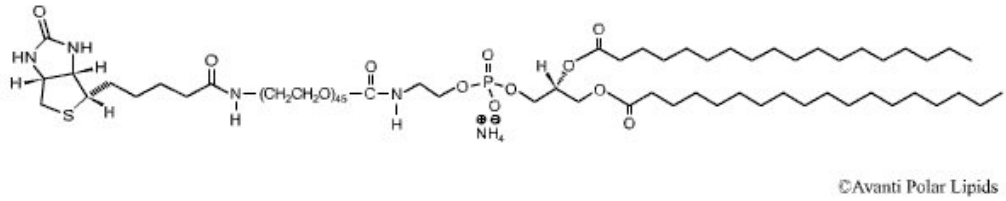

(d) 1,2-Distearoyl-sn-Glycero-3-Phosphoethanolamine-N-(Biotinyl (polyethyleneglycol)2000)(ammonium salt) **(Biotin-PEG-DSPE)**

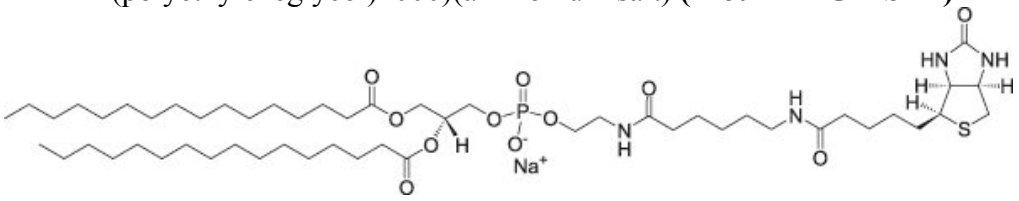

(e) 1,2-Dipalmitoyl-sn-Glycero-3 Phospho-ethanolamine-N-(Cap Biotinyl) (Sodium Salt) **(Biotin-PE)**

Fig 3.4: Structures of lipids from Table 3.1

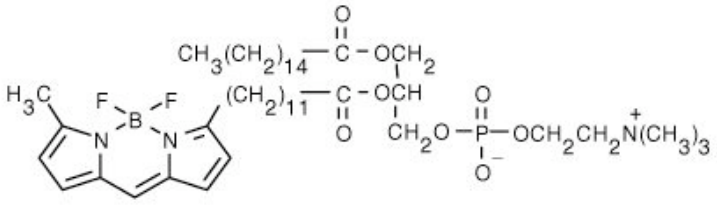

(a) 2-(4,4-difluoro-5-methyl-4-bora-3a,4a-diaza-s-indacene-3-dodecanoyl)-1-hexadecanoyl-sn-glycero-3-phosphocholine (BODIPY® 500/510 C_{12}-HPC) **(D3793)**

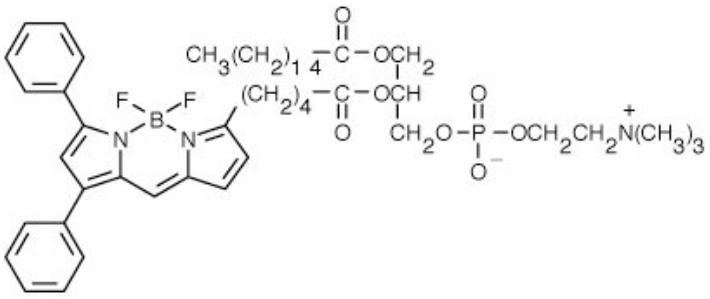

(b) 2-(4,4-difluoro-5,7-diphenyl-4-bora-3a,4a-diaza-s-indacene-3-pentanoyl)-1-hexadecanoyl-sn-glycero-3-phosphocholine (-BODIPY® 530/550 C_5-HPC) **(D3815)**

(c) 2-(4,4-difluoro-5-(4-phenyl-1,3-butadienyl)-4-bora-3a,4a-diaza-s-indacene-3-pentanoyl)-1-hexadecanoyl-sn-glycero-3-phosphocholine (-BODIPY® 581/591 C_5-HPC) (**D3806: Structure not available)**

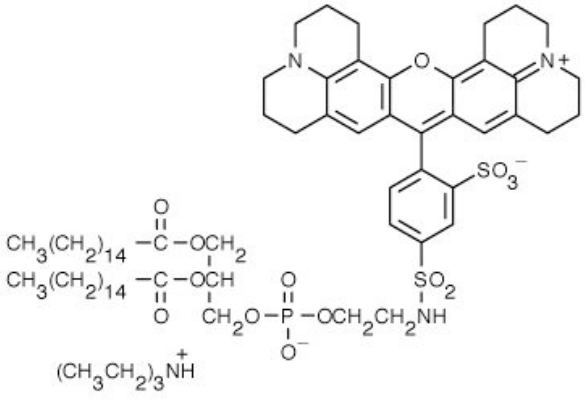

(d) TexasRed®1,2-dihexadecanoyl-sn-glycero-3-phosphoethanolamine, triethylammonium salt (Texas Red® DHPE) **(T1395)**

Fig 3.5: Structures of fluorescent lipids/lipid tags.

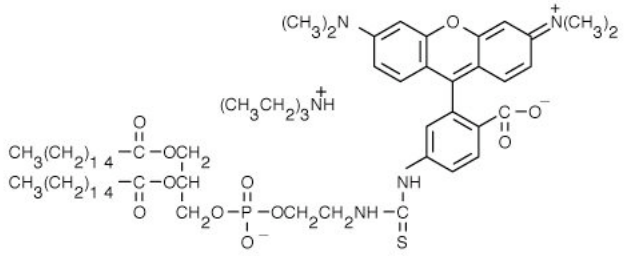

(e) N-(6-tetramethylrhodaminethiocarbamoyl)-1,2-dihexadecanoyl-sn-glycero-3-phospho ethanolamine, triethylammonium salt (TRITC DHPE) **(T1391)**

Fig 3.5 continued: Structures of fluorescent lipids/lipid tags.

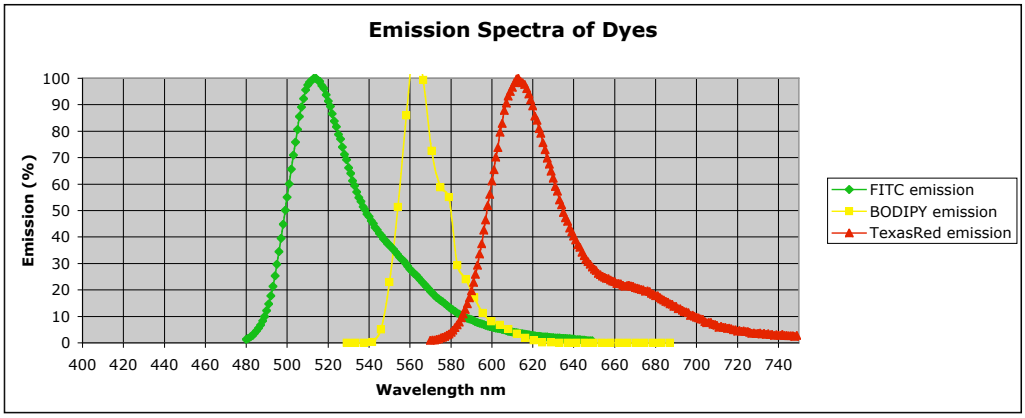

Fig 3.6: Sample emission spectra of FITC, BODIPY (530/550) and TexasRed dyes used in various fluorescence imaging experiments.

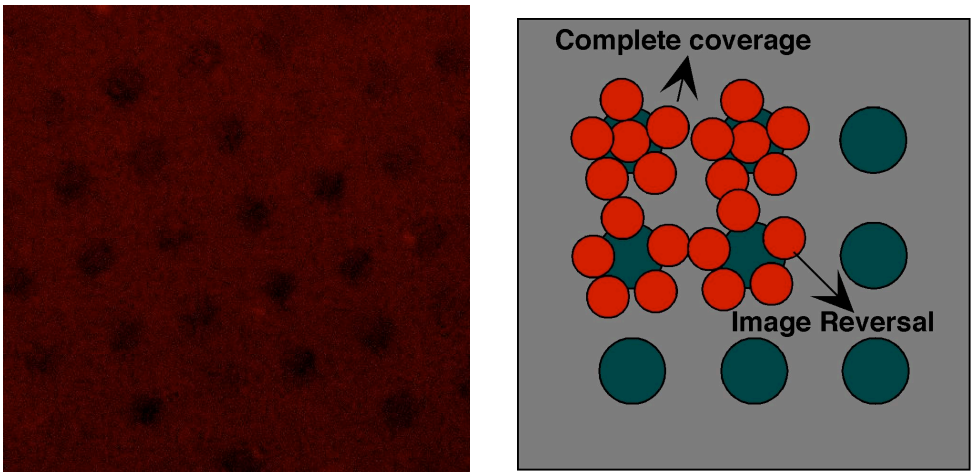

Figure 3.7: Arraying of liposomes on the planar bi-functional substrate: setback

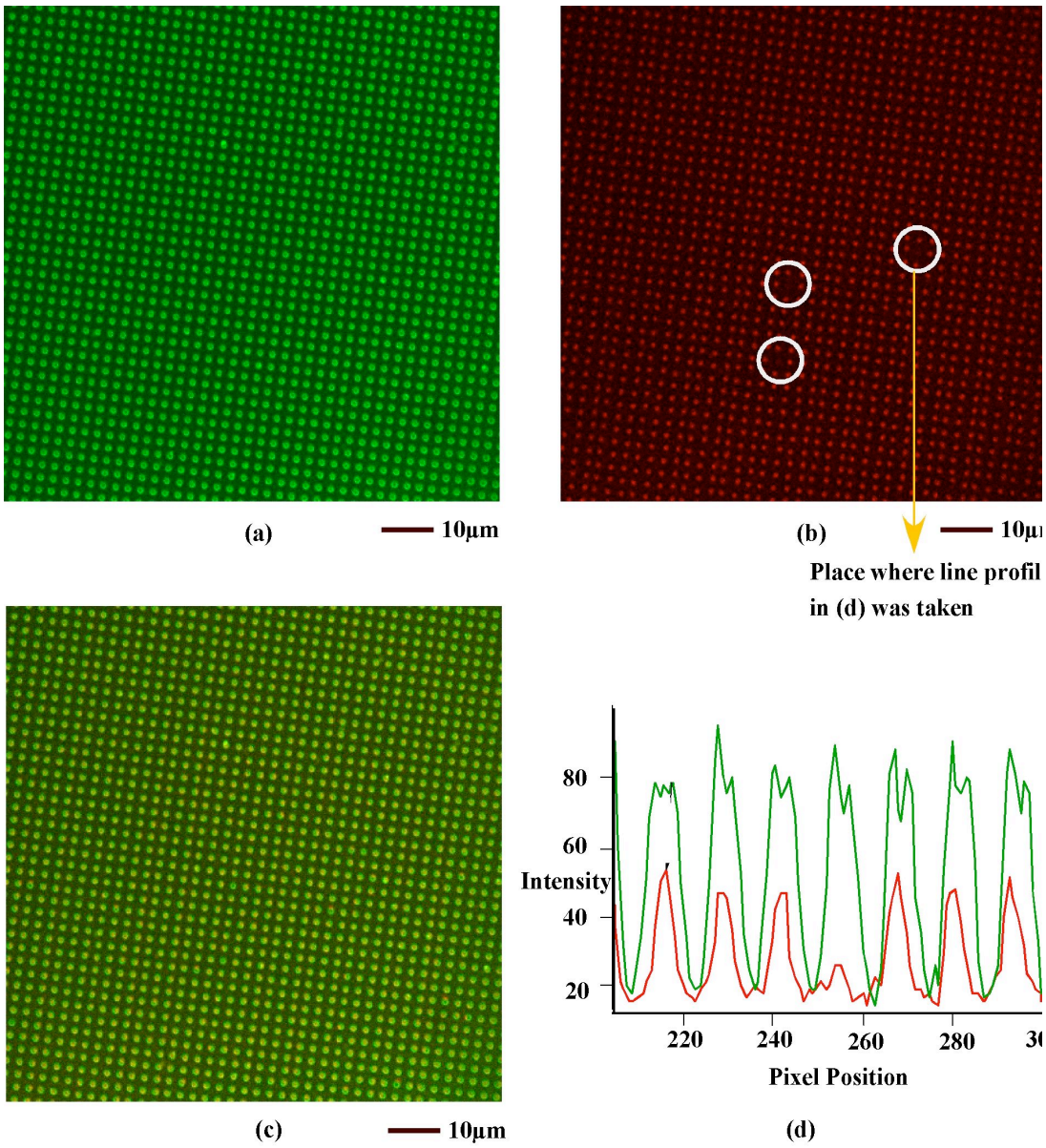

Fig 3.8: Confocal laser scanning microscopy images of the micropatterned surfaces after exposure to liposomes prepared using formulation I. (a) Neutravidin-FITC grid. (b) Dextran-Texas red inside liposomes situated on the grid. (c) Overlay image of a and b. (d) Line intensity profile incorporating one of the empty wells.

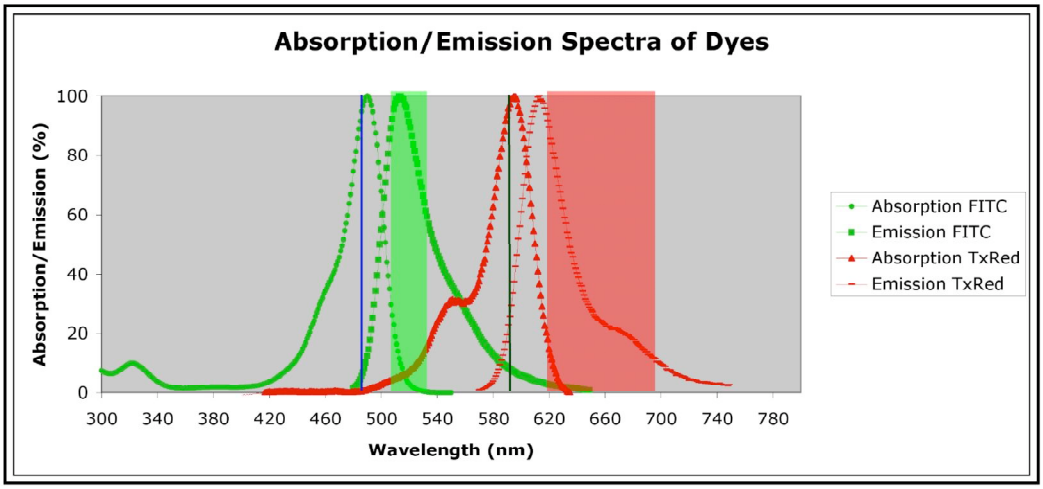

Fig 3.9: Absorption and emission spectra of FITC and TexasRed. Also shown are detection windows of corresponding dyes for experiments in figure 3.8

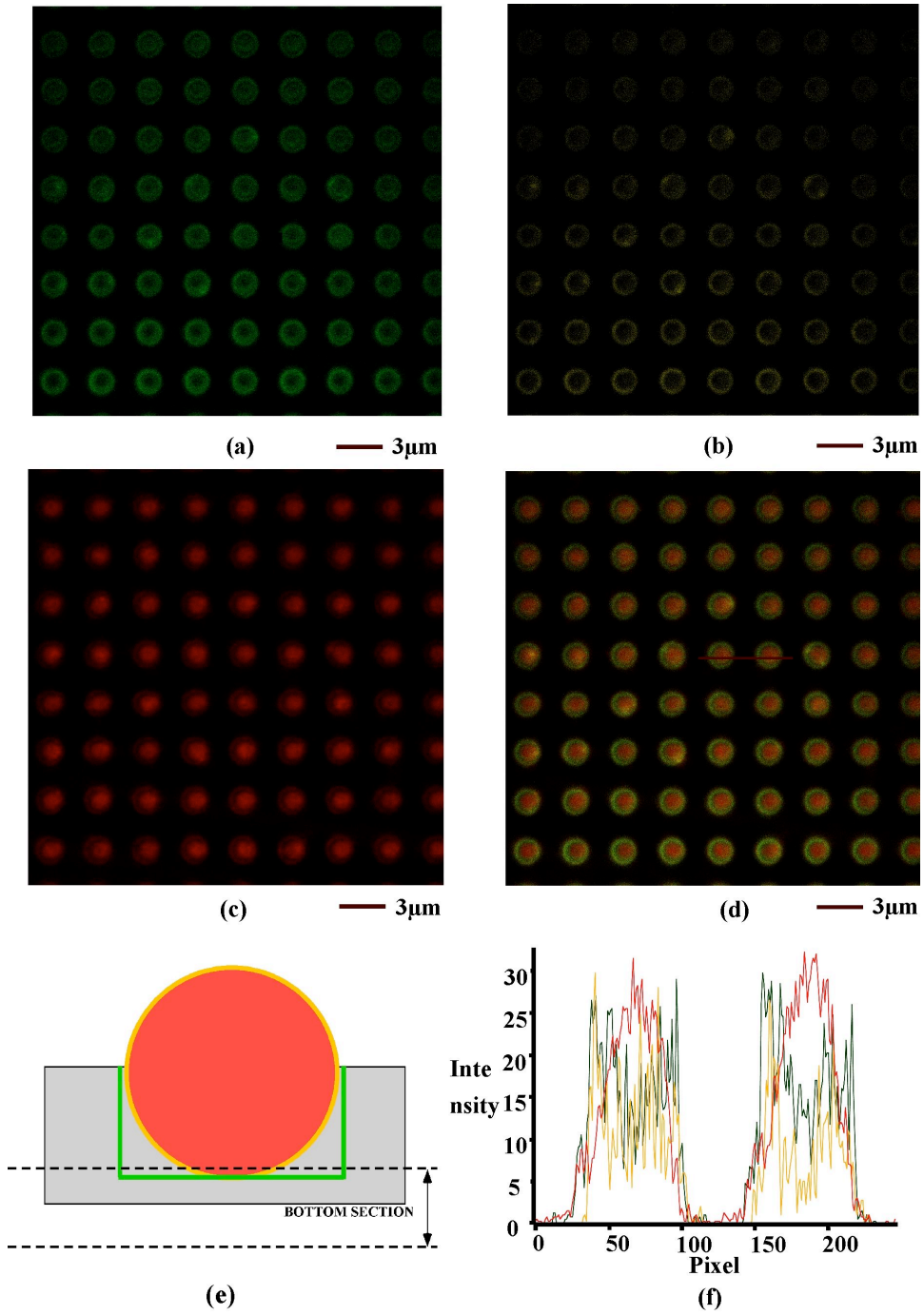

Fig 3.10: Confocal laser scanning microscopy images of the micropatterned surfaces after exposure to liposomes prepared using formulation II taken in a detection region close to the bottom of the microwells (a) Neutravidin®-FITC grid (b) BODIPY (D-3815) lipid in the lipid bilayer of the liposomes (c) Dextran-Texas Red cargo encapsulated inside liposomes situated on the grid and (d) the overlay of the three images (e) Relative location of the detection window close to the bottom of the wells (f) Line intensity profile taken across the section shown in 'd'

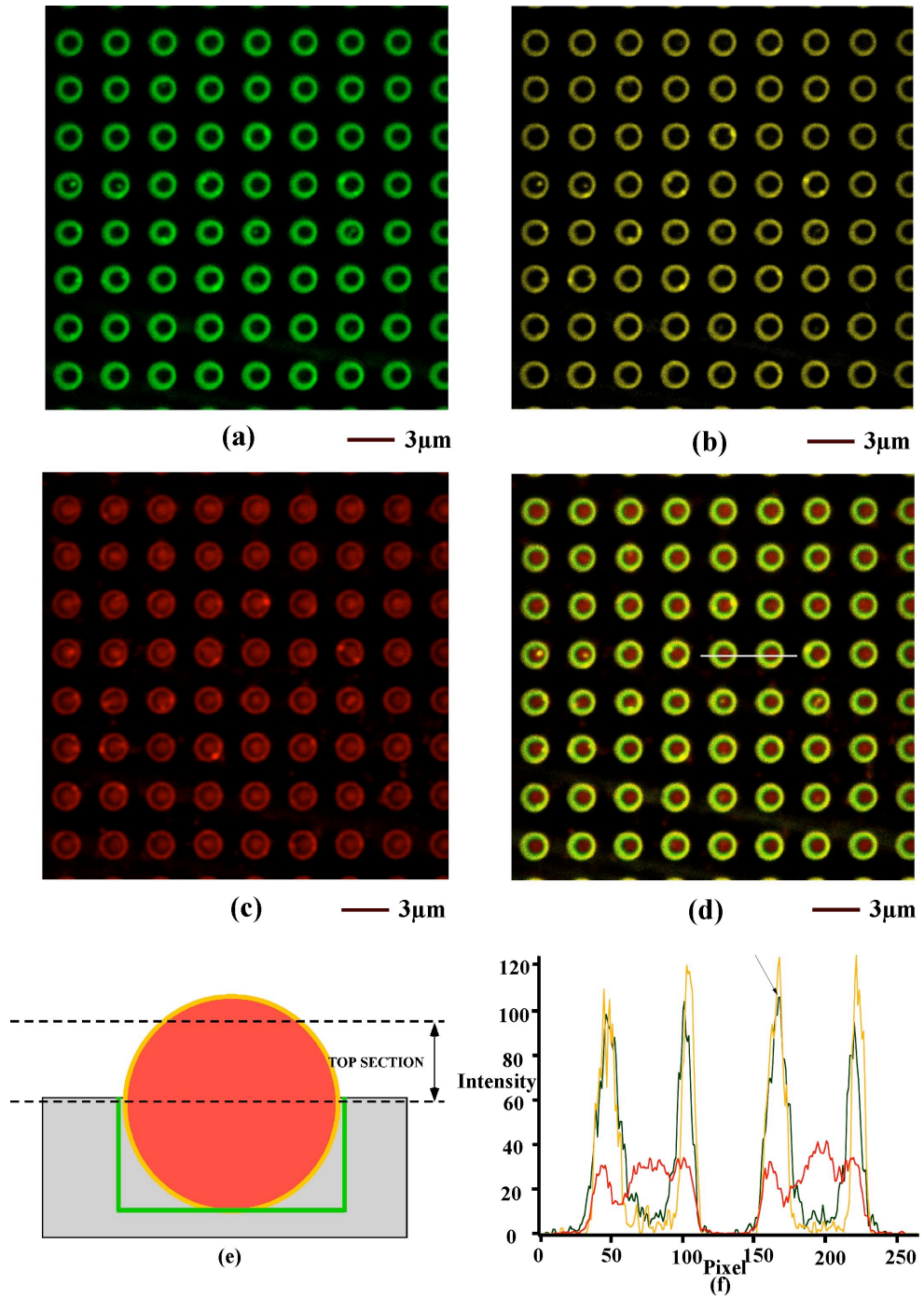

Fig 3.11: Confocal laser scanning microscopy images of the micropatterned surfaces after exposure to liposomes prepared using formulation II taken in a detection region close to the top of the the microwells (a) Neutravidin®-FITC grid, (b) BODIPY (D-3815) lipid in the lipid bilayer of the liposomes (c) Dextran-Texas Red cargo encapsulated inside liposomes situated on the grid and (d) the overlay of the three images (e) Relative location of the detection window close to the bottom of the wells. (f) Line intensity profile taken across the section shown in 'd'

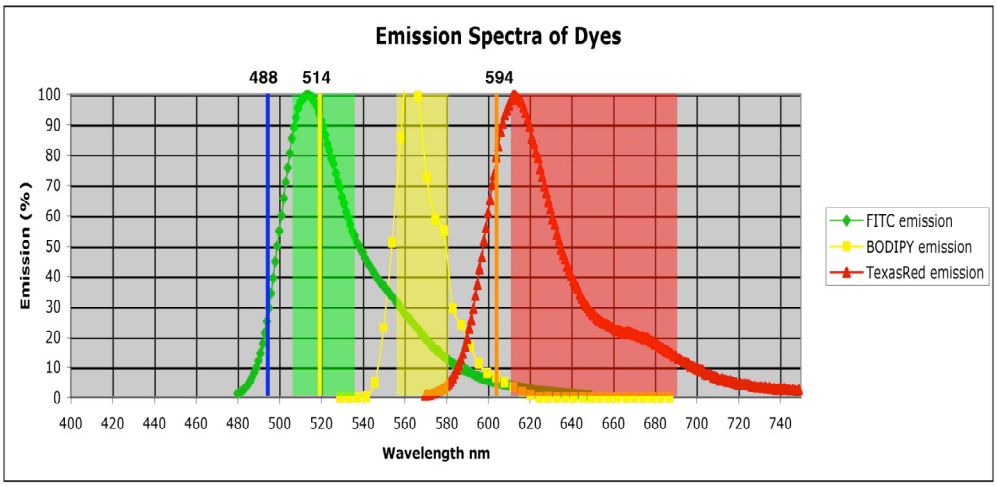

Fig 3.12: Emission spectra of FITC, BODIPY (530/550) and Texas Red tags used in experiments in data sets represented in figures 3.10 & 3.11, corresponding excitation lines and detection regions.

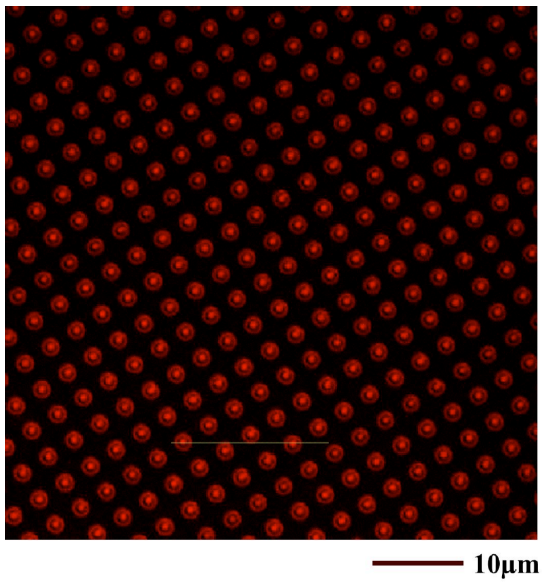

(a)

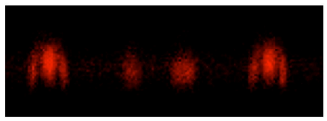

(b)

Fig 3.13: (a) Confocal laser scanning microscopy images of electrostatically arrayed microparticles inside microwells (b) y-section (xz plane) image from line as indicated in 'a'

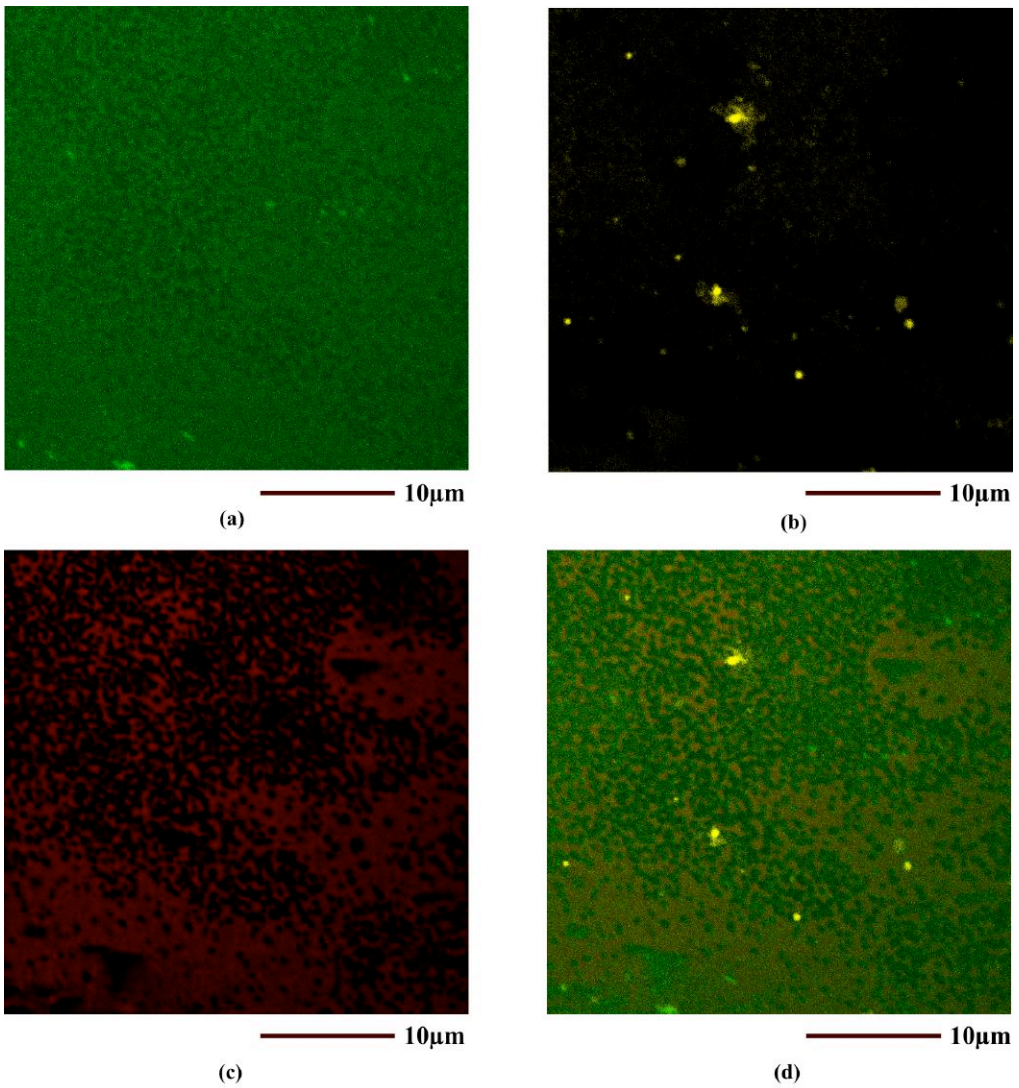

Fig 3.14: Confocal laser scanning microscopy images taken after exposing liposomes prepared using formulation II to Neutravidin^{TM}-FITC layer on a flat silicon wafer (a) Uniform Neutravidin^{TM}-FITC layer (b) BODIPY (D-3815) lipid from the broken liposomes (c) Dextran-Texas Red cargo smeared over the surface (d) Overlay of a-c.

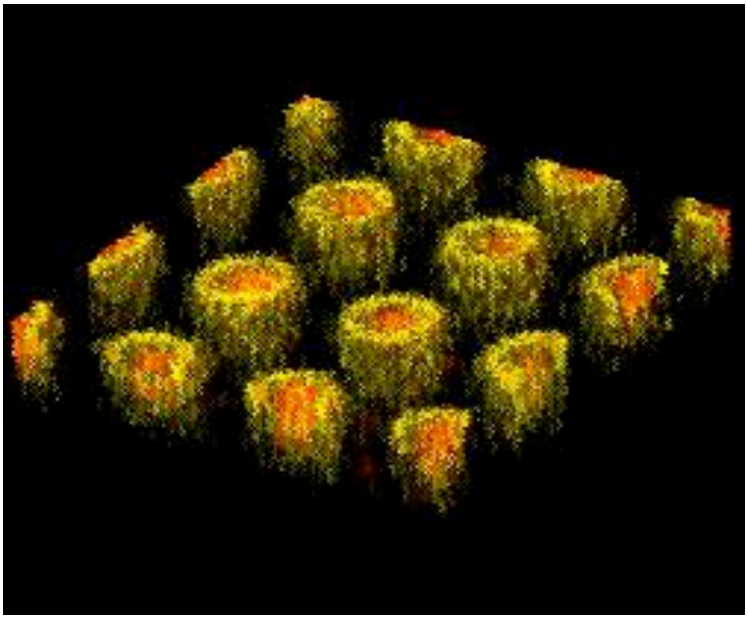

Figure 3.15: 3-D reconstruction from z-section data acquired using CLSM of the immobilized liposomes tagged with β-BODIPY® 530/550 in the lipid layer and carrying Dextran-Texas Red cargo.

Chapter 4

Arraying of liposomes with two different fluorescent lipid tags: a step towards barcoding and multi-receptor biosensor array

4.1 Need for arraying different fluorescently tagged liposome arrays

The protocol discussed in chapter 3 involves using liposomes with only one fluorescent identity (both lipid tag and cargo were identical in all liposomes arrayed on the substrate). In a working biosensor array, more than one membrane receptors are required to be arrayed on the same substrate for molecular screening type of applications involving multiple ligand-receptor interactions. Hence, there is a need to array liposomes with more than one fluorescent identity on the same substrate. This chapter discusses a protocol to array liposomes with two different fluorescent identities on the same substrate. The protocol can in general be extended to multiple liposomes with many fluorescent tags. Figure 4.1 shows a 2-D conceptualization of this concept. Two approaches were used to address this issue:

1. **Mixed adsorption:** Liposomes with two different fluorescent identities were mixed and arrayed statistically on the same substrate using the protocol described in chapter 3.
2. **Sequential adsorption:** Liposomes with one fluorescent identity were first exposed to the chemically modified substrate in such a way that some wells remain empty after the wash off step. Then the substrate was exposed to liposomes with another fluorescent identity to backfill the empty wells.

Both of these approaches face possible problems of fluorescent lipid exchange, non-specific binding of excess dye in solution etc. To exclude excess lipid and excess fluorescent dye if any, the liposome solutions were passed through a column packed with Sephadex G75 gel using a BioLogic HR workstation and a BioFrac Fraction collector setup (BIO-RAD). Typical lipid compositions used during this set of experiments is:

1. DSPC/Cholesterol/Biotin-PE in 0.475: 0.475:0.05 molar proportions.
2. Fluorescent lipid tags were added in 1:100 molar proportions to aforementioned formulations.

Three different fluorescent lipid tags (obtained from Molecular Probes) were used: T1391 (Excitation: 594nm, Detection: 610-690nm), D3815 (Excitation: 514nm, Detection: 530-590 nm) and D3793 (Excitation: 488nm, Detection: 500-535nm). More information about these lipid tags is available in Table 3.2.

4.2 Mixed attachment of liposomes with two fluorescent identities on the same substrate:

In this set of experiments, liposomes with two fluorescent tags were used: T1391 (red) and D3815 (yellow). These liposomes were passed through sephadex G75 column to remove excess lipid matter and fluorescent dyes if any. The liposomes were found to have size in the range of 0.85-0.9 μm. The surface was chemically modified to have Neutravidin-FITC in the wells. Figure 4.2 shows the data collected using confocal laser scanning microscopy after exposing the mixture of these liposomes to the substrate for 1 hr followed by multiple rinsing. Figure 4.2a is the fluorescence data collected from red T1391 incorporated liposomes, figure 4.2b is the fluorescence data collected from yellow D3815 incorporated liposomes and figure 4.2c is an overlay image, which clearly indicates that the liposomes have lost their identities. This could be due to potential exchange of fluorescent lipids either in the solution or on the substrate [93, 94]. Experiments were performed with various liposome concentrations and exposure times, but results obtained were similar to those shown in figure 4.2. Hence, this approach is not useful to array liposomes with distinct fluorescent identities.

4.3 Sequential attachment of liposomes with two fluorescent identities on the same substrate:

In this set of experiments, liposomes with two lipid tags were arrayed in sequential manner on the same substrate. Sequential method of attachment was chosen to minimize exchange of lipid tags in between two sets of liposomes [95]. Both sets of liposomes were prepared using the same formulation as described in mixed adsorption section 4.2 and with different lipid tags D3793 (green) and D3815 (Yellow) in 1:100 proportion. First green liposomes were exposed to chemically functionalized microwell substrate for 30 min followed by rinsing. Then yellow liposomes were exposed to the same substrate to occupy empty wells for 30 min followed by rinsing.

Figure 4.3 shows fluorescence data collected during this set of experiments. This data was collected using wide-field imaging by 63X objective of the confocal laser scanning microscope. It is evident that there are two different liposome colors on the substrate: green and yellow and these liposomes are only occupying the chemically functionalized microwells. Defects in figure 4.3a can be attributed to wells that stayed unoccupied during the sequential attachment of liposomes. Figure 4.3b is a zoomed in region of figure 4.3a, which further supports the claim that liposomes retain their fluorescent identity after arraying on the substrate in sequential manner. Figure 4.3c shows RGB profiles of two liposomes (green and yellow) as shown in inset in figure 4.3b. They clearly have different RGB values with one being greener than the other. Based on these results, we can claim that the protocol can potentially be used to array more than one type of membrane receptors on the same substrate. This finding is important for molecular

screening type of applications by using fluorescent lipid tags as barcodes for membrane receptor or membrane protein incorporated liposome arrays.

Since there are only limited number of organic fluorophores available and their emission profiles are usually wide, other bar-coding methods such as use of Q-dots can be explored to either tag the lipid bilayer or the core of the liposomes for use of this protocol to array several membrane proteins/receptors on the same substrate. Q-dots have various advantages including narrow emission spectra, higher quantum yields, and higher multiplicity, which can be manipulated using various combinations of size and concentrations of Q-dots [96-98]. Details about this concept are discussed in the future work section.

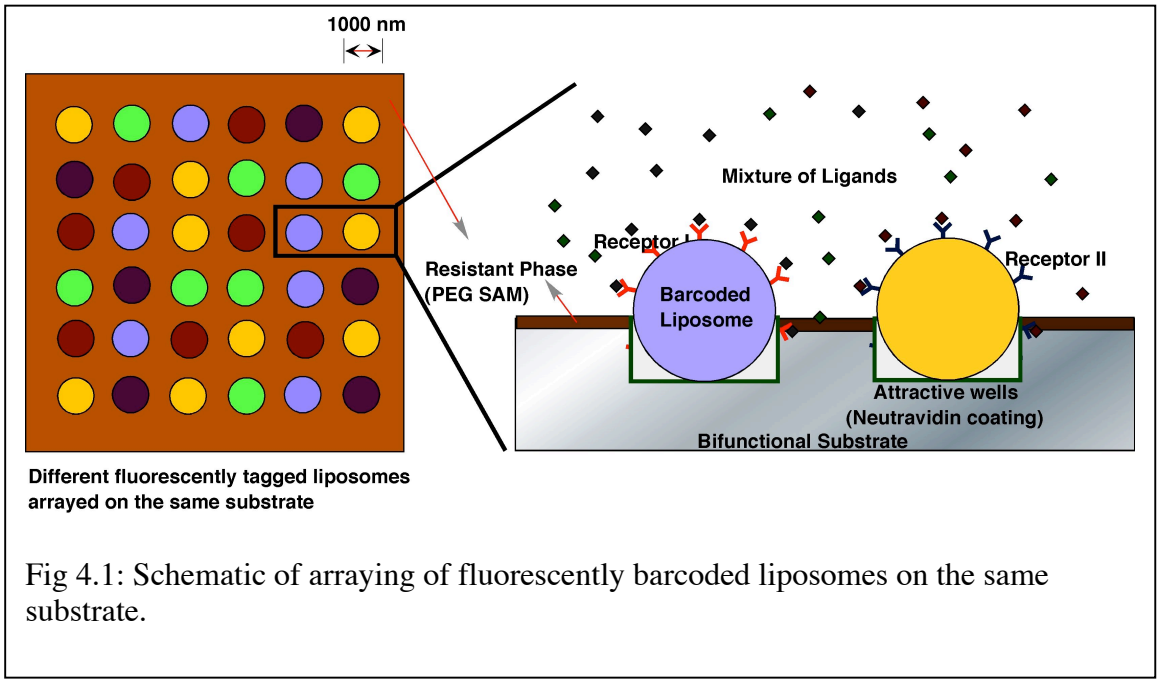

Fig 4.1: Schematic of arraying of fluorescently barcoded liposomes on the same substrate.

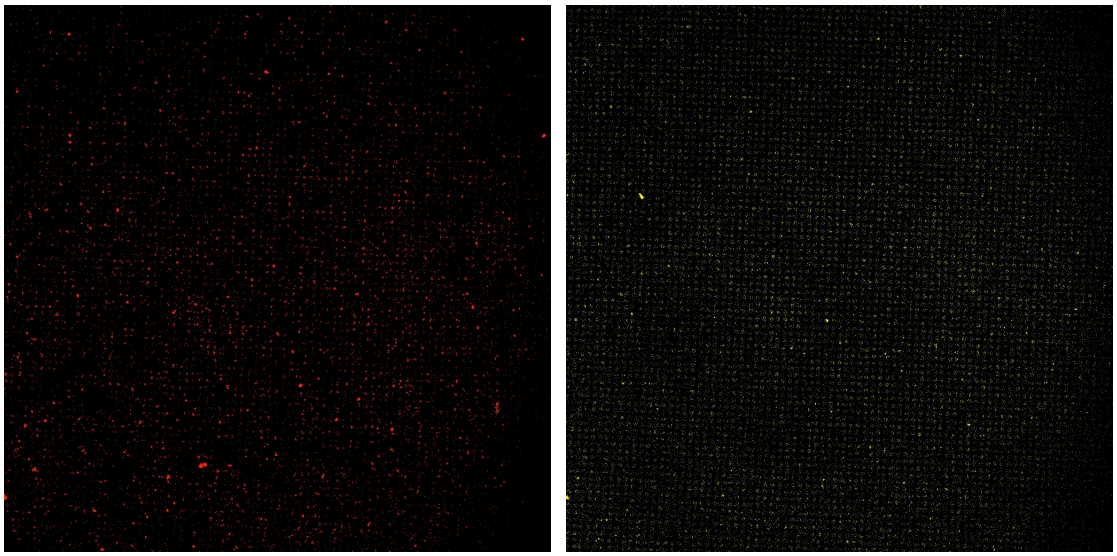

(a) (b)

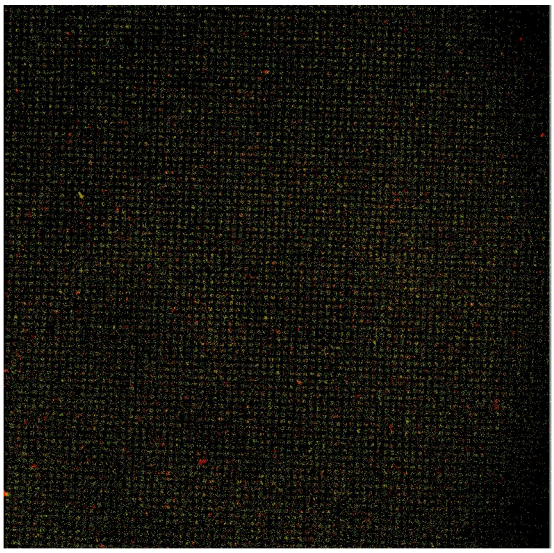

(c)

Figure 4.2: Confocal laser scanning microscopy data collected after mixed adsorption of liposomes from solution (a) T1391 fluorescence from Texas Red tag on lipid bilayer of liposomes from first set (b) D3815 fluorescence from BODIPY tag on lipid bilayer of liposomes from second set (c) Overlay image of a and b: clear indication of lipid exchange.

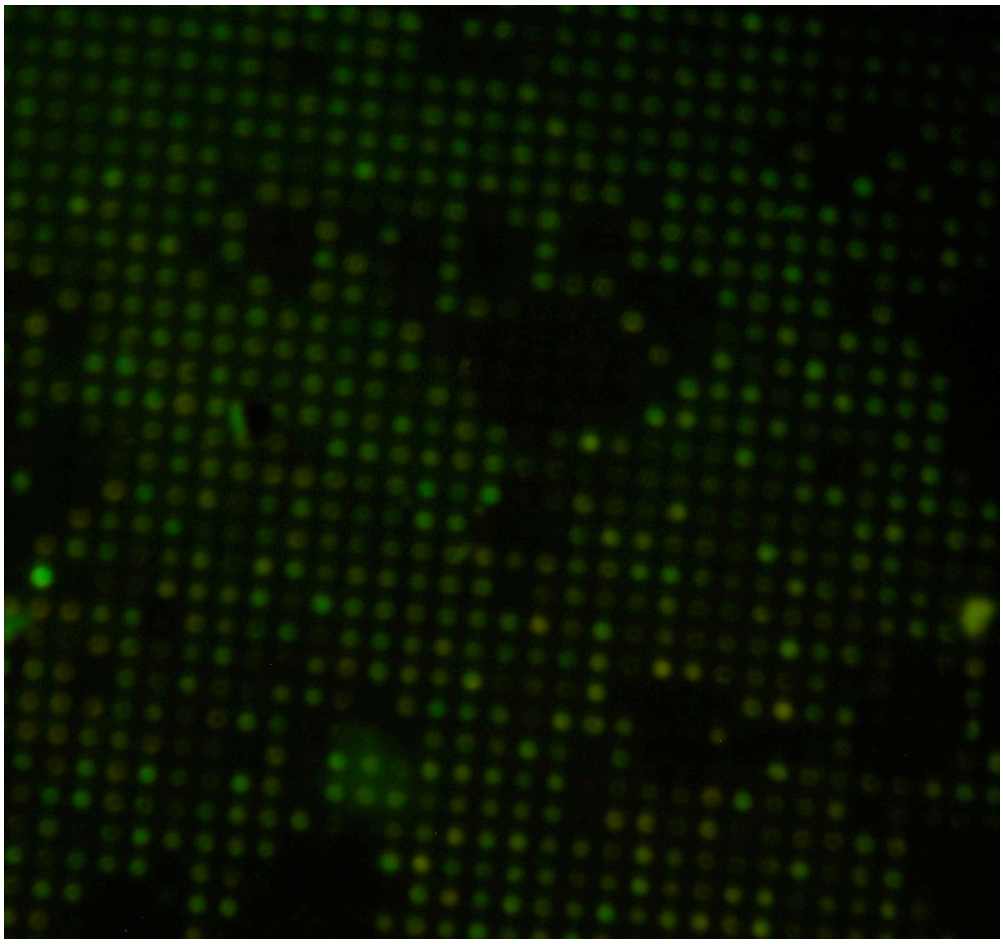

(a)

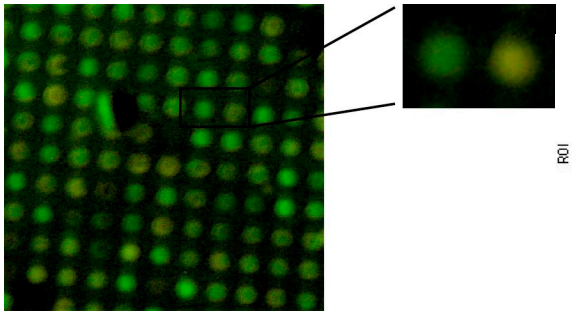

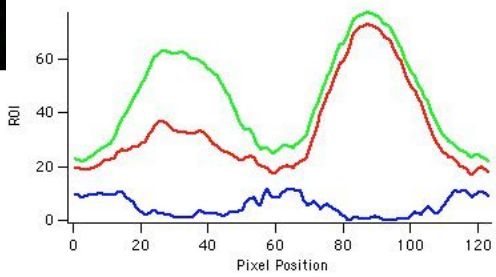

(b) (c)

Figure 4.3: Sequential attachment of two different liposomes without any receptors and with green and yellow fluorescent lipid tags. (a) widefield image taken using 63X objective on confocal microscope. (b) Zoomed in image of a (c) RGB values of two liposomes in the inset in figure b.

Chapter 5:

Application of intact liposome arrays for toxin detection

5.1 Introduction:

Biosensors are devices that use biological or chemical receptors to detect analytes in a sample. They give detailed information on the binding affinity, and in many cases also the binding kinetics of an interaction. Typically the receptor molecule must be connected in some way to a sensor that can be monitored by a computer. The majority of screens employed in drug discovery require some type of radio- or fluorescent-labeling to report the binding of a ligand to its receptor. With almost half of the drugs on the market today targeting membrane receptors[7], there is considerable interest in methods to create spatially addressable arrays of lipids or liposomes incorporating the receptors. Majority of the studies report use of solid supported lipid bilayers to array various membrane receptors on a single substrate for bio-detection purpose.[8, 99-103] The solid substrate suppresses thermally activated membrane fluctuations, limits the incorporation of membrane proteins, induces substrate-electrostatics-driven asymmetry, and hinders the translational mobilities and phase equilibration in bilayers.[102] Thus there is an increasing demand in using intact liposome microarrays for displaying membrane receptors and proteins for bio-detection.

This part of research work involves proof of concept experiments using the intact liposome microarray format and known receptor-ligand system to check the applicability of the liposome microarray platform for biodetection. In particular, Monosialoganglioside G_{M1} was incorporated in the lipid bilayer of liposomes and these receptor liposomes were arrayed onto the chemically functionalized substrates. Figure 5.1 shows the molecular structure of G_{M1} receptors. These G_{M1} receptor incorporated liposome arrays are used to detect specific binding of Cholera Toxin Subunit B (CTB) to the surface receptors using

CLSM. Cholera toxin, an enterotoxin of *Vibrio Cholerae*, is composed of two subunits: A (M_w = 27 kDa) and B (M_w = 11.6 kDa), with the stoichiometry AB_5. The protein binds to the ganglioside GM1 receptor on the cell surface via the B components. Typical cholera toxin binding affinity to whole cells is K_D = 0.46nM. [104]

Most of the studies reporting the use of G_{M1} receptor to detect the presence of cholera toxin utilize supported lipid bilayers [102, 103, 105-108]. Craighead et.al. [108] report use of micron-sized lipid domains, patterned onto planar substrates and within microfluidic channels to assay the binding of bacterial toxins using G_{M1} or G_{T1b} receptors incorporated in the SLBs. Their reported sensitivity is down to 100 pM concentrations of the toxins. Singh et.al.[106] use fluorescently labeled liposomes incorporating receptors in a sandwich fluoroimmunoassay for tetanus, botulinum, and cholera toxin detection with concentrations as low as 1 nM. Lahiri et.al.[105] describe the fabrication of microarrays of lipids containing G_{M1} and G_{T1b} receptors, using quill pin printer and 384 well microplate and their application in selective detection of cholera and tetanus toxins respectively. The supported lipid bilayer (SLB) based techniques suffer from various disadvantages as described earlier and quill pin printing technique has limitations of size to prepare the micro spots. Thus, the use of intact liposome microarray format for membrane receptor (G_{M1} ganglioside) based biosensors seems to be the next logical step towards ultra-miniaturization and lower sample detection volumes.

5.2 Methods:

Lipid films were prepared with two different formulations:

(1) Formulation-I: DSPC/Cholesterol/Biotin-PE/G_{M1} in 0.45:0.45:0.05:0.05 molar proportions.

(2) Formulation-II: DSPC/Cholesterol/Biotin-PE in 0.475: 0.475:0.05 molar proportions.

Fluorescent lipid tags, if used, were added in 1:100 molar proportions to aforementioned formulations.

These constituents were mixed using chloroform and dried overnight under vacuum resulting into approximately 2 mg of lipid films in glass vials. These vials were sealed under nitrogen using Parafilm (Fisher Scientific) and used as needed. 1 ml HEPES buffer (HEPES 20mM, sodium chloride 100mM, EDTA 1mM) of pH 7.5 was used to hydrate these films to form multilamellar vesicles. This buffer was pre-filtered using 0.2 μm syringe filter and degassed by bubbling of excess Ar gas through the solution. After three freeze-thaw cycles each lasting 15 min, this solution was extruded using 1μm pore size membrane in a mini extruder by Avanti Polar Lipids to form unilamellar vesicles (liposomes) of the same size range as the pore size of the membrane. Particle size analysis of the extruded liposomes using a Nano-series Zetasizer (Malvern Instruments) confirmed the presence of liposomes of approximately 0.9 μm average diameter. To exclude excess lipid and excess fluorescent dye if any, the liposome solution was passed through a column packed with Sephadex G75 gel using a BioLogic HR workstation and a BioFrac Fraction collector setup (BIO-RAD). After separation, the purified fraction was checked for correct particle size using the Zetasizer and using epi-fluorescense

microscopy (Nikon Eclipse TE 200 inverted microscope) to visualize the liposomes. The liposomes were also characterized for their surface charge using zeta potential measurements. Average zeta potential values for liposomes prepared using formulation-I (G_{M1} receptor liposomes)and formulation-II (liposomes with no receptors) with BODIPY lipid tag are –18mV and –11mV respectively in HEPES buffer of pH 7.5. G_{M1} receptors are inherently negatively charged [106]; hence the liposomes with G_{M1} receptors have more negative charge than those without G_{M1} receptors.

The bi-functional substrates with Neutravidin coated microwells in the background of passivating PEG-SAM (discussed in section 2.6.2) were glued to previously cleaned glass microscope slides (obtained from Fischer scientific) using Permabond® industrial grade elastomer bonding adhesive. Press-to-seal™ silicone isolators were used to prepare the sample cell around these surfaces and 500 µl of liposome solution was exposed to them for specific time duration. Multiple rinsing steps using pre-filtered HEPES buffer of pH 7.5 were used to wash off excess liposomes, which are not attached to the surface in a specific manner. Cover slips (clean and with a monolayer of PEG-silane) were used to cover the surfaces under HEPES buffer of pH 7.5 for confocal laser scanning microscopy (CLSM).

5.3 Detection of Cholera Toxin from analyte solutions using liposome microarrays with only G_{M1} receptor liposomes:

In these set of experiments, liposomes prepared using formulation I (with G_{M1} receptors) and with D3815 lipid tag (1:100 molar proportions) were arrayed on Neutravidin-FITC coated microwell substrates for 3 hrs followed by rinsing using excess

HEPES buffer (pH 7.5). This array was then exposed to 0.5 μM fluorescently tagged (AlexaFluor 647, Molecular Probes) Cholera Toxin subunit B (CT647) in HEPES buffer (pH 7.5) for 1 hr followed by rinsing using the buffer.

Two control experiments were performed to check the specificity of CT647 binding to the receptor-incorporated liposomes.

1. Liposomes prepared using formulation II (without any receptors) with D 3815 lipid tag (1:100 molar proportions) were arrayed on different Neutravidin-FITC coated microwell substrates for 3 hrs followed by rinsing using excess HEPES buffer (pH 7.5). This array was then exposed to the same concentration of CT647 for 1 hr followed by rinsing.
2. Neutravidin-FITC coated microwell substrates without any liposomes were exposed to the same concentration of CT647 for 1 hr followed by rinsing.

The data collected during these sets of experiments is discussed in figures 5.2, 5.3, and 5.4.

Figure 5.2 shows fluorescence data collected after the exposure of G_{M1} receptor liposomes arrayed on a chemically functionalized substrate (with Nu-FITC coated microwells in the background of PEG terminal SAM) to fluorescently tagged cholera toxin (CT647). The fluorophores were chosen on the basis of their well-separated emission spectra in order to minimize crosstalk between detection channels. Appropriate spectral detection regions were chosen while imaging using confocal laser scanning microscopy in sequential scanning mode. In this mode of data collection, each fluorescent dye is separately excited in a sequential manner to suppress signal cross talk or bleed-through.

Figure 5.2a shows the fluorescence (Excitation: 488nm, Detection: 500-530 nm) from the green FITC tag on Neutravidin molecules present inside the microwells on the micropatterned surfaces. Neutravidin is present both along the walls and at the bottom of the wells [109]. Figure 5.2b shows the fluorescence (Excitation: 514nm, Detection: 530-590 nm) from BODIPY fluorescent tag present in the lipid bilayer of the liposomes. Figure 5.2c shows the fluorescence (Excitation: 633nm, Detection: 650-750nm) from cholera toxin attached to G_{M1} receptors present on the surface of liposomes.

Figure 5.3a,which is an overlay image of figures 5.2a, 5.2b and 5.2c, clearly shows the co-localization of the fluorescence from the three dyes. This suggests that liposomes are residing inside the chemically functionalized microwells and are intact based on previous findings [109]. Based on the 0.90 μm average diameter of the liposomes, measured using a Malvern Zetasizer, which is of the order of the microwell dimensions (1.2 μm), it can be claimed that there is only one liposome in each microwell. Figure 5.3 also shows negligible attachment of cholera toxin and lipid matter in the background of the wells. Hence PEG silane SAM is very effective in preventing non-specific adsorption of Cholera Toxin and liposomes. Figure 5.3b is a line intensity profile plotted along a section shown in figure 5.3a. It further supports the claim that cholera toxin got selectively attached only to G_{M1} receptor liposomes arrayed on the substrate.

Two control experiments were performed in order to support the claim that cholera toxin attachment as shown in figure 5.2C was specific to the presence of G_{M1} receptors in the lipid bilayer of arrayed liposomes. Figure 5.4 shows fluorescence data collected using CSLM after exposing fluorescently tagged cholera toxin (CT647) to Neutravidin-FITC array without any liposomes. Figure 5.4a is the fluorescence of FITC

fluorescent tag on the Neutravidin present inside the wells (Excitation: 488nm, Detection: 500-530 nm). Figure 5.4b is the fluorescence data collected after exposing the Neutravidin-coated microwells to CT647 (Excitation: 633nm, Detection: 650-750nm). Figure 5.4b indicates that there is negligible attachment of cholera toxin to Neutravidin present inside the microwells. Figure 5.4c is an overlay image of a and b. Figure 5.4d is a line intensity profile taken along the section shown in figure 5c. It further supports the claim of negligible cholera toxin attachment to Neutravidin. In second set of control experiments, liposomes prepared with formulation-II (without G_{M1} receptor) were arrayed on Neutravidin-coated microwell surfaces and were exposed to the same concentration of CT647 for same time duration. The observation was similar to data in figure 5.4 (data not shown). Thus for attachment of cholera toxin to arrayed liposomes, presence of G_{M1} receptors is essential.

5.4 Detection of Cholera Toxin from analyte solutions using microarrays with G_{M1} receptor liposomes and non-G_{M1} receptor liposomes arrayed on the same substrate:

In this set of experiments, liposomes with and without G_{M1} receptors were arrayed on the same substrate using the sequential attachment protocol discussed in chapter 4. This data is the first step towards a more realistic biosensor array where more than one receptor is arrayed on the same substrate and specific ligand-receptor interactions are identified.

Liposomes prepared using formulation-I (G_{M1} receptor liposomes) had no fluorescent lipid tag and liposomes prepared using formulation-II (No receptor liposomes) had yellow (D3815) lipid tag. After arraying these two sets of liposomes on

the same substrate in sequential attachment manner, these microarrays were exposed to 0.5 μM CT647 solution in HEPES buffer (pH 7.5) for 30 min. This set of data shows selectivity of cholera toxin binding to G_{M1} receptor liposomes arrayed on the substrate. Confocal laser scanning microscopy (CLSM) was used to image the fluorescently labeled microwells, liposomes and cholera toxin attached to liposome microarrays using the Leica TCS SP2 AOBS confocal microscope.

Figure 5.5 shows the data collected using CSLM during the set of experiments in which both G_{M1} and non-G_{M1} receptor liposomes were arrayed on the same substrate as described earlier. G_{M1} receptor liposomes, prepared using formulation-I have no fluorescent lipid tag and non-G_{M1} receptor liposomes have a yellow fluorescent lipid tag (D3815) (Excitation: 514nm, Detection: 530-590 nm). The cholera toxin has alexafluor647 fluorescent tag (CT647)(Excitation: 633nm, Detection: 650-750nm). Data was collected using sequential scanning mode.

Figure 5.5a is an overlay image of the two sets of fluorescence data, which clearly shows that yellow and blue colors are distinguishable beyond doubt. Figure 5.5b is a zoomed in overlay image and figure 5.5c is a line intensity profile taken along the section shown in figure 5.5b. The line intensity profile implies that cholera toxin doesn't attach to liposomes without G_{M1} receptors (negligible binding). The presence of slight yellow fluorescence in places where cholera toxin has attached can be attributed to possible lipid exchange between the two sets of liposomes, but their lipid bilayer fluorescence intensities are 1/3 of the liposomes without any receptors. Thus this data proves that this protocol can be used to selectively detect the presence of a toxin from analyte solutions. This result also supports the claim that the protocol can be potentially used for molecular

screening type of applications, where there is a need to have more than one membrane receptors/proteins arrayed on the same substrate.

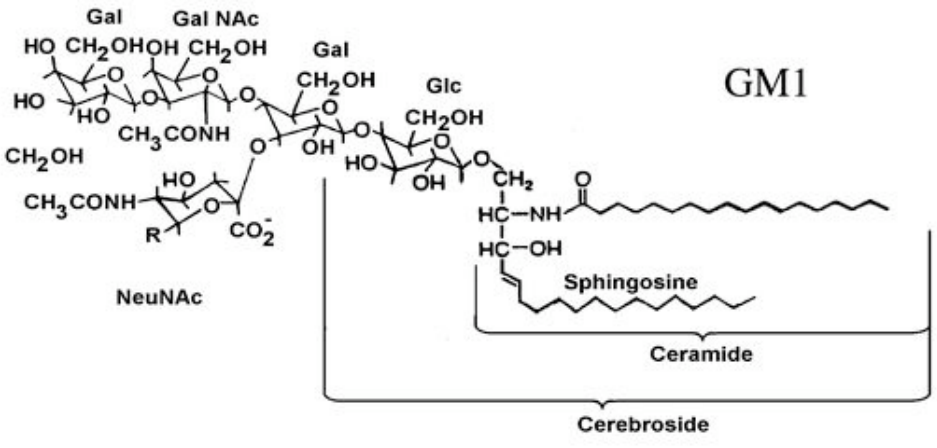

Fig 5.1 Monosialoganglioside G_{M1} cell membrane receptor.

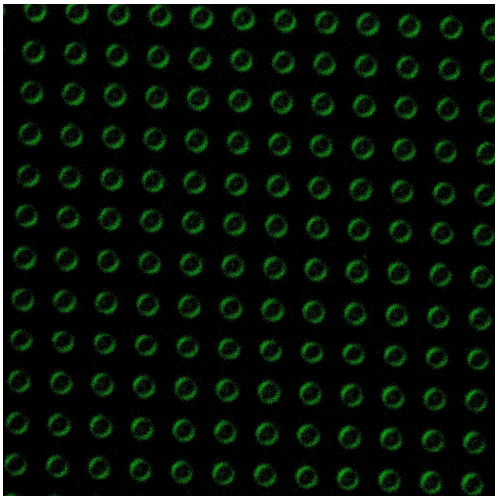

(a)

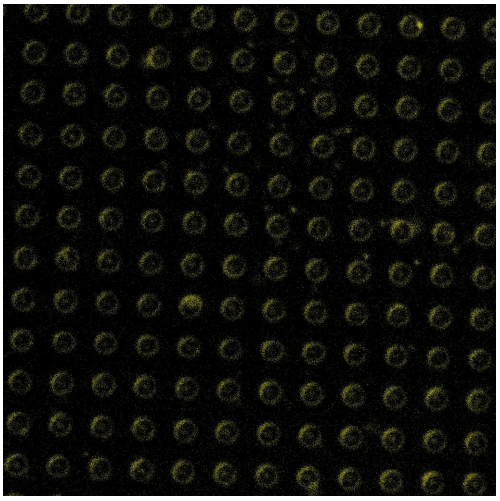

(b)

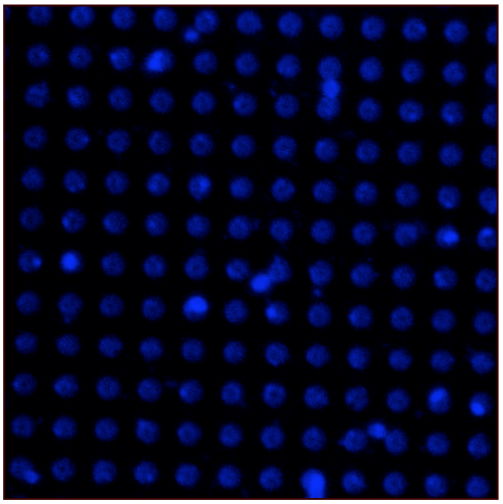

(c)

Fig 5.2: Detection of cholera toxin using microarrays prepared using liposomes with G_{M1} receptors: fluorescence data collected using confocal laser scanning microscopy (a) Nu-FITC fluorescence from the microwells (b) BODIPY fluorescence from the lipid bilayer of liposomes (c) CT647 fluorescence from cholera toxin attached to G_{M1} receptors in the lipid bilayer of liposomes.

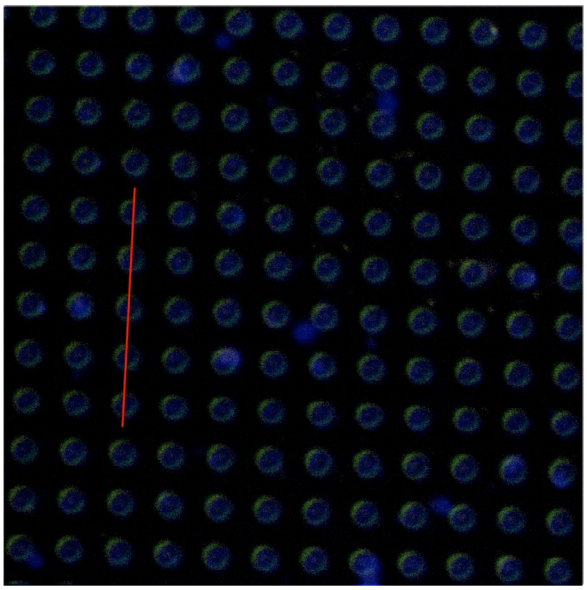

(a)

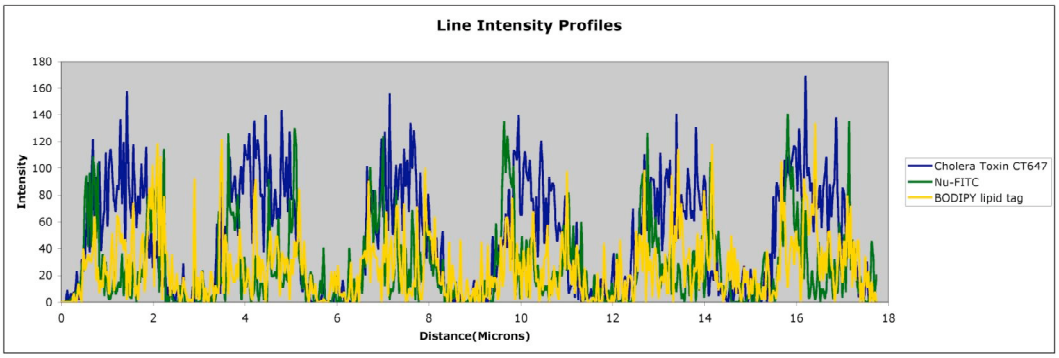

(b)

Fig. 5.3: (a) Overlay image of a, b and c from figure 3 (b) Line intensity profile along the section shown in the overlay image.

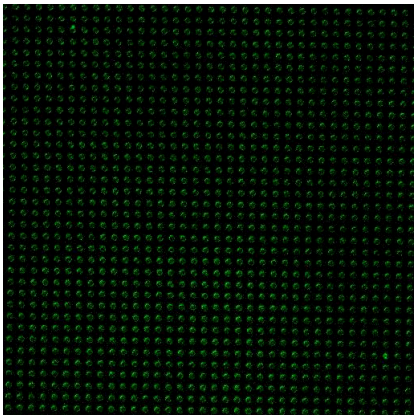

(a)

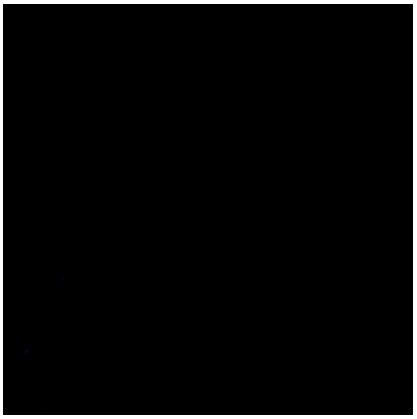

(b)

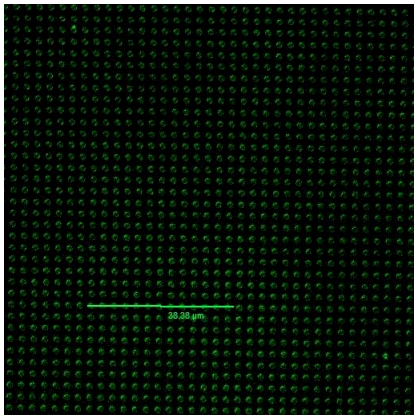

(c)

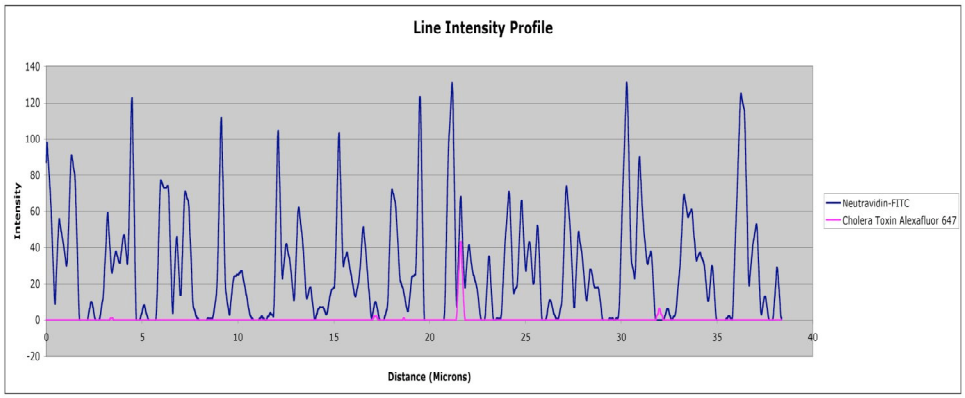

(d)

Fig 5.4: Exposure of cholera toxin (CT647) to Nu-FITC microwells without any liposomes: (a) Neutravidin-FITC fluorescence (b) CT647 fluorescence collected after exposure of cholera toxin to Nu-FITC array for 1 hr (c) overlay image of a and b (d) Line intensity profile along the section shown in figure c.

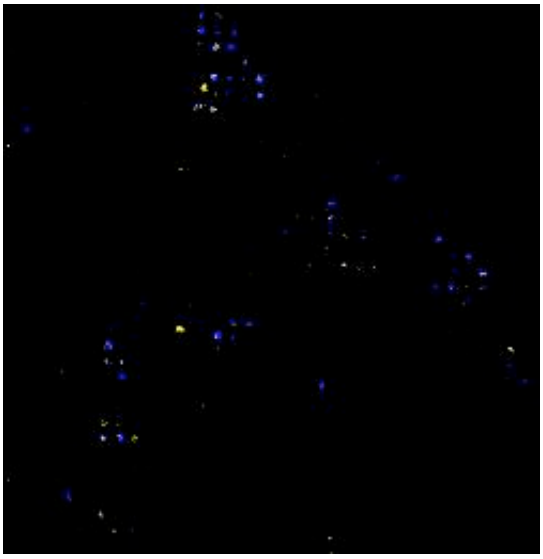

(a)

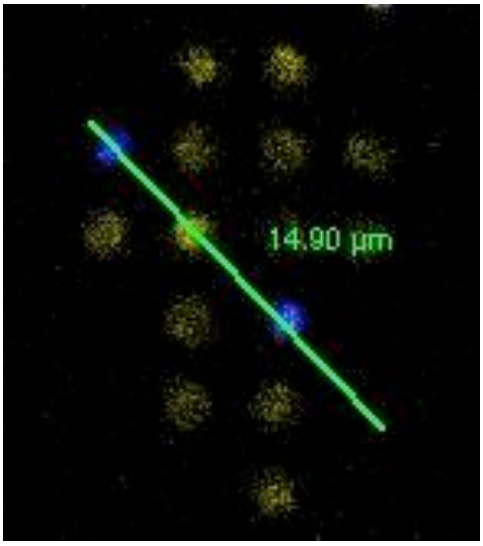

(b)

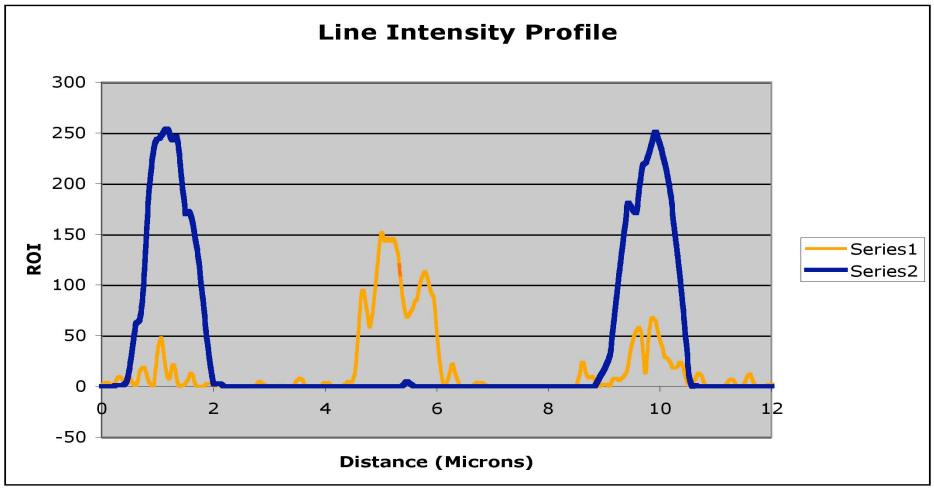

(c)

Figure 5.5: Selective attachment of cholera toxin to G_{M1} liposomes.

(a) Overlay of sequential scanning data for BODIPY (yellow) tag on liposomes without receptor and cholera toxin (CT647, blue) attached to G_{M1} receptors on the surfaces of liposomes without any fluorescent tag. These liposomes are arrayed on the same substrate using sequential attachement protocol.

(b) Zoomed in overlay shows two distinct colors.

(c) Line intensity profile taken along section shown in overlay b.

Series 1: BODIPY fluorescence from lipid bilayer of non-G_{M1} liposomes

Series 2: CT647 fluorescence from cholera toxin attached to G_{M1} liposomes.

6. Summary and Future work

This thesis describes a highly robust method of arraying individual intact liposomes onto chemically functionalized microwell substrates. The thesis outlines a strategy to prepare bi-functional substrates for arraying of liposomes in the chapter 2 followed by the methodology to array individual liposomes using specific interactions in the chapter 3. Chapter 4 outlines a method to fluorescently barcode the lipid bilayers of liposomes and array liposomes with different fluorescent identities on the same substrate using sequential attachment technique. Chapter 5 elaborates on application of the liposome microarray platform for detection of cholera toxin from solution as a proof of concept study. This platform has widespread applications in arraying of various membrane proteins or receptors for bio-detection applications pertaining to pharmaceutical industry and national defense related applications.

The practical difficulty in this platform is the broad emission profiles of organic fluorophores and their limited availability. This limits the number of fluorescent identities for liposomes, and hence the number of receptors or membrane proteins that could be arrayed on a single substrate. Ideally, at least a few hundred receptors need to be arrayed on the same substrate for high-throughput screening type of applications. Hence, new methods to fluorescently barcode liposomes need to be developed. Our research group is working on the development of optical barcodes inside silica and polystyrene microbeads, which in turn could then be incorporated in the core of liposomes. The silica microbeads are prepared using well-known Stober synthesis of silica nanoparticles [110, 111]. The polystyrene microbeads are prepared using spraying suspension polymerization [112]. Various methods exist in literature to incorporate luminescent barcodes into these microbeads using quantum dots [113-119]. Quantum dots provide a range of emission

intensities based on variation in their loading and various extremely narrow emission profiles based on their particle size (REF). Figure 6.1 illustrates a group of CdSe/ZnS core shell semiconductor nanocrystals (quantum dots) emission spectra using a single excitation source. One of the disadvantages of incorporating beads inside the liposomes could be the close proximity of the bead surface to the lipid bilayers of liposomes, which may result in loss of mobility of lipid bilayers and could potentially affect the structure and function of incorporated membrane proteins or receptors. This problem can be circumvented by using molecular tethers to distance the lipid bilayer from the solid substrate as described in our research group's recent study.[120]

A library of various beads with different fluorescence emission profiles and intensities can then be created with each type of bead corresponding to one single receptor liposome. Liposome solutions with different membrane receptors or proteins could be prepared each incorporating one type of beads with its own fluorescent signature. These liposomes can then be arrayed statistically on a single substrate as elaborated in chapter 4. This array would then be exposed to the solution containing mixture of ligands or potential drug molecules. The spots on the liposome grid where binding events have occurred can be located using fluorescence based techniques and corresponding emission profiles from the beads incorporated in those liposomes will result in determination of the membrane protein or receptors responsible for the binding. Figure 6.2 illustrates the schematic of the biosensor array with several membrane receptors and barcoded beads incorporated in the core of liposomes.

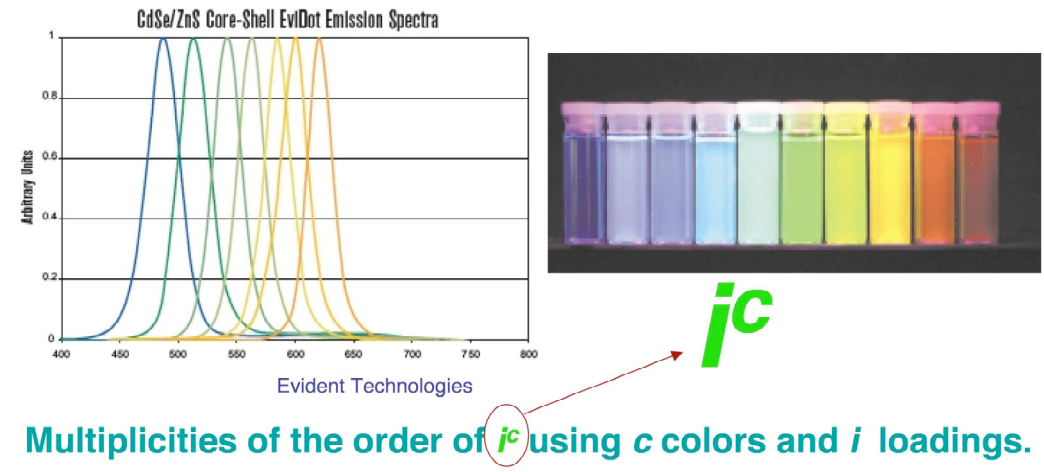

Fig 6.1 Multiplicities obtained using various sizes and concentrations of quantum dots.

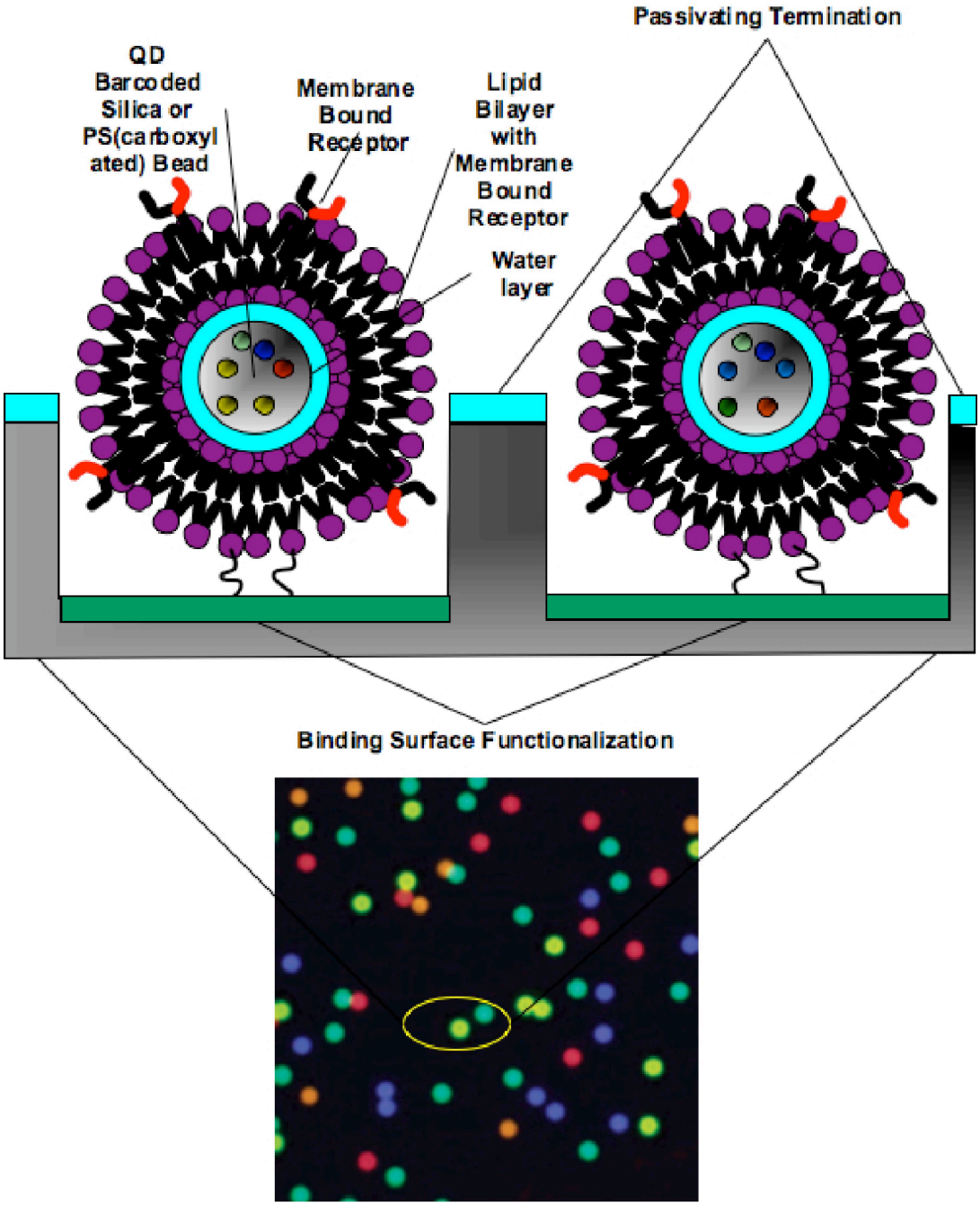

Fig 6.2 Schematic of the multi-receptor biosensor array: each color of the bead represents a different fluorescent barcode.

Bibliography

1. Cooper, M.A., *Advances in membrane receptor screening and analysis*. J.Mol.Recognit., 2004. **17**: p. 286-315.
2. Terstappen G. C., A.R., *In silico research in drug discovery*. Trends Pharmac. Sci, 2001. **22**: p. 23-26.
3. Lahiri, Y.F.Y.H.B.W.J., *Applications of Biomembranes in Drug Discovery*. MRS Bulletin, 2006. **31**(July): p. 541-545.
4. Paternostre, M.O.C.M.M., *Review: Vesicle Reconstitutaion from lipid-detergent mixed micelles*. Biochimica et Biophysica Acta, 2000. **1508**: p. 34-50.
5. Marie, R.J.L.P., *Mechanisms of membrane protein insertion into liposomes during reconstitution procedures involving use of detergents.2. Incorporation of the light driven proton pump bacteriorhodopsin*. Biochemistry, 1988. **27**: p. 2677-2688.
6. Marie, R.J.L.P., *Mechanisms of membrane protein insertion into liposomes during reconstitution procedures involving the use of detergents.1. Solublization of large unilamellar liposomes (prepared by reverse phase evaporation) by triton x-100, octyl glucoside, and sodium cholate*. Biochemistry, 1988. **27**(2668-2677).
7. Lasic, D.D. and P. D., *Liposomes revisited*. Science, 1995. **267**: p. 1275-1276.
8. Iwasaki, Y., et al., *Stablilization of Liposomes Attached to Polymer Surfaces Having Phosphorylcholine Groups*. Journal of Colloid and Interface Science, 1997. **192**: p. 432-439.

9. Keller, C.A. and B. Kasemo, *Surface specific kinetics of lipid vesicle adsorption measured with a quartz crystal microbalance*. Biophys J, 1998. **75**(3): p. 1397-1402.

10. Egawa, H. and K. Furusawa, *Liposome Adhesion on Mica Surface Studied by Atomic Force Microscopy*. Langmuir, 1999. **15**: p. 1660-1666.

11. Keller, C.A., et al., *Formation of supported membranes from vesicles*. Phys Rev Lett, 2000. **84**(23): p. 5443-6.

12. Thomson, N.H., et al., *Atomic Force Microscopy of Cationic Liposomes*. Langmuir, 2000. **16**: p. 4813-4818.

13. Kumar, S. and J.H. Hoh, *Direct visualization of Vesicle-Bilayer Complexes by Atomic Force MIcroscopy*. Langmuir, 2000. **16**: p. 9936-9940.

14. Jass, J., T. Tjarnhage, and G. Puu, *From Liposomes to Supported, Planar Bilayer Structures on Hydrophilic and Hydrophobic Surfaces: An Atomic Force Microscopy Study*. Biophysical Journal, 2000. **79**(Dec.2000): p. 3153-3163.

15. Ahmed, K., P. Gribbon, and M.N. Jones, *The application of confocal microscopy to the study of liposome adsorption onto bacterial biofilms*. Journal of liposome research, 2002. **12**(4): p. 285-300.

16. Reimhult, E., F. Hook, and B. Kasemo, *Intact vesicle adsorption and supported biomembrane formation from vesicles in solution: Influence of surface chemistry, vesicle size, temperature and osmotic pressure*. Langmuir, 2003. **19**: p. 1681-1691.

17. Tokumasu, F., et al., *Atomic Force Microscopy of Nanometric Liposome Adsorption and Nanoscopic Membrane Domain Formation*. Ultramicroscopy, 2003. **97**: p. 217-227.

18. Schonherr, H., et al., *Vesicle Adsorption and Lipid Bilayer Formation on Glass Studied by Atomic Force Microscopy*. Langmuir, 2004. **20**: p. 11600-11606.

19. Liang, X., G. Mao, and K.Y.S. Ng, *Mechanical properties and stability measurement of cholesterol-containing liposome on mica by atomic force microscopy*. Colloid and interface science, 2004. **278**: p. 53-62.

20. Helfrich, W., *Elastic properties of lipid bilayers: theory and possible experiments*. Z. Naturforsch, 1973. **28c**: p. 693-703.

21. Lipowsky, R.S., U, *Adhesion of vesicles and membranes*. Mol.Cryst.Liq.Cryst., 1991. **202**: p. 17-25.

22. Sofou, S., James L. Thomas, *Stable adhesion of phospholipid vesicles to modified gold surfaces*. Biosensors & Bioelectronics, 2003. **18**: p. 445-455.

23. Sackmann, E., Science, 1986. **271**: p. 43.

24. Dustin, J.T.G.M.L., J.Immunol.Meth., 2003. **278**: p. 19.

25. S.G.Boxer, J.T.G., Acc. Chem. Res., 2002. **35**: p. 149.

26. C.M.Yip, J.E.S.A.S., J.Am.Chem.Soc., 2003. **125**: p. 11838.

27. M.P.Shrinivasan, T.V.R., P.Stroeve, and M.L.Longo, *Patterned Supported Bilayers on Self-Assembled Monolayers: Confinement of Adjacent Mobile Bilayers*. Langmuir, 2001. **17**: p. 7951-7954.

28. Sen, A.G., P.K.;Mukherjea, M., Mol.Cell.Biochem., 1998. **187**: p. 183-190.

29. Chapman, D., Langmuir, 1993. **9**: p. 39-45.

30. Glasmastar, K., et al., Journal of Colloid and Interface Science, 2002. **246**: p. 40-47.

31. Martinez, K., et al., *Ligand Binding to G Protein-Coupled Receptors in Tethered Cell Membranes*. Langmuir, 2003. **19**(10925-10929).

32. Merrill, E.W., in *Poly(ethylene glycol): Biotechnical and Biomedical Applications*, J. Harris, Editor. 1992, Plenum Press: New Yorl. p. 199-220.

33. Du, H., P. Chandaroy, and S. Hui, *Grafted Poly-(ethylene glycol) on lipid surfaces inhibits protein adsorption and cell adhesion*. Biochim. Biophys. Acta., 1997. **1326**: p. 236-248.

34. Huang, N.P., et al., *Biotin derivatized poly(L-lysine)-g-poly(ethylene glycol): A novel polymeric interface for bioaffinity sensing*. Langmuir, 2002. **18**: p. 220-230.

35. Huang, N.P., et al., *Poly(L-lysine)-g-poly(ethylene glycol) layers on metal oxide surfaces: Surface Analytical characterization and resistance to serum and fibrinogen adsorption*. Langmuir, 2001. **17**: p. 489-498.

36. Lussi, J.W., et al., *A novel generic platform for chemical patterning of surfaces*. Progress in Surface Science, 2004. **76**(3-5): p. 55-69.

37. Prime, K.L. and G.M. Whitesides, *Self-Assembled Organic Monolayers: Model System for Studying Adsorption of Proteins at Surfaces*. Science, 1991. **252**: p. 1164-1167.

38. Prime, K. and G. Whitesides, Journal of the American CHemical SOciety, 1993. **115**: p. 10714.

39. Harder, P., et al., *Molecular conformation in oligo(ethylene glycol)-terminated self-assembled monolayers on gold and silver surfaces determines their ability to*

resist protein adsorption. Journal of Physical Chemistry B, 1998. **102**(2): p. 426-436.

40. Chapman, R.G., et al., *Surveying for surfaces that resist the adsorption of proteins*. Journal of the American CHemical SOciety, 2000. **122**(34): p. 8303-8304.

41. Shibata-Seki, T., et al., *In Situ atomic force microscopy study of lipid vesicles adsorbed on a substrate*. Thin Solid Films, 1996. **273**: p. 297-303.

42. Stanish, I., J. Santos, and A. Singh, *One-Step, Chemisorbed Immobilization of Highly Stable, Polydiacetylenic Phospholipid Vesicles Onto Gold FIlm*. Journal of the American CHemical SOciety, 2001. **123**: p. 1008-1009.

43. Patolsky, F., A. Lichtenstein, and I. Willner, *Electrochemical Transduction of Lipsomome-Amplified DNA Sensing*. Agnew. Chem. Int. Ed., 2000. **39**: p. 940-941.

44. Yoshina-Ishii, C. and S. Boxer, *Arrays of Mobile Tethered Vesicles on SUpported Lipid Bilayers*. Journal of American Chemical Society, 2003. **125**: p. 3696-3697.

45. Yoshina-Ishii, C., et al., *General Method for Modification of Liposomes for ENcoded Assembly on SUpported Bilayers*. Journal of the American CHemical SOciety, 2005. **127**: p. 1356-1357.

46. Benkoski, J.J. and F. Hook, *Lateral Mobility of Tethered Vesicle-DNA Assemblies*. Journal of Physical CHemistry B, 2005. **109**: p. 9773-9779.

47. Jung, L.S., et al., *Quantification of Tight Binding to Surface-Immobilized Phospholipid Vesicles Using Suface Plasmon Resonance: Binding Constants of*

Phospholipase A2. Journal of the American CHemical SOciety, 2000. **122**: p. 4177-4184.

48. Boukobza, E., A. Sonnenfeld, and G. Haran, *Immobilization in Surface-Tethered Lipid Vesicles as a New Tool for Single Biomolecule Spectroscopy*. Journal of Physical Chemistry B, 2001. **105**: p. 12165-12170.

49. Vermette, P., et al., *Immobilized liposome layers for drug delivery applications: inhibition of angiogenesis*. Journal of COntrolled Release, 2002. **80**: p. 179-185.

50. Vermette, P., et al., *Characterization of Surface-Immobilized Layers of Intact Liposomes*. Biomacromolecules, 2004. **5**: p. 1496-1502.

51. Pignataro, B., et al., *Specific Adhesion of Vesicles Monitored by Scanning Force Microscopy and Quartz Crytal Microbalance*. Biophysical Journal, 2000. **78**: p. 487-498.

52. Okumus, B., *Vesicle Encapsulation Studies Reveal that Single Molecule Ribozyme Heterogeneities Are Intrinsic*. Biiophysical Journal, 2004. **87**: p. 2798.

53. Cremer, P.S. and T. Yang, *Creating Spatially Addressed Arrays of Planar Supported Fluid Phospholipid Membranes*. J. Am. Chem. Soc., 1999. **121**(35): p. 8130-8131.

54. Hovis, J.S. and S.G. Boxer, *Patterning Barriers to Lateral Diffusion in Supported Lipid Bilayer Membranes by Blotting and Stamping*. Langmuir, 2000. **16**: p. 894-897.

55. Yoshinobu, T., et al., *Chemical imaging sensor and its application to biological systems*. Electrochimica Acta, 2001. **47**(1-2): p. 259-263.

56. Yoshinobu, T., et al., *AFM fabrication of oxide patterns and immobilization of biomolecules on Si surface*. Electrochimica Acta, 2003. **48**(20-22): p. 3131-3135.

57. Groves, J. and S. Boxer, *Micropattern Formation in Supported Lipid Membranes*. Accounts of Chemical Research, 2002. **35**: p. 149-157.

58. Kam, L. and S. Boxer, *Formation of Supported Lipid Bilayer Composition Arrays by Controlled Mixing and Surface Capture*. Journal of American Chemical Society, 2000. **2000**: p. 12901-12902.

59. Grove, J.T. and S. Boxer, *Micropattern Formation in Supported Lipid Membranes*. Accounts of Chemical Research, 2002. **35**(3): p. 149-157.

60. Stadler, B., et al., *Micropatterning of DNA Tagged Vesicles*. Langmuir, 2004. **20**: p. 11348-11354.

61. Stamou, D., et al., *Self-assembled microarrays of attoliter molecular vessels*. Angewandte Chemie-International Edition, 2003. **42**(45): p. 5580-5583.

62. Michel, B., et al., *Printing meets lithography: Soft approaches to high-resolution patterning*. Chimia, 2002. **56**(10): p. 527-542.

63. Catherine Pale-Grosdemange, E.S.S., Kevin L.Prime, George M.Whitesides, *Formation of self assembled monolayers by chemisorption of derivatives of oligoethylene glycol on Gold*. J.Am.Chem.Soc, 1991. **113**: p. 12-20.

64. Colin D. Bain, G.M.W., *Formation of two component surfaces by the spontaneous self assembly of monolayers on gold from solutions containing mixtures of organic thiols*. J.Am.Chem.Soc, 1988. **110**: p. 6560-6561.

65. Colin D. Bain, G.M.W., *Correlation between wettablity and structure in monolayers of alkanethiols adsorbed on gold*. J.Am.Chem.Soc, 1988. **110**(3665): p. 3665-3666.

66. Colin D. Bain, G.M.W., *Molecular level control over surface order in self assembled monolayer films of thiols on gold*. Science, 1988. **240**(April): p. 62-63.

67. Colin D. Bain, G.M.W., *formation of monolayers by the coadsorption of thiols on gold:variation in the length of the alkyl chain*. J.Am.Chem.Soc, 1988. **111**: p. 7164-7175.

68. J.B.Brzoska, I.B.A.a.F.R., *Silanization of solid substrates: a step towards reproducibility*. Langmuir, 1994. **10**: p. 4367-4373.

69. Piner, R.D.Z., J.; Xu, F.; Hong, S.; Mirkin, C.A., *Dip Pen Nanolithography*. Science, 1999. **283**: p. 661-663.

70. Liu, J.J.G.F.M.W.Y.J., *Self-Assembled Monolayers into the 21st Century: Recent Advances and Applications*. Electroanalysis, 2003. **15**(2): p. 81-96.

71. Kim, M.-S.L.S.-C.H.D., *Direct Photochemical Lithography of Gold (111) Film*. Japanese Journal of Applied Physics, 2004. **43**(12): p. 8347-8348.

72. Taschner, J.H.Y.L.C.K.J.M.E.K.T.J.M.I.S., *Photochemical Patterning of a Self-Assembled Monolayer of 7-Diazomethylcarbonyl-2,4,9-trithiaadmantane on Gold Films via Wolff Rearrangement*. Langmuir, 2004. **20**(12): p. 4933-4938.

73. Nitin Kumar, C.M., Carol Steiner, Alexander Couzis, *Formation of nanometer domains of one chemical functionality in a continuous matrix of a second chemical functionality by sequential adsorption of silane self assembled monolayers*. Langmuir, 2001. **17**: p. 7789-7797.

74. Fengqiu Fan, C.M., Alexander Couzis, *Fabrication of surfaces with nanoislands of chemical functionality by the phase separation of self-assembling monolayers on silicon*. Langmuir, 2003. **19**: p. 3254-3265.

75. Xia, Y.N., et al., *Microcontact printing of alkanethiols on copper and its application in microfabrication*. Chemistry of Materials, 1996. **8**(3): p. 601-&.

76. H.A.Biebuyck, N.B.L., E.Delamarche,B.Michel, *Lithography beyond light:Microcontact Printing with monolayer resists*. IBM J.Res.Develop., 1997. **41**(1/2): p. 159-170.

77. Younan Xia, G.M.W., *Soft lithography*. Angew.Chem.Int.Ed., 1998. **37**: p. 550-575.

78. T.Pompe, A.F., S.Herminghaus, *Submicron contact printing on silicon using stamp pads*. Langmuir, 1999. **15**: p. 2398-2401.

79. Cherniavskaya Oksana, D.M.A., *Edge transfer lithography of molecular and nanoparticle materials*. Langmuir, 2002. **18**: p. 7029-7034.

80. Rebecca J Jackman, J.L.W., George M.Whitesides, *Fabrication of submicrometer features on curved substrates by microcontact printing*. Science, 1995. **269**(August).

81. Emmanuel Delamarche, H.S., Bruno Michel, Hans Biebuyck, *Stability of molded Polydymethylsiloxane microstructures*. Advanced Materials, 1997. **9**(9): p. 741-746.

82. E. Delamarche; A. Bietsch; N.B. Larsen; H. Rothuizen, B.M.H.B., *Transport Mechanisms of Alkanethiols during Microcontact Printing on Gold*. J.Phys.Chem.B., 1998. **102**: p. 3324-3334.

83. Libioulle, L., et al., *Contact-inking stamps for microcontact printing of Alkanethiols on gold*. Langmuir, 1999. **15**(2): p. 300-304.

84. Souheng, W., *Polymer Interface and Adhesion*. 1982: p. 88.

85. Raj, H.P.R., *Principles of Colloid and Surface Chemistry*. 1997.

86. Francis Szoka Jr., D.P., *Comparative properties and methods of preparation of lipid vesicles*. Ann.Rev.Biophys.Bioeng., 1980. **9**: p. 467-508.

87. Kang, M.C., et al., *Nanowell-array surfaces prepared by argon plasma etching through a nanopore alumina mask*. Langmuir, 2005. **21**(18): p. 8429-8438.

88. Yap, F.L. and Y. Zhang, *Protein micropatterning using surfaces modified by self-assembled polystyrene microspheres*. Langmuir, 2005. **21**(12): p. 5233-5236.

89. Jahnig, F., *Lipid Exchange between Membranes*. Biophysical Journal, 1984. **46**(6): p. 687-694.

90. G. Duckwitz-Peterlein, a.H.M., *Transport of lipids through water as exchange mechanism between two liposome populations*. European Biophysics Journal, 1978. **4**(4): p. 315-326.

91. Jahnig, F., *Lipid exchange between membranes*. Biophys J, 1984. **46**(6): p. 687-694.

92. Chan, W.C.W. and S.M. Nie, *Quantum dot bioconjugates for ultrasensitive nonisotopic detection*. Science, 1998. **281**(5385): p. 2016-2018.

93. Bruchez, M., et al., *Semiconductor nanocrystals as fluorescent biological labels*. Science, 1998. **281**(5385): p. 2013-2016.

94. Alivisatos, A.P., *Semiconductor clusters, nanocrystals, and quantum dots*. Science, 1996. **271**(5251): p. 933-937.

95. Susan Daniel, F.A., and Paul S. Cremer, *Making lipid membranes rough, tough, and ready to hit the road*. MRS Bulletin, 2006. **31**(July): p. 536-540.

96. Ye Fang, A.G.F., Joydeep Lahiri, *Membrane Protein Microarrays*. JACS Communications, 2001. **124**(11): p. 2394-2395.

97. Ye Fang, J.L.a.L.P., *G Protein Coupled Receptor Microarrays for Drug Discovery*. Drug Discovery Today, 2003. **8**: p. 755-761.

98. Groves, A.N.P.a.J.T., *Materials science of supported lipid membranes*. MRS Bulletin, 2006. **31**(July): p. 507-509.

99. Yulong Hong, B.L.W., Hui Su, Eric J. Mozdy, Ye Fang, Qi Wu, Li Liu, Jonathan Beck, Ann M. Ferrie, Srikanth Raghvan, John Mauro, Alain Carre, Dirk Mueller, Fang Lai, and Joydeep Lahiri, *Functional GPCR microarrays*. JACS Communications, 2005. **127**: p. 15350-15351.

100. Biltonen, M.E.G.R.L., *Characterization of the interaction of phospholipase A(2) with phosphatidylcholine-phosphatidylglycerol mixed lipids*. Biochemistry, 2000. **39**: p. 9623-9631.

101. Ye Fang, A.G.F., Joydeep Lahiri, *Ganglioside Microarrays for Toxin Detection*. Langmuir, 2003. **19**: p. 1500-1505.

102. Anup K. Singh, S.H.H., and Joseph S. Schoeniger, *Gangliosides as Receptors for Biological Toxins: Development of Sensitive Fluoroimmunoassays Using Ganglioside-Bearing Liposomes*. Analytical Chemistry, 2000. **72**: p. 6019-6024.

103. Soohyoun Ahn-Yoon, T.R.D., Antje J. Baeumner, and Richard A. Durst, *Ganglioside-Liposome Immunoassay for the Ultrasensitive Detection of Cholera Toxin*. Analytical Chemistry, 2003. **75**: p. 2256-2261.

104. Jose M. Moran-Mirabal, J.B.E., Grant D. Meyer, Dan Throckmorton, Anup K. Singh, and Harold G. Craighead, *Micrometer - sized Supported Lipid Bilayer Arrays for Bacterial Toxin Binding Studies through Total Internal Reflection Fluorescence Microscopy*. Biophysical Journal, 2005. **89**(July): p. 296-305.

105. Kalyankar, N.D., et al., *Arraying of intact liposomes into chemically functionalized microwells*. Langmuir, 2006. **22**(12): p. 5403-5411.

106. W.Stober, A.F., E.Bohn, J.Colloid Interface Sci, 1968. **26**: p. 62.

107. D.L.Green, J.S.L., Yui-Fai Lam, M.Z.C.Hu, Dale W. Schaefer, and M.T.Harris, *Size, volume fraction, and nucleation of Stober silica nanoparticles*. J.Colloid Interface Sci, 2003. **266**: p. 346-358.

108. Chengli Yang, H.L., Yueping Guan, Jianmin Xing, Junguo Liu, Guobin Shan, *Preparation of magnetic poly(methylmethacrylatedivinylbenzene-glycidylmethacrylate) microspheres by spraying suspension polymerization and their use for protein adsorption*. Journal of Magnetism and Magnetic Materials, 2005. **293**(2005): p. 187-192.

109. O'brien, P., et al., *Quantum dot-labelled polymer beads by suspension polymerisation*. Chemical Communications, 2003(20): p. 2532-2533.

110. Riegler, J., O. Ehlert, and T. Nann, *A facile method for coding and labeling assays on polystyrene beads with differently colored luminescent nanocrystals*. Analytical and Bioanalytical Chemistry, 2006. **384**(3): p. 645-650.

111. Li, Y., et al., *Synthesis and characterization of CdS quantum dots in polystyrene microbeads*. Journal of Materials Chemistry, 2005. **15**(12): p. 1238-1243.

112. Haes, A.J., et al., *Using solution-phase nanoparticles, surface-confined nanoparticle arrays and single nanoparticles as biological sensing platforms*. Journal of Fluorescence, 2004. **14**(4): p. 355-367.

113. Chan, W.C.W., et al., *Luminescent quantum dots for multiplexed biological detection and imaging*. Current Opinion in Biotechnology, 2002. **13**(1): p. 40-46.

114. Bradley, M., N. Bruno, and B. Vincent, *Distribution of CdSe quantum dots within swollen polystyrene microgel particles using confocal microscopy*. Langmuir, 2005. **21**(7): p. 2750-2753.

115. Han, M.Y., et al., *Quantum-dot-tagged microbeads for multiplexed optical coding of biomolecules*. Nature Biotechnology, 2001. **19**(7): p. 631-635.

116. Sharma, M.K., Jattani H. and Gilchrist M.L., *Bacteriorhodopsin conjugates as anchors for supported lipid bilayers*. Bioconjugate Chemistry, 2004. **15**(4): p. 942-947.